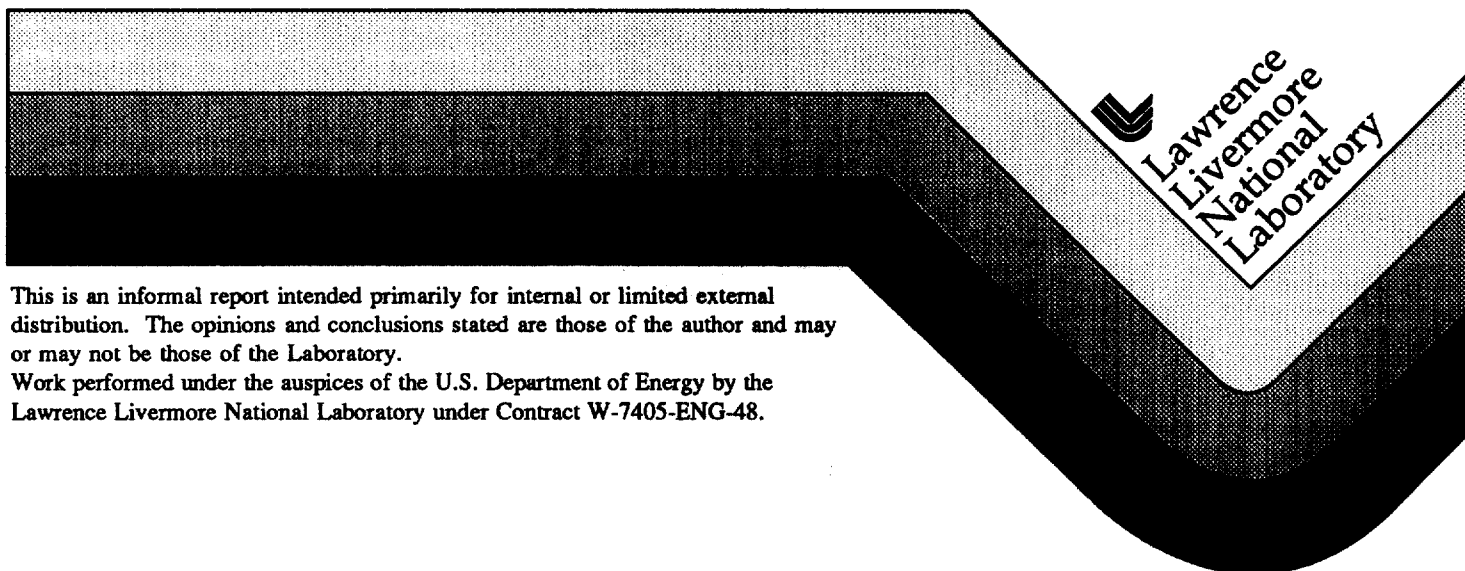


Science and Engineering Research Semester Internship Fall 1996 Abstracts and Research Papers

Brian Beaubien, Eric Brown, Michael Davis, Jolene Downs, Kari Fox,
Charity Hayden, Eric Jacobsen, Erin Kraut, Sheila Lawrence,
Tina Legler, Shane Oram, Samihah Ragland, Timm Wulff

Beverly Williams
SERS Program Coordinator

December 1996



This is an informal report intended primarily for internal or limited external distribution. The opinions and conclusions stated are those of the author and may or may not be those of the Laboratory.

Work performed under the auspices of the U.S. Department of Energy by the Lawrence Livermore National Laboratory under Contract W-7405-ENG-48.

DISCLAIMER

This document was prepared as an account of work sponsored by an agency of the United States Government. Neither the United States Government nor the University of California nor any of their employees, makes any warranty, express or implied, or assumes any legal liability or responsibility for the accuracy, completeness, or usefulness of any information, apparatus, product, or process disclosed, or represents that its use would not infringe privately owned rights. Reference herein to any specific commercial product, process, or service by trade name, trademark, manufacturer, or otherwise, does not necessarily constitute or imply its endorsement, recommendation, or favoring by the United States Government or the University of California. The views and opinions of authors expressed herein do not necessarily state or reflect those of the United States Government or the University of California, and shall not be used for advertising or product endorsement purposes.

This report has been reproduced
directly from the best available copy.

Available to DOE and DOE contractors from the
Office of Scientific and Technical Information
P.O. Box 62, Oak Ridge, TN 37831
Prices available from (615) 576-8401, FTS 626-8401

Available to the public from the
National Technical Information Service
U.S. Department of Commerce
5285 Port Royal Rd.,
Springfield, VA 22161

SCIENCE & ENGINEERING

SERS

RESEARCH SEMESTER

Lawrence Livermore National Laboratory

Fall 1996

December 12-13, 1996



**ABSTRACTS
FOR
STUDENT SYMPOSIUM**



Sponsored by:

**The U.S. Department of Energy
Office of Energy Research**

**Science and Engineering Research Semester
Fall 1996 Internship Program
at
Lawrence Livermore National Laboratory**

Authors

**Brian Beaubien
Eric Brown
Michael Davis
Jolene Downs
Kari Fox
Charity Hayden
Eric Jacobsen
Erin Kraut
Sheila Lawrence
Tina Legler
Shane Oram
Samihah Ragland
Timm Wulff**

Affiliations: Brian Beaubien, University of Minnesota; Eric Brown, University of California, Berkeley; Michael Davis, Mississippi State University; Jolene Downs, Ohio State University; Kari Fox, University of California, Santa Cruz; Charity Hayden, Norwich University; Eric Jacobsen, University of Dayton; Erin Kraut, St. Mary's College; Sheila Lawrence, Auburn University; Tina Legler, University of Wisconsin, Stevens Point; Shane Oram, Ithaca College; Samihah Ragland, Spelman College; Timm Wulff, California State University Chico

SCIENCE & ENGINEERING
SERS
 RESEARCH SEMESTER

Table of Contents

Abstracts	i -viii
Brian Beaubien	Hexahedral Mesh Generation For a 3D Finite Element Model of the Human Hand	1
Eric Brown	Modeling Source-Area VOC Transport in Ground Water	10
Michael Davis	3D Imaging of Bacterial Processes in Subsurface Environments: Selection of Bacteria.....	29
Jolene Downs	Progress in the Synthesis of a Photoactivatable, Reversible Linker	38
Kari Fox	Experimental and Computational Approach to VOC Transport in Ground Water.....	58
Charity Hayden	Evaluating the Sewer Satellite Stations for Future Alterations ...	78
Eric Jacobsen	Real-Time Earthquake Warning Using Artificial Neural Networks	108
Erin Kraut	Identifying Barriers and Facilitators to Curriculum Reform.....	120
Sheila Lawrence	Mapping Genes on Chromosome 19.....	140
Tina Legler	Optimization of the Biodegradation of Trichloroethylene.....	151
Shane Oram	Pericentric Inversion Frequency for High- and Low- LET Radiation Measured by Fluorescence <i>in situ</i> Hybridization FISH	165
Samihah Ragland	Optimization of Chromosome Painting Probes for Scoring of Incomplete Translocations.....	180
Timm Wulff	Cyber Sight, a 3D Motion Camera, Moves to the PC Platform..	192

A Finite Element Model of the Human Hand

Brian Beaubien
University of Minnesota
Computations

ABSTRACT

We are developing a 3D finite element model to study the biomechanics of the human hand. Data obtained from high resolution CTscans are used to create hexahedral, volumetric meshes for analysis by NIKE3D, a finite element code developed at LLNL. Once complete, this model will be a valuable tool in prosthetics design, surgical planning, and research and education in anatomy and biomechanics.

Modeling Source-Area VOC Transport in Ground Water

Eric Brown
University of California, Berkeley
Mechanical Engineering

ABSTRACT

The purpose of this study is to develop a tool that will allow us to predict time to remediate volatile organic compounds (VOCs) in ground water. An adaptive-grid finite element model was created using PDEase software. Results indicate that convergence to analytical solutions, field data, and conceptual mass-transport models was successful. Contaminants in fine-grained zones were proved to be long term sources that are difficult to remediate.

Bacterial-Contaminant-Particle Interactions in Subsurface Environments: Selection of Bacteria

Michael Davis
Mississippi State University
Biology and Biotechnology Research Program

ABSTRACT

The purpose of this project is to study bacterial-contaminant-particle interactions in subsurface environments; therefore, we must first select a bacterium that can (1) survive in and (2) function normally in our porous medium and refractive index matched solution. We grew bacteria in a solution similar to the aqueous phase of our system, and counted cells at various time points. We analyzed the resultant plots and decided that of the strains tested, *Alcaligenes xylosoxidans* has the best survival rate. Provided *A. xylosoxidans* can be sufficiently fluoresced, it will be used to study bacterial transport in modeled subsurface environments.

Progress in the Synthesis of a Photoactivatable, Reversible Linker

Jolene Downs
Ohio State University
Environmental Programs

ABSTRACT

The objective of this study is the synthesis of a photoactivatable molecule that will reversibly link biotin to biological macromolecules. Isolation of the macromolecules can then be achieved through biotin-avidin affinity chromatography. The synthesis plan has five steps, and results from completion of the first three steps will be presented.

The product from the Step-1 condensation of a lactone and a triamine was coupled with a photoactive species in Step 2 to yield the photoactivatable segment of the linker. The condensation of biotin and tetraethylene glycol in Step 3 provided the linker segment useful for biotin-avidin affinity chromatography.

The products have been characterized by infrared spectroscopy and mass spectrometry, showing that desired products were obtained and that light conditions for the Step-2 reaction were adequate to protect the photoactive product.

In Step 4 the biotin segment will be attached to a silane, followed by attachment of the photoactivatable segment to the silane in Step 5. It is anticipated that these reactions will be straightforward once suitable conditions are determined for avoiding di-substitution on the silane in Step 4.

Experimental Approach to VOC Transport in Ground Water

Kari Fox
University of California, Santa Cruz
Plant Operations

ABSTRACT

The object of this study is to evaluate the physical and chemical retardation processes that impede cleanup in low organic carbon aquifers. Innovative laboratory column and diffusion experiments were performed to measure the transport mechanisms of retardation, diffusion, and tortuosity for four volatile organic compounds (VOCs) commonly found in ground water.

Resolution of problems with experimental methods is in progress. Field and experimental parameters are used to bound the uncertainty in computational modeling efforts.

Sewer Satellite Stations

Charity Hayden
Norwich University
Plant Operations

ABSTRACT

Unauthorized releases of contaminants into the sanitary sewer during the 80's led the City of Livermore Sewage Treatment Plant to request additional monitoring measures. Corrections proposed by Lawrence Livermore National Laboratory (LLNL) included sewer satellite stations to identify instantaneous or chronic sewer spill sources.

The purpose of my project is to perform a technical evaluation of these stations functionality and their current applicability. A quantification of past operational findings will be used as a basis for the assessments.

Ten sewer satellite stations were built, beginning in 1989, in response to historical problems with site discharges. The initial concept for these was to perform spill traceback by locating the source of a spill which could have an environmental impact or cause damage to the Livermore Water Reclamation Plant.

Stations that are evaluated to be beneficial to LLNL in monitoring spills or illicit discharges may have to be moved, repaired or upgraded. This project will graph the historical operations of the satellites and from the graph develop criteria for future practices. Operational parameters and equipment for a reliable trace back system will be proposed.

Real Time Earthquake Warning Using Artificial Neural Networks

Eric Jacobsen
University of Dayton
Electrical Engineering

ABSTRACT

This report describes a neural network based earthquake early warning system. The system would estimate the complete time series envelope and earthquake magnitude immediately after the beginning of an earthquake and continuously updating the estimate as the earthquake evolves. The estimates can be used to trigger automatic shut off systems or sound alarms before the most damaging shaking occurs.

A set of recorded time-series earthquake signals is prepared. Several signal pre-processing algorithms and neural network architectures will be tested to minimize estimation error. The network will be trained with a large portion of the available data, while some data will be set aside for testing. Successful estimation is determined by the networks performance with the previously unseen data. Because of recent damaging earthquakes such as Mexico City, Loma Prieta, Northridge, and Kobe, previously unavailable strong-motion recordings are now available.

With this new data, we will try to further the research by addressing two important issues:

- First, can the neural network be trained to estimate over a wide dynamic range of ground motion including very large (>8.0 MI) earthquakes?
- Second, can a neural network be trained to provide warning to a network of stations using recorded signals from all the stations as training input, as opposed to using data only from a single site?

Identifying Barriers and Facilitators to Curriculum Reform

Erin Kraut
St. Mary's College
Education Program - University Relations

ABSTRACT

The purpose of this study is to review and synthesize the research literature referring to barriers and facilitators to implementing new curriculum and instructional techniques.

The methodology consisted of an extensive literature search of the ERIC database and the MELVYL database. There was also an Internet search to locate titles and references to original sources. Several research reports on schools attempting to implement new curriculum programs and/or instructional techniques were examined.

Results from the review identified ten conditions that appear to facilitate successful implementation: 1) leadership, 2) teacher empowerment, 3) professional development, 4) guidelines, 5) embrace problems, 6) program monitoring, 7) district support, 8) resources, 9) incentive programs, 10) information dissemination. Successful schools implemented at least five of the conditions concurrently.

The major consensus is that successful reform requires established goals and a vision, fundamental pedagogical changes and time. Changes that take place over time must be inclusive and tied to established goals.

Mapping Genes on Chromosome 19

Sheila Lawrence
Auburn University
Biology and Biotechnology Research Program

ABSTRACT

In order to increase the utility of the physical map of chromosome 19, more genes need to be isolated along the entire length of the chromosome. The purpose of my project is to define several Expressed Sequence Tags (EST's), which are portions of genes, and then further characterize them. Eleven cDNA clones chosen from the databank of the I.M.A.G.E. Consortium were initially hybridized to high density filters containing cosmid clones, and positive signals were verified by PCR. Four clones were chosen for further characterization by sequencing and Northern Hybridization to determine mRNA size and tissue specificity. The results are the addition of four EST's to the Human Genome databank, which will increase the resolution of the physical map of chromosome 19. Also, the genes in this study were previously undiscovered. By characterizing them, more was learned about their position on the chromosome as well as their role and function based on sequence homologies.

Optimization of the Biodegradation of Trichloroethylene

Tina Legler
University of Wisconsin, Stevens Point
Environmental Programs

ABSTRACT

As an interim step towards optimizing the biodegradation of trichloroethylene (TCE), the lowest concentration of methanol that could support cellular growth and yet not inhibit TCE degradation needed to be determined. Population growth and TCE degradation rates were determined by analyzing growth curves and gas chromatograph assays. The data from these analyses showed that at concentrations of 0.001% methanol, cultures continued to grow, and TCE degradation remained significant. Although all data analysis is not yet complete, these results suggest that it will be possible to support a bacterial culture on methanol, while allowing TCE degradation to occur.

Pericentric Inversion Frequency for High-LET and Low-LET Radiation Using FISH

Shane Oram
Ithaca College
Environmental Programs

ABSTRACT

The purpose of this study is to measure the ratio of translocations to pericentric inversions for high-LET radiation and low-LET radiation using fluorescence *in situ* hybridization (FISH). The method to measure pericentric inversions employs fluorescent probes generated by degenerate oligonucleotide-primed-polymerase chain reaction (DOP-PCR). Probes consisting of a composite chromosome 1p telomeric region specific probe, a chromosome 1 heterochromatin probe and a pan-centromere probe were developed to identify pericentric inversions. A chromosome 1 paint probe was employed to measure translocations on chromosome 1 as described by Lucas *et al.* (1989, 1992). A pericentric inversion is made distinct by the position change of the fluorescent signals relative to the chromosome centromere. This allows for easy identification of pericentric inversions.

Facilitating the measurement of a signature for high-LET radiation will make it easy to distinguish between high-LET and low-LET radiation. This will allow for quick diagnosis of victims exposed to unknown sources.

Optimization of Whole Chromosome Probes for Use in Scoring Incomplete Translocations

Samihah Ragland
Spelman College
Biology and Biotechnology Research Program

ABSTRACT

The purpose of this project is to synthesize a two color whole chromosome probe mixture for use in scoring incomplete translocations. An incomplete translocation occurs when one chromosome derivative fails to rejoin, leaving one bicolor chromosome and one painted chromosome segment. The painted chromosome segment has a centromere. Flourogreen labeled probes for chromosomes 3,5, and 6 were generated by DOP-PCR and Random Priming techniques. Spectrum Orange labeled probes for chromosomes 1,2, and 4 were purchased from VYSIS. After ethanol precipitation, the probe DNA was resuspended in buffer and visualized by FISH on metaphase spreads.

The signals produced by this bicolored probe mix provide a rapid and sensitive means of scoring incomplete translocations. These probes will facilitate the understanding and quantification of incomplete translocations by providing a sharper image of small translocated segments on bicolored chromosomes.

Cyber Sight, 3D Motion Camera, Moves to the PC Platform

Timm Wulff
California State University, Chico
Electrical Engineering

ABSTRACT

The advent of the PCI bus on the Personal Computer (PC) has suggested that the PC may have become a more effective platform from which the Cyber Sight project could be executed. The purpose of this paper is to document the steps made to convert the Cyber Sight project from a UNIX to a PC platform, including evaluation of possible hardware and software options.

Research Methods

- 1.) exploring the Targa 2000 hardware as a source of video input.
- 2.) exploring 3D Studio MAX software as a imaging output tool.
- 3.) development of software to convert 3D image data to a format that is supported by 3D Studio MAX.

Research Results

- 1.) Targa video format is compressed to keep up with real time video data rate. The video format is in 60 fields per second, and 2 fields per frame.
- 2.) images could be imported into 3D Studio MAX in a dxf format.
- 3.) a program was developed to convert output image data to a dxf format.

Based on Results

- 1.) The fields of the Targa video image make the Targa video useless to application in the Cyber Sight project.
- 2.) Importing the dxf format into 3D Studio MAX is an effective method of displaying system output.
- 3.) Software has been developed to build a series of DXF files from a series of 3D data sets.

**HEXAHEDRAL MESH GENERATION FOR A 3D FINITE
ELEMENT MODEL OF THE HUMAN HAND**

Brian Beaubien

**University of Minnesota Institute of Technology
Minneapolis, Minnesota
e-mail bpb@redhook.llnl.gov**

**Mentor - Karin Hollerbach
Institute for Scientific Computing Research
Lawrence Livermore National Laboratory
Livermore, California 94550**

December 20, 1996

Prepared in partial fulfillment of the requirements of the Science and Engineering Research Semester under the direction of Karin Hollerbach, Research Mentor, in the Lawrence Livermore National Laboratory.

***This research was supported in part by an appointment to the US. Department of Energy Science and Engineering Research Semester (hereinafter called SERS) program administered by LLNL under Contract W-7405-Eng-48 with Lawrence Livermore National Laboratory.**

ABSTRACT:

Hexahedral mesh generation techniques were developed for a 3D finite element model of the human hand to be used in biomechanics research. Using these techniques, meshes were generated from CT scans for all 27 bones in the human hand. NIKE3D finite element software has accepted all meshes, and analysis on the carpo-metacarpal joint has produced encouraging results. Once complete, this model will provide researchers with a better understanding of the complex biomechanics of the hand, which can be used in education, surgery planning, and prosthetic device development.

INTRODUCTION:

Osteoarthritis is a debilitating disease that deteriorates the bones and cartilage of the body's joints, causing pain, swelling, and sometimes a loss of joint function. Joint implants are often the answer for sufferers of severe joint problems associated with osteoarthritis and other pathological disorders in the joints of the hand. With an aging population and increased life expectancy we can expect to see dramatic increases in the number of joint implants conducted each year [2]. While these implants have the ability to immediately increase mobility and nearly eliminate joint pain, they usually fail within the patient's lifetime, requiring dangerous and expensive revision surgeries to alleviate the pain and restore mobility [2].

Prosthetic joint breakdown is most often associated with failure to duplicate healthy joint kinematics, material failure at the articular surface, and failure at the implant/bone interface[2]. The Institute for Scientific Computing Research at LLNL is developing a hexahedral finite element model capable of three dimensional non-linear analysis of the complex kinematics of a healthy or diseased joint. Using this model, researchers would gain an understanding of the natural biomechanics of the joint which could be imitated in designing new prosthetic devices. New designs inspired by this understanding could also be tested using the model, providing a more accurate and less expensive alternative to clinical testing.

Hand biomechanics analysis using the finite element method (FEM) to date has mostly been linear and two dimensional, which we feel is an invalid simplification. The mechanics of the hand are complex and three dimensional in nature, and can only be accurately modeled using a three dimensional approach. Another simplification often made is assuming a fixed rotational axis of a given joint. We do not constrain joint movement to a pre-determined axis, but instead allow bone geometry and soft tissue attachments to determine this axis.

Doctors and surgeons would also benefit from this model. The model will be a valuable tool in anatomy and biomechanics education, and with further developments, the model could be used to create a pre-operative model of each patient's unique anatomy and physiology. Surgeons may even be able to conduct surgery on these models, analysing their procedures computationally before they are performed in the operating room.

THE PROCESS OF FINITE ELEMENT MODEL GENERATION

Data is acquired for the bone models using Computed Tomography scans taken by Non Destructive Evaluation (NDE) at LLNL. Our current data set was obtained from the fresh frozen cadaver hand of a 53 yr. old Caucasian woman using industrial CT scanners at NDE with a spatial resolution of approximately 160 microns.

After the scans are taken, bone is segmented from the CT scan layers using VISU, a semi-automatic edge detection program developed at LLNL, which traces and fills in the bone outline. Manual intervention is required on several layers to correct deterioration at the joint surfaces scans due primarily to pathological bone deterioration and scanning artifacts.

Using a marching cubes algorithm, 3D polygonal surfaces are triangulated from the segmentation results for use in mesh generation. The number of surface nodes is reduced by approximately 70% using DECIMATE (General Electric) which reduces computation time while maintaining the spatial resolution.

Hexahedral, volumetric meshes are generated using TrueGrid (*xyz Scientific*) to closely match the triangulated bone definition. Although the meshing of hexahedral elements is more time consuming than that of tetrahedral elements, hexahedral elements are more appropriate for mechanical simulations. Material properties, load curves, and sliding surfaces are also defined in TrueGrid to help prepare the mesh for analysis. This process is done primarily interactively, but commands are saved in a file for batch processing in NIKE3D.

After the mesh is complete, boundary conditions are defined in AVS™. AVS is a scientific visualization package developed by Advanced Visualization Systems that allows the operator to apply boundary conditions, which define force vectors, moments and motion constraints to be applied to the mesh in analysis [1].

NIKE3D, a finite element code developed at LLNL, is used to conduct the analysis. Displacements and forces can be applied in NIKE which then performs 3D, non-linear, large displacement analysis. Resulting stresses, deformations, and displacements are calculated by NIKE3D, and represent the actual three dimensional mechanics experienced in the joint.

METHOD:

Since we are allowing bone geometry and soft tissue attachment define the range of motion of the model, it is extremely important to take advantage of the high resolution data set by closely matching the mesh to the surface definition . This objective is complicated by the fact that each element must remain roughly block shaped, or orthogonal. Elements which are extremely thin, wedge shaped or twisted will prevent NIKE3D from converging, or will produce erroneous results.

The process used to create the meshes in TrueGrid has been compiled from personal experience and the previous meshing experience of Karin Hollerbach, Jonathan Pearlman, and Scott Perfect. The process we have developed will be broken down into the following five steps:

- **Block Definition** - Select a block of elements to roughly match the bone geometry.
- **Curve Placement** - Define guideline curves at key locations along the surface definition.
- **Point Attachment** - Attach nodes to and project edges to the curves to mold the mesh closer to the surface definition.
- **Surface Projection** - Map nodes on the surface of the mesh to the surface definition and interpolate internal nodes.
- **NIKE3D Preparation** - Relax the surface of the mesh and define sliding surfaces and materials.

After completing these five steps we apply the boundary conditions, and perform analysis on the meshes.

Block Definition

The first step in the meshing process is initiating a set of blocks that roughly match the shape of the bone. Selecting an initial block of elements for the phalanges and metacarpals generally involves a simple rectangular shape. Choosing a shape for the irregularly shaped carpals is usually a more difficult task, and often involves experimentation. An L shaped block, for example, was finally chosen to match that of the hamate.

At this point the block has a square cross-section, which must be mapped to the nearly circular cross-section of the bone. If this were done directly, adjacent edges of the block's cross section would intersect in angles approaching 180 degrees. These large angles in the cross section would cause one side of the element to be pushed through another when forces are applied normal to the long axis of bones. The result is an element with a negative volume, which NIKE3D recognizes as a physically impossible event.

In order to avoid these large angles we use the "iron cross" or "butterfly" approach in which the corner columns of the block are deleted and the mesh is stretched into a nearly cylindrical shape (see Figure 1).

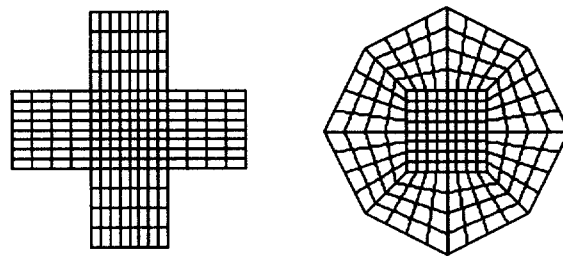


Figure 1. Cross section of block illustrating butterfly mesh before (left) and after it has been stretched.

Curve Placement

After the block is created, curves are placed along the surface definition to act as guidelines in positioning the mesh. In order to capture the detail of the articular surfaces, a curve is interactively drawn along the outer edges of each of these surfaces. Curves are then defined along the bone by intersecting planes perpendicular to the long axis of the bone with the surface definition. It is important to place these curves at points that highlight the features of the bone being meshed (i.e. head-shaft intersection, condyles, and other protrusions). Failure to properly place these curves often leads to missed bone features or distorted elements after projection.

Point Attachment

Once guideline curves have been defined, cross sections are systematically translated and scaled to approximate the curve outline. Nodes on the edges of each cross-section near the curves are interactively selected and attached to the curves. Only certain nodes explicitly

described during block formation can be directly attached to the curves. After these nodes have been attached, intermediate nodes are projected to the curves. At this point the mesh closely resembles the surface definition of the bone, and is ready for projection.

Surface Projection

Surface projection captures the details of the surface definition, and is the final step in the process of mesh generation. In this stage, nodes on the surface of the mesh are mapped to their closest respective position on the surface definition. Internal nodes are automatically interpolated to form highly orthogonal hexahedral elements throughout the volume of the mesh.

After projection, a relaxation algorithm is applied to smooth the surface of the mesh, and make the elements more orthogonal.

NIKE3D Preparation

In order to further prepare the projected mesh for analysis, it is necessary to define regions as “sliding surfaces” which are expected to contact other tissues. By labeling these sliding surfaces on adjacent tissues, NIKE3D will prevent the nodes of one tissue from passing through those of the other.

Regions of the mesh are also given material properties at this stage. An entire mesh or a section of a mesh is assigned a material number which is later categorized as having specific material properties such as elasticity, viscoelasticity, or rigidity.

Although the bone has been created from one block, overlapping nodes are present as a result of the butterfly technique, and must be merged, or combined. This is done by specifying a minimum tolerance between nodes which causes all nodes within this tolerance to be merged. It is important to verify that all overlapping nodes have been merged to avoid the occurrence of separate sections within the mesh.

At this point the mesh is ready for boundary conditions to be defined using the AVS software, and later applied to the mesh in the finite element analysis stage.

RESULTS:

Using this process, meshes have been generated for each of the 27 bones in the human hand, and all bones have been accepted by NIKE3D. Analysis has been conducted on the first metacarpal and its respective articular surface on the trapezium, as well as for several designs of prosthetic implants for this joint. Quantitative clinical testing information for the implants has not been compared to our model as of yet, but the FEM results appear to correlate closely with wear patterns seen in clinical testing[2].

I have recently finished mesh generation for ligaments in the second proximal interphalangeal joint. Surfaces were created manually to represent the collateral ligaments, and a dorsal ligament was used to represent the remainder of the joint capsule. Meshes have been made for these surfaces and await dynamic analysis in NIKE3D.

CONCLUSIONS:

While our current meshing techniques will produce a high quality hexahedral mesh, they are very time consuming, and require highly specialized operators. In order to expedite the meshing process and increase the feasibility of a patient-specific finite element model, it is recommended that the meshing process be automated as much as possible as the need for new meshes arises.

The ISCR is developing a set of templates that will take a step toward automating the meshing process. These templates will exploit the similarities between the anatomy of each patient by allowing the mesh builder to begin the process with a block very similar to the actual geometry of the bone. By selecting the proper template and making minor adjustments to the mesh as necessary, a mesh builder will be able to generate a quality mesh much more quickly than is currently possible.

REFERENCES:

[1] Abramowitz, MarcS. A Computational Model of Human Hand Kinematics Using AVS. *SERS Research Papers*, Fall, 1995.

[1] Hollerbach, Karin, S Perfect, A.Hollister, M. Truman, C. Nielsen, E. Ashby. 3-D Finite Element Analysis of Prosthetic Implants or the Thumb CMC Joint. XVIth Congress of the International Society of Biomechanics, Aug 25-27, 1997 (submitted).

Modeling Source-Area VOC Transport in Ground Water



Eric Brown

Lawrence Livermore National Laboratory
Environmental Restoration Division

This research was supported in part by an appointment to the U. S. Department of Energy Science and Engineering Research Semester program administered by LLNL under Contract W-7405-Eng-48 with Lawrence Livermore National Laboratory.

Modeling Source-Area VOC Transport in Ground Water

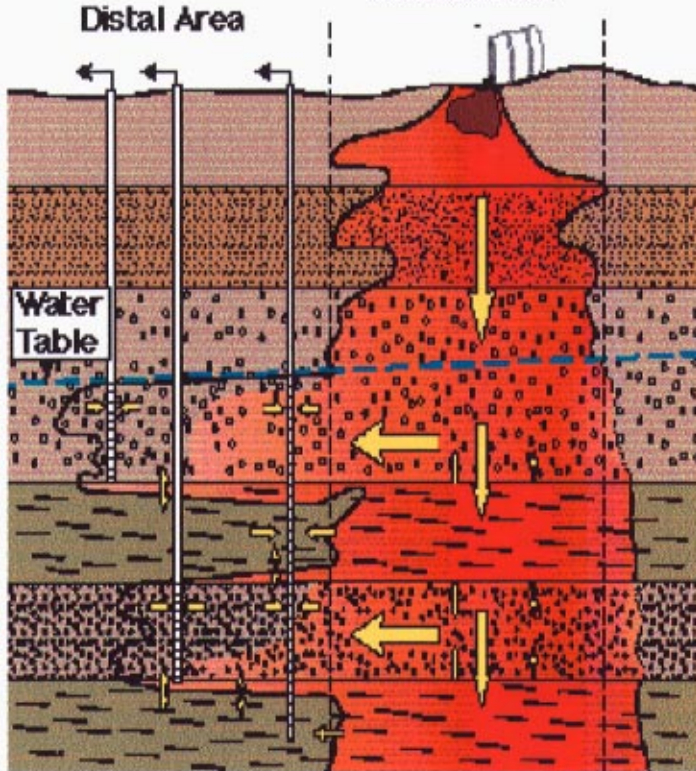
ABSTRACT

The purpose of this study is to develop a tool that will allow us to predict time to remediate volatile organic compounds (VOCs) in ground water. An adaptive-grid finite element model was created using PDEase software. Results indicate that convergence to analytical solutions, field data, and conceptual mass-transport models was successful. Contaminants in fine-grained zones were proved to be long-term sources that are difficult to remediate.

INTRODUCTION

The aquifers beneath the Lawrence Livermore National Laboratory (LLNL) have been contaminated by VOCs since World War II. Efficient cleanup of the resulting contaminant plume requires the ability to simulate VOC transport under potential remediation strategies. This report describes a computational modeling effort to achieve this simulation.

According to the conceptual model established by LLNL hydrogeologist Fred Hoffman (Hoffman, 1996), VOC plumes can be represented as two independent units: the source area and the distal plume. Source areas are characterized by high contaminant concentrations in zones of all hydraulic conductivities, while distal-plume contamination is largely found in high-hydraulic conductivity (HK) zones.



Although sufficient models exist for the simulation of distal-plume contaminant migration (CFEST, FEFLOW), modeling source-area contaminant transport poses unique challenges that will be the focus of this paper.

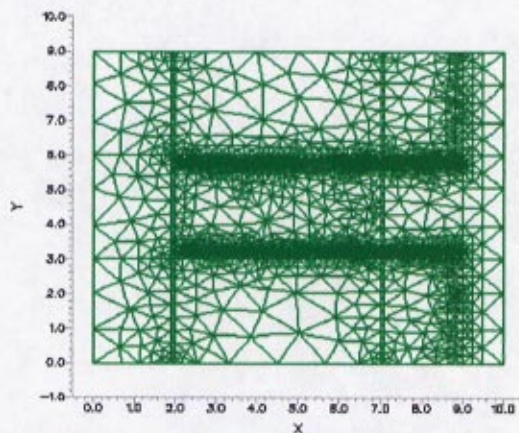
The specific goals of this modeling effort are:

- examination of contaminant transport across geologic boundaries: interfaces between areas of low (LK) and high hydraulic conductivity
- computational evaluation of the conceptual model outlined above
- solution of the advection-dispersion transport equation with sufficient detail as to allow analysis of all the parameters governing dispersion
- determination of the extent of the ability of LK zones to act as diffusive contaminant reservoirs during source-area pump-and-treat cleanup procedures.

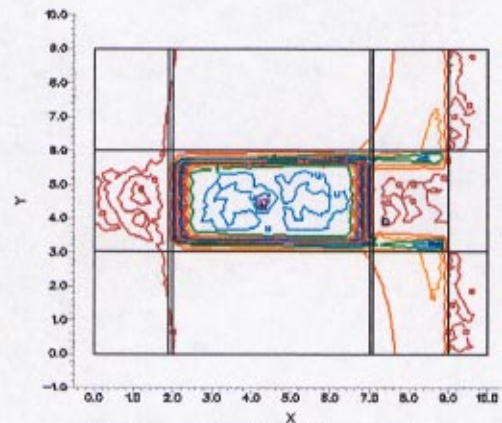
Description of Software Used

We used PDEase, adaptive-grid finite element analysis software, to find approximate numerical solutions to the partial differential equations (PDEs) governing VOC flow and transport. PDEase approximates these equations by discrete algebraic expressions at every node, using the Galerkin weighted-residual Finite Element Method (FEM).

This software is unique in that the nodal density of its solution grid automatically refines in areas of high gradient at every time step. This capability is critical, because realization of accuracy limits depends upon the presence of sufficient nodal density at every point in the domain. While this resolution is automatic in PDEase, it is difficult or impossible to obtain with standard fixed or moving-grid FEM techniques. This is because of the complexity of evolutionary source-area contaminant transport patterns.



**FEM PDE Discretization Grid
at time t**



**Concentration Isocontours
at time t**

PDEase uses allows us to select the order of the polynomial functions used to extrapolate its solution between nodes. Attempts to utilize order 1 functions led to the development of pockets of extremely high nodal density, resulting in consumption of large amounts of CPU. Order 2 functions were instead used throughout the modeling process.

PDEs Governing Contaminant Transport

14

Our model performs *decoupled* analysis of ground water flow and contaminant transport equations. This powerful approach gives us increased control over the final solution, as we can adjust and evaluate flow and transport parameters, boundary conditions, and equation form separately. Furthermore, this decoupling of the PDE system greatly speeds computation.

Ground water advection is assumed to follow Darcy's Law (Fetter, 1994):

$$v = \frac{k \cdot \nabla h}{\phi} \quad \text{where:} \quad (1)$$

v = ground water advection velocity

k = hydraulic conductivity

h = hydraulic head

ϕ = porous medium porosity.

PDEase determines spatially-dependent advection velocities from the solution of the PDE:

$$\nabla \cdot (k \cdot \nabla h) = 0. \quad (2)$$

Darcy's Law velocities outputted from the solution of (2) are imported as coefficients into the Advection-Dispersion Equation (ADE) (Cherry and Freeze, 1979):

$$R \frac{\partial C}{\partial t} = \nabla \cdot (-v \cdot C) + \nabla \cdot (D \cdot \nabla C) \quad \text{where:} \quad (3)$$

R = retardation factor

C = VOC concentration

D = hydrodynamic dispersivity

$D \cdot \nabla C$ = hydrodynamic dispersion.

Form of ADE

15

PDEase solution methodology is determined by the way the equations it solves are written. Explicit form implies direct differentiation; Gaussian (div, grad, curl) form implies integration by parts.

Numerical experimentation led to the discovery that writing first-order (advective) terms of the ADE in Gaussian form results in the development of a pocket of extremely high nodal density in the upper-right corner of the domain. This area appears when the HK advection front crosses the domain's half-way point.

Experimentation shows that explicit expression of the advective terms eliminates this problem:

$$R \frac{\partial C}{\partial t} = \frac{\partial v_x}{\partial x} \cdot C + \frac{\partial v_y}{\partial y} \cdot C + \nabla \cdot (D \cdot \nabla C). \quad (4)$$

Analysis of Hydrodynamic Dispersion

Hydrodynamic dispersion includes velocity-dependent (mechanical dispersion) and velocity-independent (molecular diffusion) terms. In order to construct D , a single second-order term incorporating both dispersion and diffusion, we define:

$$D = D_{mechanical} + D_{molecular} \quad \text{where:} \quad (5)$$

$D_{mechanical}$ = mechanical dispersivity

$D_{molecular}$ = molecular diffusivity.

Further, we define:

$$D_{mechanical} = \begin{bmatrix} D_{11} & D_{12} \\ D_{21} & D_{22} \end{bmatrix} \quad \text{where:} \quad (6)$$

$$D_{ij} = \alpha_T \bar{v} \delta_{ij} + (\alpha_L - \alpha_T) v_i v_j / \bar{v} \quad (7)$$

D_{ij} = mechanical dispersivity tensor

α_T = transverse mechanical dispersivity

α_L = longitudinal mechanical dispersivity

δ_{ij} = Delta Kronecker operator and:

$$D_{molecular} = D_w \cdot \Omega \quad \text{where:} \quad (8) \quad 16$$

$D_{molecular}$ = molecular diffusion scalar
 D_w = VOC diffusion coefficient in water
 Ω = porous medium tortuosity.

Inserting (6) and (8) into (5), we obtain:

$$D = \begin{bmatrix} D_{11} & D_{12} \\ D_{21} & D_{22} \end{bmatrix} \cdot \nabla C + D^* \cdot \nabla C. \quad (9)$$

Here, we multiply both the tensor $D_{mechanical}$ and the scalar $D_{molecular}$ by the vector ∇C . This "vectorizes" the terms into the same two-component (x, y) form, conditioning them for linear superposition.

Resolution of Geologic Interfaces

PDEase resolves the complex concentration gradients that characterize source areas by refining its solution grid. The local nodal density resulting from this process is roughly proportional to the magnitude of the local concentration gradient. When concentration gradient becomes near-infinite, then, so does nodal density. At this limit, the FEM scheme operates with undesirably small time-stepping, leading to a drastic reduction in computational speed.

Near-infinite gradients tend to form adjacent to sharp geologic boundaries, as VOCs are rapidly flushed out of HK zones, leaving contaminants in relatively stagnant LK zones "stuck" behind. We realized that the existence of a "buffer zone" through which hydraulic conductivity is graduated (from LK to HK levels) would serve to selectively retain contaminants. This retention "smoothes" concentration gradients at HK / LK interfaces.

We use the Super Gaussian function to accomplish this smoothing: 17

$$k(y) = k_h - (k_h - k_l) \cdot e^{-\left(\frac{y-y_0}{\mathcal{E}}\right)^{nn}} \quad \text{where:} \quad (10)$$

k_h = HK Hydraulic conductivity

k_l = LK Hydraulic conductivity

y_0 = midpoint of LK region

\mathcal{E} = width of LK region

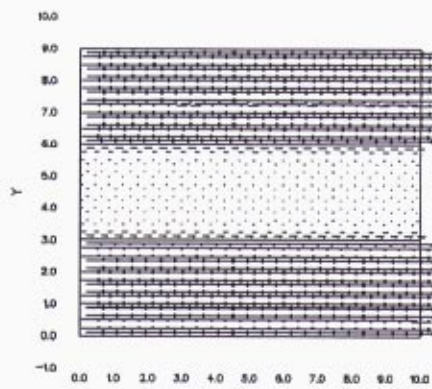
nn = Super Gaussian exponent (determines slope of curve).

Conductivity gradation is reflected in advective rates through Darcy's Law.

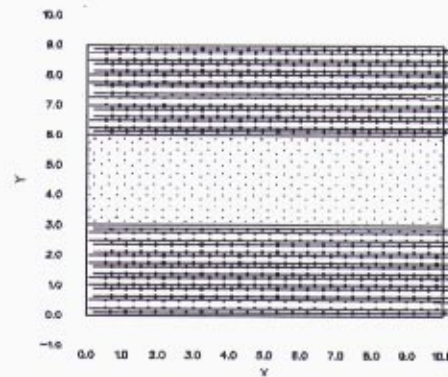
Introduction of Interfacial Texture Parameter

Although our motivation for the incorporation of the Super Gaussian function was to eliminate extreme concentration gradients, we found that the smoothing function also introduced a new modeling parameter: interfacial texture.

Different values of nn result in different degrees of interfacial smoothing, ranging from very sharp to very gradual. A sharp boundary, such as that represented below by $nn = 40$, is characterized by the little or no interfacial mixing between bordering subsurface layers. An example is a coarse gravel bed lying directly on top of clay sediments. On the other hand, a gradual boundary, such as that represented by $nn = 8$, results from smooth transition between or blending of HK and LK materials. Representative examples include a clay / sand / gravel transition and an interfacial-zone mixing of the above materials.

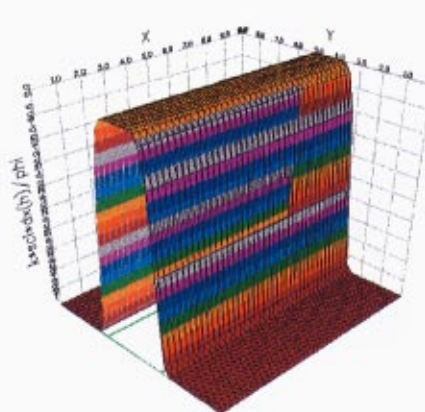


nn = 8

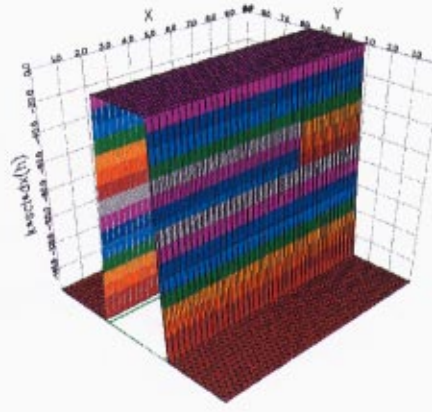


nn = 40

velocity vector field



nn = 8



nn = 40

velocity surface plot

The ability to adjust interfacial smoothing is important in accurately modeling geologic boundaries. Our model can represent the wide variety of different interfaces that exist in the subsurface.

Definition of Model Domain

We constructed a domain, or solution space, to simulate typical source-area conditions. It is a vertical cross section 9 meters in the y-direction by 300 meters in the x-direction. We define subsurface parameters of hydraulic conductivity, tortuosity, porosity, and retardation factor according to the hydrostratigraphic unit (HSU) approach: in "layer cake" regions. To allow for examination of contaminant transport across geologic interfaces, our domain consists of three horizontal layers: a LK zone sandwiched between two HK channels.

The FEM scheme operates on a scaled domain of 9 units in the y direction by 30 units in the x-direction, an approximately 1 to 3 object ratio. This scaling of the domain is necessary for two reasons: (1) to provide the adaptive-grid finite element solver with an object ratio which it can process, and (2) to allow for the desired vertical grid resolution (nodal density). The validity of resulting matrix transformations can be verified through symbolic computation.

Because the ADE is a parabolic PDE (containing first derivatives with respect to time but second-order spacial derivatives), it is a boundary value problem. Solution of this class of problem requires specification of conditions describing the variable being solved for on the edges of the solution space.

We define zero Neumann, or no flux, boundary conditions along the domain's top and bottom edges:

$$\nabla \cdot (n \cdot \nabla C) = 0 \quad \text{where:} \quad (11)$$

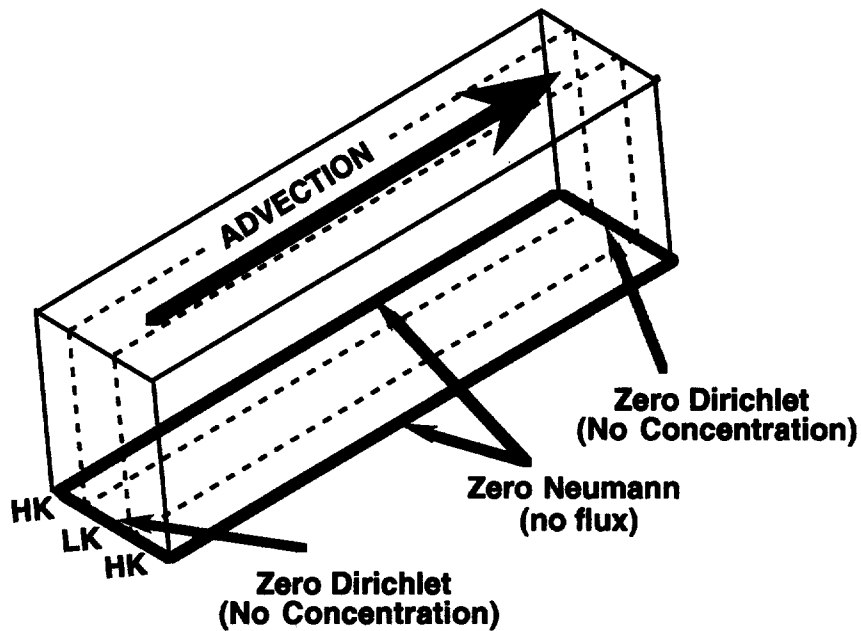
n = unit vector normal to boundary.

These Neumann conditions imply that there is no outflow of contaminants through the outer edges of the HK zones.

We pose Zero Dirichlet, or no concentration, conditions on the left and right edges of the domain:

$$C = 0. \quad (12)$$

A concentration of zero on the left simulates the inflow of clean ground water to flush and remediate the source area. The right-most Dirichlet condition represents the complete capture of contaminated ground water by the pumping zone.



Source-Area Domain

RESULTS

Analytical Verification of Model

After the governing equations and solution methodology were defined, we verified that our model was mathematically accurate.

We performed the coordinate transformation:

$$\mathfrak{X} - v\mathfrak{T} = x, \quad (13)$$

$$\mathfrak{T} = t \quad (14)$$

on the analytical solution of the 1-D diffusion equation:

$$R \cdot \frac{\partial C}{\partial t} = D \cdot \frac{\partial^2 C}{\partial x^2}, \quad (15)$$

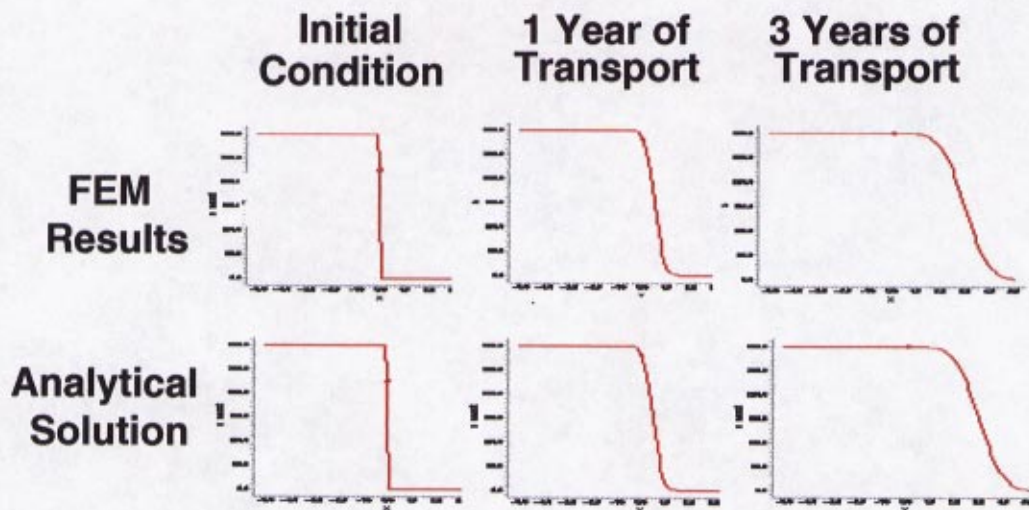
$$\text{solution: } C_{\text{exact}} = C_0 \cdot \text{ERFC}\left(\frac{x}{2\sqrt{Dt/R}}\right).$$

This gives an analytic, or mathematically exact, solution the one-dimensional (1-D) ADE: 21

$$R \cdot \frac{\partial C}{\partial t} = -v \cdot C + D \cdot \frac{\partial^2 C}{\partial x^2}. \quad (16)$$

$$\text{solution: } C_{\text{exact}} = C_0 \cdot \text{ERFC}\left(\frac{x - vt / R}{2\sqrt{Dt/R}}\right). \quad (17)$$

Results from FEM analysis of the 1-D ADE match the analytic solution within the adjustable error limit of the FEM scheme. Below, we show the solutions converging precisely at the practical error limit of one part in ten-thousand.

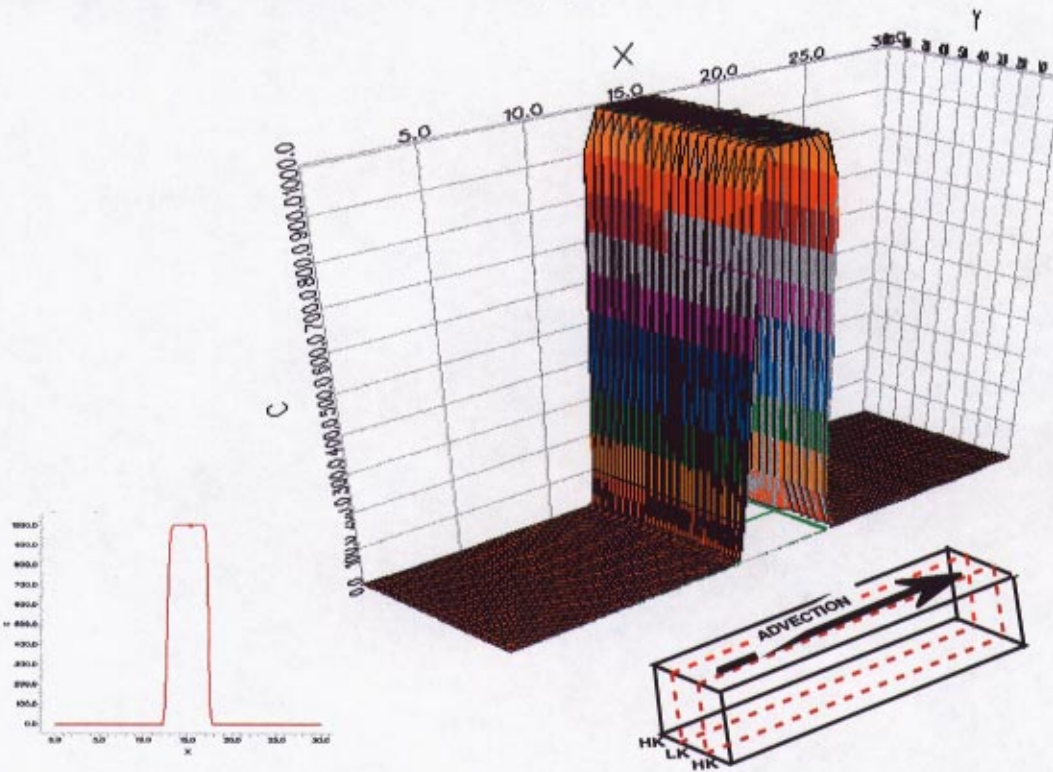


This mathematical verification encouraged us to increase the complexity and dimensionality of our domain to a level at which no analytical solution exists: a 2-D source-area.

Source-Area Modeling Results

In addition to well-posed boundary conditions, transient (time-dependent) parabolic PDEs require definition of an initial condition. Our model's initial condition is a 50 meter wide plug of contaminant in the center of the domain. This plug has a concentration of 1000 parts per billion (ppb) and stretches through both LK and HK zones. These conditions simulate those near the LLNL Treatment Facility A (TFA).

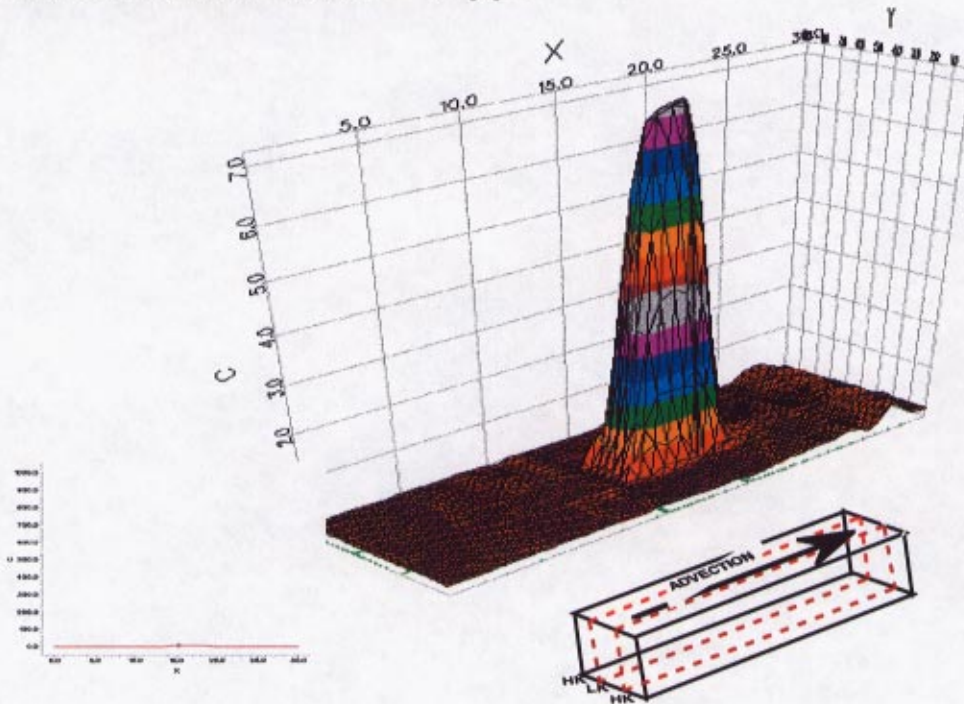
Time = start
Concentration Scale = 1000 ppb



Clean ground water is advected through the model under a head gradient of .05, similar to that near the largest pumping wells in the TFA area. After three months of this pumping, we see contaminants in HK zones being flushed toward the right boundary of the domain, while VOCs in relatively stagnant LK regions are left behind.

After eighty years of this pump-and-treat remediation, maximum concentration levels (MCLs) of 5 ppb are finally approached in the LK zone.

Time = 80 years
Concentration Scale = 7 ppb



Why has the cleanup of the fine-grained region taken so long? The answer can be found in the ADE. Of the three transport mechanisms, only molecular diffusion is independent of local ground water velocity: only this process can occur in the stagnant LK zones. Molecular diffusion is driven by random (Brownian) motion of molecules in solution. Because of the tiny scale of the forces involved, this mechanism is orders of magnitude slower than advection or dispersion.

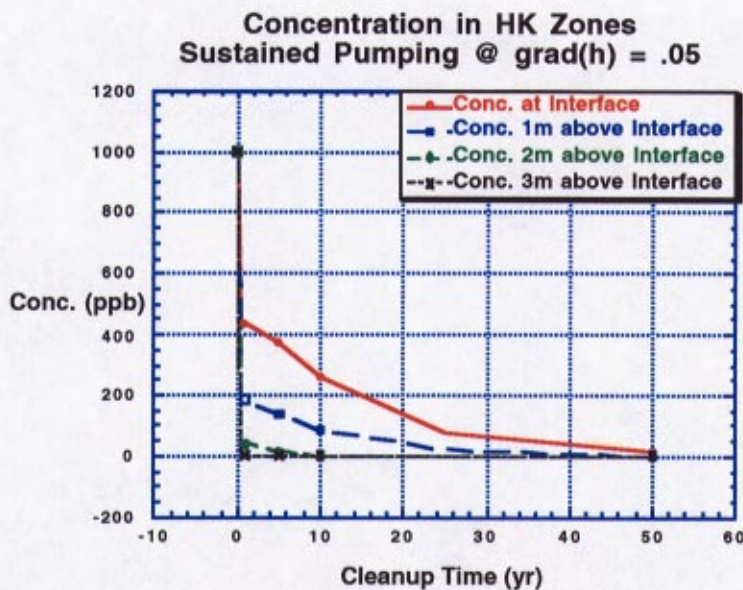
Comparison of Conceptual and Computational Models

Our model predicts that source-area contaminant transport follows the conceptual model outlined in the introduction: VOCs in HK zones are spread to the distal plume, while source areas retain LK contaminants.

Contaminant Concentration in HK Zones

Ecological impact downgradient of source areas is determined by contaminant concentrations in the source-area aquifers (HK regions). These regions seem easy to remediate using the pump-and-treat strategy modeled above.

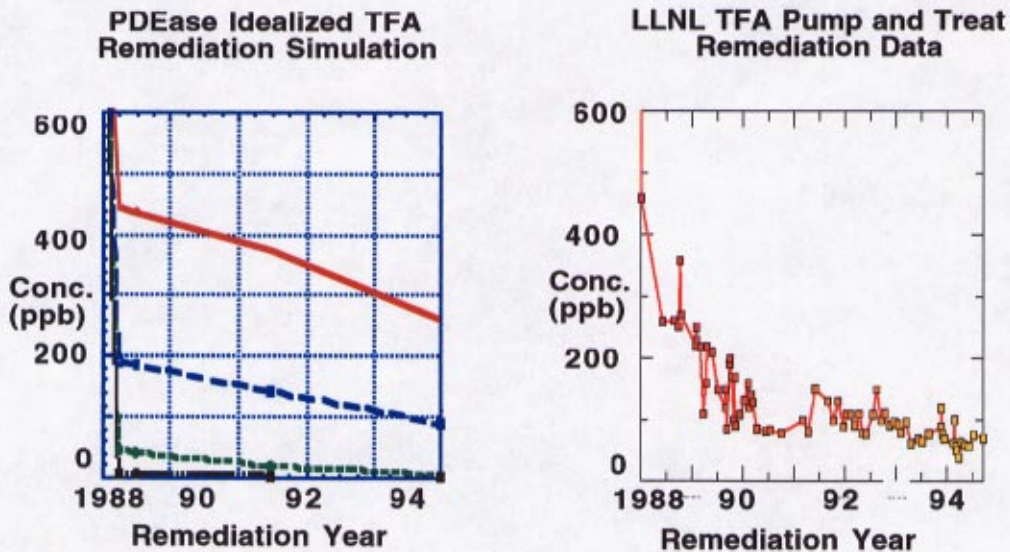
We showed above that LK zones slowly diffuse VOCs into these aquifers. To determine whether LK zones serve as a significant contaminant source to these aquifers, we plotted the HK concentrations predicted by our model over 50 years of cleanup.



The significant concentrations present in the HK zones indicate that LK concentrations do serve as significant sources to mobile ground water. This fact is of essential importance to those designing source-area remediation strategies.

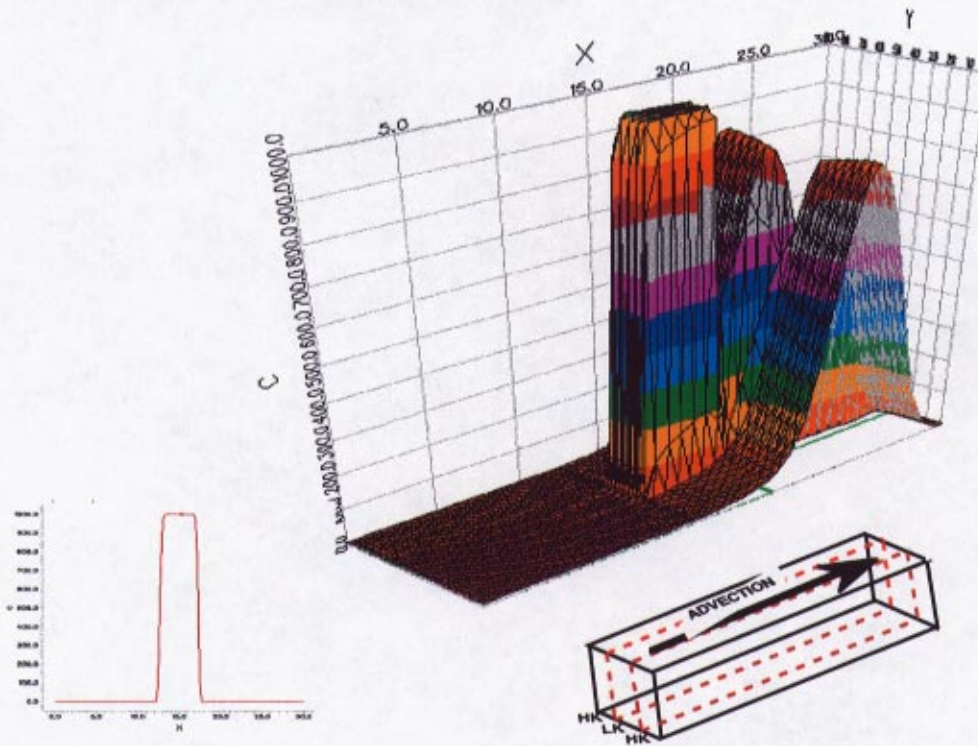
Comparison with Field Data

In plotting HK concentrations during source-area remediation, we created a powerful method for the validation of our model against real-world conditions. Since 1988, the LLNL Environmental Restoration Division (ERD) has been engaged in the pump-and-treat cleanup of the TFA area. The ERD has continually logged the concentration of the contaminated ground water being pumped out of TFA's main downgradient extraction well. VOCs in effluent extracted at this well represent average concentration in source-area HK zones. We plotted field data from TFA against our model's prediction.



The convergence of the concentration trends predicted by the model to those actually observed in the field is compelling evidence that our model accurately simulates source-area conditions.

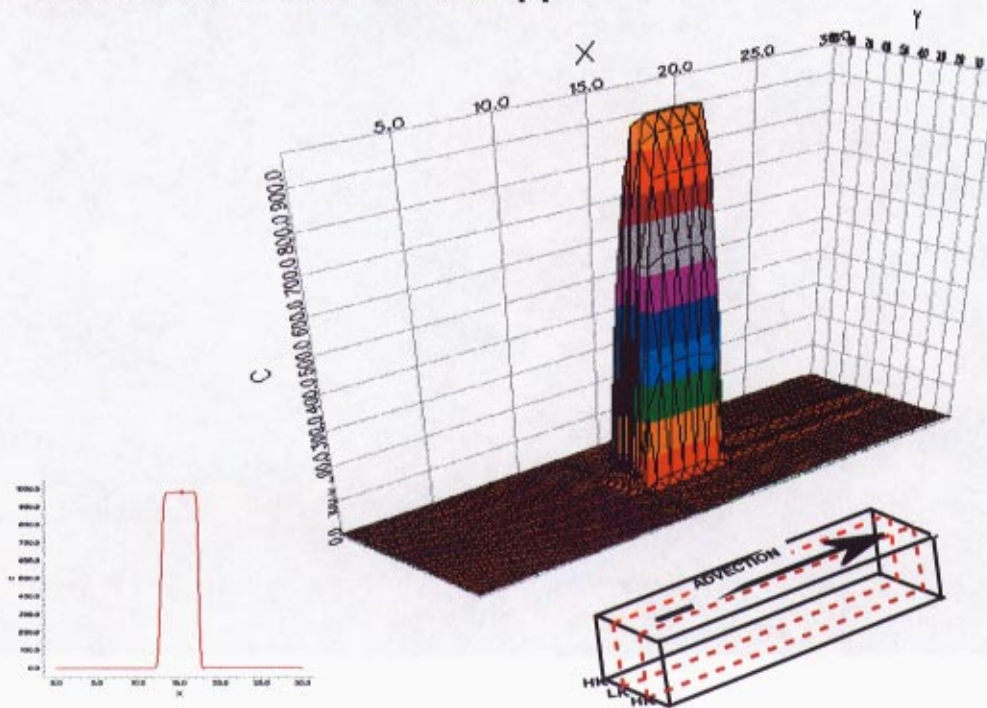
Concentration Scale = 1000 ppb



Three years of pumping later, the "wave" of contaminant advecting through the HK zones has been completely pumped out of the source area. However, LK VOCs remain at near-initial concentrations.

Time = 3 years

Concentration Scale = 950 ppb



We have shown that our FEM model successfully simulates VOC transport in ground water. We began with an examination of Darcy's Law and the ADE, the two equations governing subsurface contaminant migration. Then, we investigated two distinguishing modeling techniques, adaptive-gridding and the Super Gaussian interfacial smoothing function. Following a discussion of the model's domain, we examined the results of a simulation of source-area cleanup. Finally, we examined the implications of these results in terms of downgradient ecological impact and compared these predictions with conceptual expectations and field data.

AREAS OF CONTINUING RESEARCH

- Incorporation of further geometric and geologic complexity and continued study in model parameterization to more accurately simulate flow and transport in the subsurface.
- Examination of the effect of various scales and classes of interfacial geometrical complexity on interfacial contaminant transport to improve ability to model geologic boundaries.

SOURCES

Cherry, John A., and Freeze, R. Allan. Groundwater. Prentice-Hall, Inc., New York, 1979, pp. 549-552.

Fetter, C. W. Applied Hydrogeology. Prentice-Hall, Inc., New York, 1994, p. 143.

Hoffman, Fredric. "A New Conceptual Model and Remediation Strategy of VOCs in Low Organic Carbon Unconsolidated Sediments." Submitted to *Ground Water*, September, 1996, Preprint UCRL-JC-125199, Lawrence Livermore National Laboratory, Livermore, California.

Acknowledgments

28

Fred Hoffman oversaw this modeling effort. LLNL scientists Said Doss, Kari Fox, and Bob Gelinas provided essential leadership and direction during the model's construction and evaluation.

Special thanks to Kim Heyward for graphics support, and to Fred Bancalari and Kirk Fitzgerald for UNIX assistance.

3D Imaging of Bacterial Processes in Subsurface Environments: Selection of Bacteria

Michael A. Davis

Mississippi State University

Lawrence Livermore National Laboratory

Livermore, California 94550

December 18, 1996

Prepared in partial fulfillment of the requirements of the Science and Engineering Research Semester under the direction of Mehdi Rashidi Ph.D., Research Mentor, in the Lawrence Livermore National Laboratory.

*This research was supported in part by an appointment to the U.S. Department of Energy Science and Engineering Research Semester (hereinafter called SERS) program administered by LLNL under Contract W-7405-Eng-48 with Lawrence Livermore National Laboratory.

Abstract

For bioremedial purposes, we wish to study bacterial transport in subsurface environments ; however, we must first select a bacterium that can (1) survive in and (2) function normally in the porous medium and refractive index-matched solution of our imaging system. We grew bacteria in a solution similar to the aqueous phase of our system, and counted cells at various time points. We then analyzed the resultant plots to confirm that three of the four test strains could not only survive but could prosper in our imaging system. Once the surviving bacterial strains are fluorescently labeled, we will tally the data to determine the most suitable strain for our system.

Introduction

Our goal is to quantitatively investigate the microscale processes that govern bacterial transport within subsurface environments, and provide the basis for improved modeling of transport and contaminant treatment in natural porous systems. To do so, we shall be implementing a non-intrusive fluorescence imaging system. The system will consist of a rectangular column packed with lithium fluoride crystals and an aqueous refractive index-matched solution. Through the column will flow fluoresced bacteria that are illuminated by a scanning, planar laser beam and digitally captured by a CCD camera. Once captured, the images will be stored and processed via VCR and computer. However, before bacterial transport can be studied, a bacterium capable of surviving in and functioning normally in the refractive index-matched solution must be identified.

In order to match the refractive index of the solution to that of the lithium fluoride, large amounts of sucrose were added. Due to the high osmotic pressure and low water availability, few organisms are expected to function in such an extreme environment (Atlas 358). Therefore, to increase the likelihood of near-normal functionality, we decided to add a small amount of yeast extract, which contains trace elements, amino acids, and other molecules required for normal metabolic functions. With a solution more capable of sustaining life, we began testing for survivability in our refractive index-matched solution.

Methods and Materials

A. Equipment

1. Shimadzu UV-VIS Recording Spectrophotometer UV-160A
2. Beckman Avanti J-25 High Performance Centrifuge
3. Beckman J-Lite JLA-10.500 Fixed Angle Rotor
4. VWR Scientific Incubator; Model #: 1545
5. New Brunswick Scientific Co., Inc. Incubator Shaker; Model #: G-25
6. The Baker Company Laminar Flow Hood Class II Type B1; Model #: NCB-C6

B. Materials

1. *Pseudomonas fluorescens* NC1MB 11764
2. *Pseudomonas putida* ATCC 12633
3. *Pseudomonas putida* F1 Gibson
4. *Alcaligenes xylooxidans* ATCC 11764
5. Bacto Nutrient Agar (dehydrated)
6. Bacto Nutrient Broth (dehydrated)
7. Bacto Yeast Extract ("DIFCO" Certified)
8. EM Science Sucrose GR

C. Procedures

In order to measure cells/ml solution, we spread cells sampled from each culture onto nutrient agar plates and allowed them to grow at 26°C. Since each cell will form a single colony, colonies are counted and used to determine cells/ml solution. However, if the cell density is too high, then one colony can not be

distinguished from another and measurements are inaccurate. Therefore, each sample is diluted so that cell numbers may be accurately counted.

Addition of cells to sucrose/yeast extract solution

Isolated colonies of desired bacteria are first grown on nutrient agar plates. Cells from an isolated colony are used to aseptically inoculate 10 ml nutrient broth. The suspension is then incubated in a shaker incubator at 26°C and at 200 RPM for up to 24 hours. After the allotted time, one ml of the homogenized suspension is aseptically combined to 49 ml of fresh nutrient broth. This preculture is then allowed to incubate at 26°C and at 200 RPM until the absorbance at 600 nm falls between 0.5 and 1.0 (cells are in the log phase and assumed to be healthy).

Once the absorbance has reached the appropriate level, the cells can be washed of the nutrient broth by centrifugation. Cells are spun at 8000 RPM for 15 min, the supernatant is removed, and the cells are resuspended in 10 ml sucrose/yeast extract solution. They are again spun and decanted, but the cells are now resuspended with 20 ml sucrose/yeast extract solution. Finally, the culture is incubated at 26°C and at 200 RPM and 1 ml samples are taken at various time points.

Ten-fold Serial Dilutions

Five eppendorf microfuge tubes are labeled A, B, C, D, and E. One ml of homogenized (shaken or vortexed) solution is placed into tube A. Tube A is vortexed, and 0.01 ml suspension from tube A is added to 0.99 nutrient broth in tube B. Tube B is vortexed, and 0.1 ml of the suspension in Tube B is added to 0.9 ml nutrient broth in Tube C. Tube C is vortexed, and 0.1 ml of the suspension in Tube C is added to 0.9 ml nutrient broth in Tube D. Tube D is vortexed, and 0.1 ml of the suspension in Tube D is added to 0.9 ml nutrient broth in Tube E. If further dilutions are necessary, then the preceding trend can be continued.

Quantification of population density

For Tubes C, D, and E, 0.1 ml suspension is spread onto each of two prepared agar plates, providing final dilutions of 10^{-4} , 10^{-5} , and 10^{-6} respectively. The plates are incubated at 26°C until colonies can be easily counted--for statistical accuracy, a plate is counted if it contains between 3 and 300 colonies. Since each colony arises from a single cell, cells/ml solution is determined by multiplying the number of colonies by the reciprocal of the dilution.

D. Precautions

When possible, procedures were carried out under aseptic conditions to prevent the contamination of pure cultures and the inaccuracy of collected data.

Results

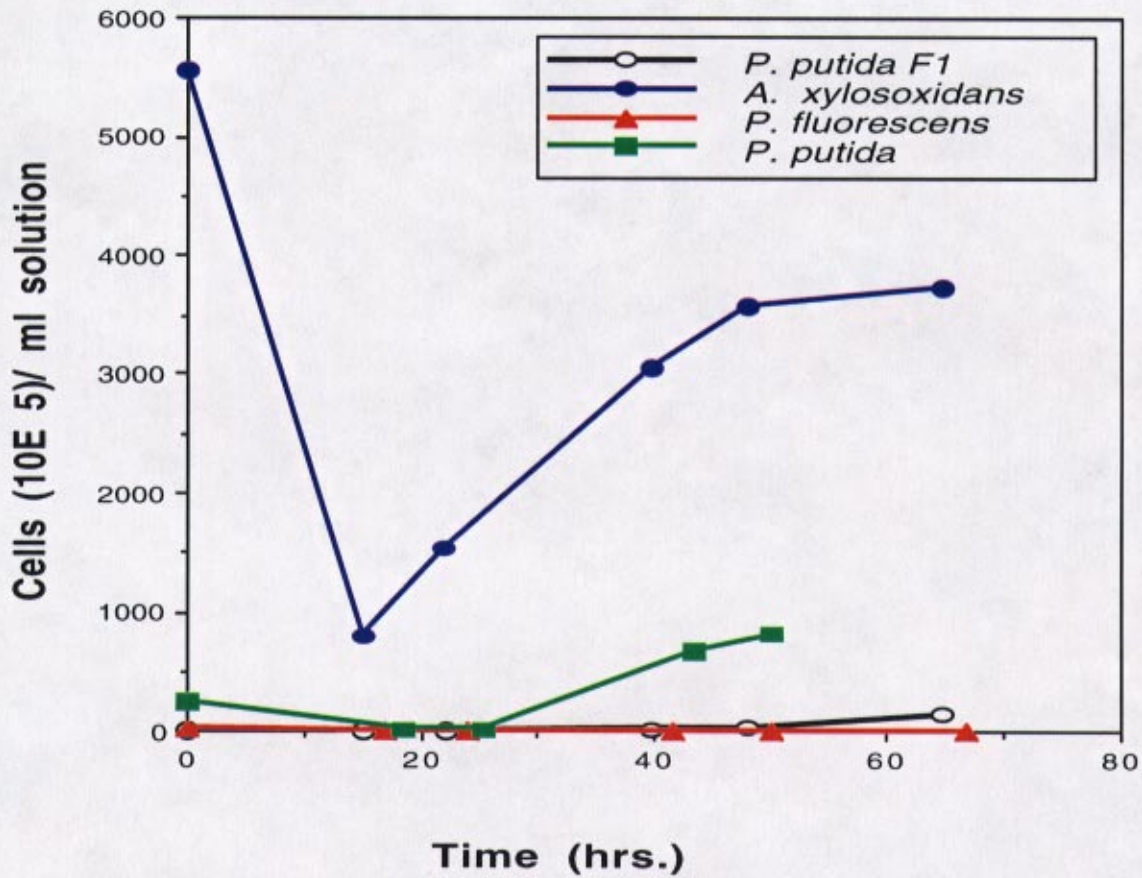


Figure 1: Bacteria Grown in Refractive Index-Matched Solution

Bacteria were grown in refractive index-matched solution and cells counts were calculated for various time intervals. As shown in the graph, three of the strains grew in the solution.

Discussion/ Conclusions

From results presented, we know of three bacterial strains that will grow in our refractive index-matched solution. However, their ability to grow does not assure their use in our system. Neither does *A. xylooxidans*'s superior growth rate in our solution give it precedence over *P. putida* and *P. putida* F1.

First of all, the strains must be labeled with a fluorescent molecule that allows near normal function and growth. We are currently investigating molecules that are cleaved within the bacterium and activated. Once activated, the fluorescent molecule will bind (depending on the molecule) to phospholipids (in membranes), primary amines (such as lycein residues), or thiol groups. However, the concentration must be such that cell function is uncompromised while fluorescent emission is maximized.

Secondly, as each labeled bacterium divides, any fluorescent molecule contained within the parent bacterium will be divided among the two daughter cells. Although the system's overall fluorescent intensity should remain the same, each division reduces a cell's fluorescence by half. Therefore as time progresses, cells will become increasingly difficult to image, and results may be skewed.

For reasons mentioned, it may be necessary to decrease the doubling time (time required for a doubling of population size) of strains tested or to use a bacterium whose doubling time is already low. Once cells are sufficiently labeled, all data produced (on growth and labeling) will be compared in determining a suitable bacterium for our study of bacterial transport in subsurface porous systems.

References

Atlas, Ronald M. Principles of Microbiology. Mosby 1995.

D.T. Gibson, J.R. Kock, R.E. Kallio. "Oxidative Degredation of Aromatic Hydrocarbons by Microorganisms: I. Enymatic Formation of Catechol from Benzene." Biochem. 1968, Vol 7. 2653-2662.

Aknowledgements

Mehdi Rashidi allowed me to work on this project.

Joanne Horn taught me the necessary techniques.

Eric Dickenson and Jamshid Dehmeshki provided technical assistance.

**Progress in the Synthesis of a
Photoactivatable, Reversible Linker***

Jolene T. Downs

The Ohio State University

Lawrence Livermore National Laboratory
Livermore, California 94550

December 18, 1996

Prepared in partial fulfillment of the requirements of the Science and Engineering Research Semester under the direction of Kenneth T. Bogen, Research Mentor, in the Lawrence Livermore National Laboratory.

*This research was supported in part by an appointment to the U.S. Department of Energy Science and Engineering Research Semester (hereinafter called SERS) program administered by LLNL under **Contract W-7405-Eng-48 with Lawrence Livermore National Laboratory.**

Progress in the Synthesis of a Photoactivatable, Reversible Linker

Jolene T. Downs

Abstract

The objective of this study is the synthesis of a photoactivatable molecule that will reversibly link biotin to biological macromolecules. Isolation of the macromolecules can then be achieved through biotin-avidin affinity chromatography. The synthesis plan has five steps, and results from completion of the first three steps are presented.

The product from the Step-1 condensation of a lactone and a triamine was coupled with a photoactive species in Step 2 to yield the photoactivatable segment of the linker. The condensation of biotin and tetraethylene glycol in Step 3 provided the linker segment useful for biotin-avidin affinity chromatography.

The products have been characterized by infrared spectroscopy and mass spectrometry, showing that desired products were obtained and that light conditions for the Step-2 reaction were adequate to protect the photoactive product.

In Step 4 the biotin segment will be attached to a silane, followed by attachment of the photoactivatable segment to the silane in Step 5. It is anticipated that these reactions will be straightforward once suitable conditions are determined for avoiding di-substitution on the silane in Step 4.

Table of Contents

	Page
List of Figures	iv
Introduction	1
Experimental	2
Materials	2
Methods	2
Results	3
Discussion	4
Conclusions	6
Acknowledgments	7
References	7

List of Figures

	Page
Figure 1. Proposed reaction scheme for the linker	2a
Figure 2. A spacefilling model of the proposed linker	2c
Figure 3. The linker shown in the first step of two-step affinity chromatography	2d
Figure 4. The FT-IR and mass spectra of the Step-1 amide product	3a
Figure 5. The FT-IR and mass spectra of the photoactivatable segment	4a
Figure 6. UV/Visible absorption spectra showing wavelength range for photoactivation	4b
Figure 7. The FT-IR spectrum of the Step-3 ester product	4c
Figure 8. The mass spectrum of the Step-3 ester product	4d

Introduction

In the study of biological macromolecules, a means for selectively isolating molecules is often required. One method of isolation uses biotin-avidin affinity chromatography, in which selected macromolecules have been labeled with biotin, and avidin has been attached to a solid support. The strong binding of avidin and biotin ensures selective isolation.

A common means of attaching biotin to macromolecules is with a linker molecule. The linker may have biotin at one end and a species such as an antibody or substrate at the other end for selecting a specific biological molecule. The linker is first attached to a macromolecule and then allowed to attach to avidin on a solid support.

The conditions required for detaching most available linkers from the solid support can damage sensitive macromolecules; therefore, linkers have been proposed which can cleave under mild aqueous conditions. The process of selecting biomolecules by attachment to a solid support and then cleaving a linker under mild conditions is referred to as "two-step affinity chromatography."¹

In this study, a linker molecule is sought which can be used in two-step affinity chromatography and which will be selective toward specific target molecules. The desired properties of the linker are:

- ❑ attaches readily to a specific biological macromolecule
- ❑ has adequate length so as not to interfere with biotin-avidin binding
- ❑ suitable for use with targets containing proteins sensitive to thiol denaturation
- ❑ cleaves under mild aqueous conditions

A five-step plan has been proposed for the synthesis of the linker, as shown in Figure 1 on the following pages. Figure 2 shows a space-filling model of the proposed linker, and Figure 3 gives an illustration of the linker as it could be used in two-step affinity chromatography for the isolation of selected biomolecules.

Methods used in the first three synthesis steps will be described. In addition, results from these steps will be discussed and recommendations for future work will be given.

Experimental

Materials

Anhydrous *N,N*-dimethylformamide (DMF), γ -butyrolactone, 3,3'-diamino-*N*-methyldipropylamine, and 1-cyclohexyl-3-(2-morpholinoethyl)carbodiimide metho-*p*-toluenesulfonate (CMDI) were purchased from Aldrich. Triethylamine, d-biotin, tetraethylene glycol, and 4-dimethylaminopyridine (DMAP) were purchased from Sigma Chemical Co. Absolute ethyl alcohol was purchased from Aaper Alcohol and Chemical Co., and 4-fluoro-3-nitrophenyl azide was purchased from Fluka. All chemicals were used without further purification.

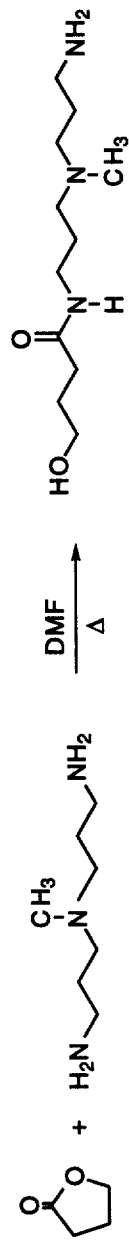
Methods

Step 1. First γ -butyrolactone (1.69 g; 20 mmol) was dissolved in 20 mL DMF and added to a 250 mL round-bottom flask. The dipropylamine (5.71 g; 39 mmol) was dissolved in 20 mL DMF and added to the flask with stirring. The solvent was brought to a total of 120 mL and the solution was heated to about 55 °C and left stirring overnight. After 23 hours the solvent was removed under vacuum, leaving a colorless oil.

The product was distilled under vacuum using a short-path apparatus. The second fraction yielded a yellowish oil (1.68 g; 37.1% yield), which was analyzed using Fourier transform-infrared spectroscopy (FT-IR) and mass spectrometry (MS).

Figure 1. Proposed reaction scheme for the linker

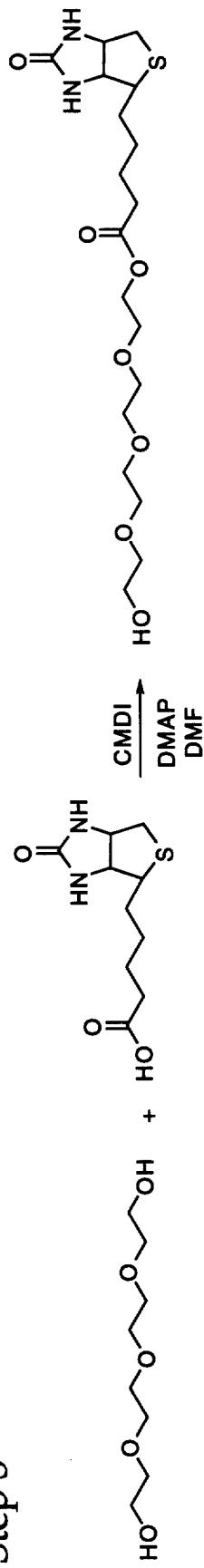
Step 1



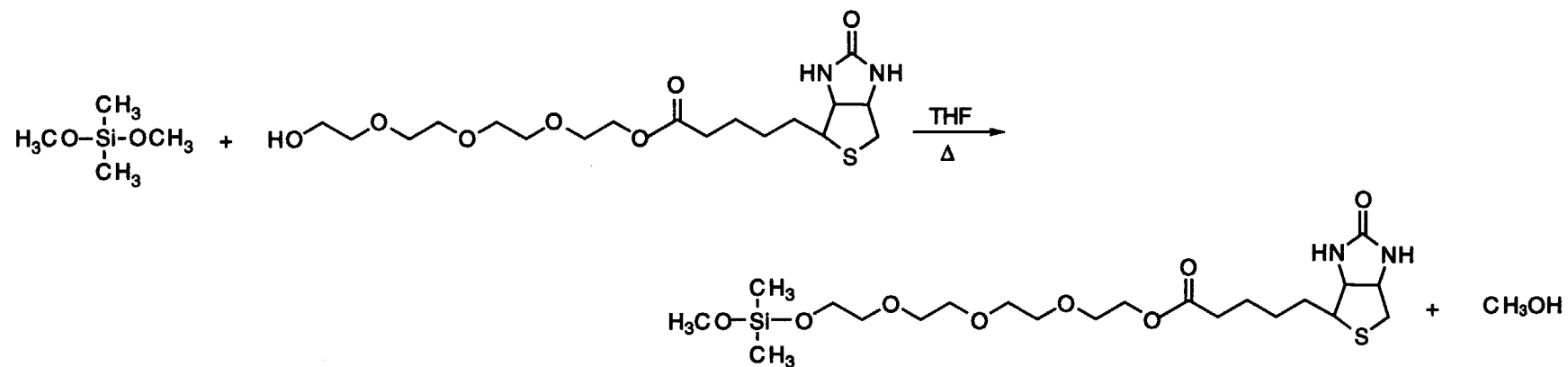
Step 2



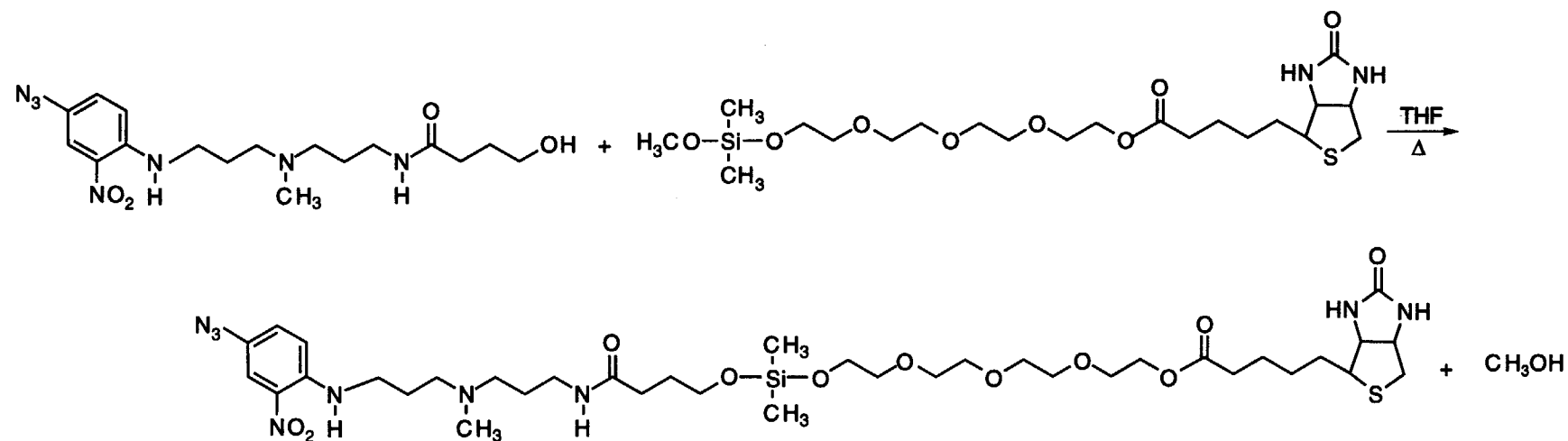
Step 3



Step 4



Step 5



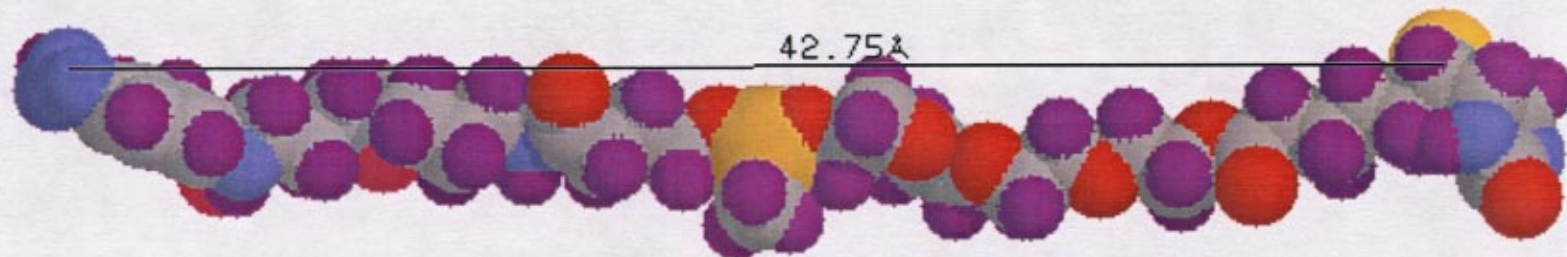


Figure 2. A spacefilling model of the proposed linker, showing the approximate length of the molecule.



Figure 3. The linker shown in the first step of two-step affinity chromatography, with a myoglobin molecule attached to the photoactivatable end (left) and the biotin end bound to the protein avidin (right). The avidin molecule is attached to a solid support (not shown). The second step involves cleavage of the linker on either side of the central silicon atom in order to release the myoglobin for study.

Step 2.² The reaction was carried out with the fluorescent lights off in the hood. The Step-1 product (0.112 g; 0.49 mmol) was weighed into a 50 mL round-bottom flask and dissolved in 5 mL absolute ethanol. Triethylamine (0.105 g; 1.04 mmol) was dissolved in 5 mL ethanol and added to the flask with stirring. Next 4-fluoro-3-nitrophenyl azide (0.079 g; 0.43 mmol) was dissolved in 5 mL ethanol and added. The solution was stirred at room temperature.

The progress of the reaction was followed using thin-layer chromatography. Silica plates were developed in 50:50 ethyl acetate/methanol and visualized with iodine crystals and short-wave ultraviolet light. After 29 hours a significant amount of azide starting material remained, so the reaction was allowed to stir over a weekend, for approximately 96 hours total. The solvent was removed under vacuum, leaving a red-orange oil.

The product was purified with thin-layer chromatography on 20 cm x 20 cm alumina plates, using 95:5 ethyl acetate/methanol. The band at R_f 0.29 was collected (0.060 g; 35.0% yield) and analyzed using FT-IR and MS.

Step 3.³ Biotin (0.255 g; 1.04 mmol) was weighed into a 100 mL round-bottom flask and dissolved in 50 mL anhydrous DMF. Tetraethylene glycol (0.54 mL; 3.13 mmol), CMDI (0.498 g; 1.18 mmol), and DMAP (0.016 g; 0.13 mmol) were added with stirring. The flask was flushed with nitrogen gas and placed under positive nitrogen pressure. The solution was stirred at room temperature for 66 hours, after which the solvent was removed under vacuum, leaving a colorless oil.

An attempt was made at purification using a silica column. However, the yield of product eluted from the column was so small that it was not measured. The product was analyzed using FT-IR and MS.

Results

Figure 4 shows the infrared and mass spectra for the Step-1 amide product. Of note on the FT-IR spectrum are the amide carbonyl peak at 1637 cm^{-1} and the broad

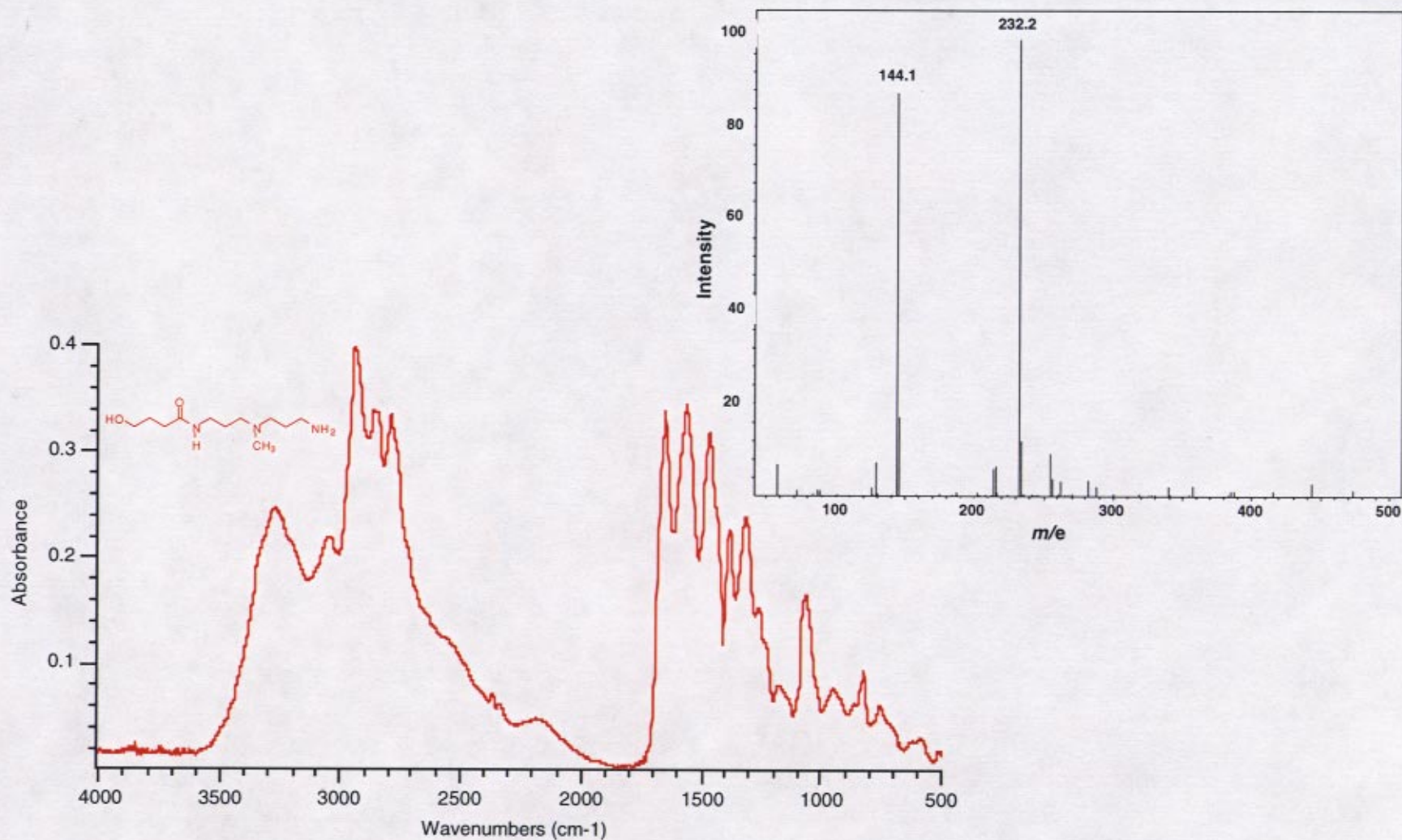


Figure 4. The FT-IR and mass spectra of the Step-1 amide product. The FT-IR spectrum shows the amide carbonyl peak at 1637 cm⁻¹ and the broad O-H band at 3300 cm⁻¹. The protonated molecular ion peak is shown at 232.2 on the mass spectrum.

O-H peak at 3300 cm^{-1} . The mass spectrum shows the protonated molecular ion peak at 232.2, while the peak at 144.1 corresponds to the amine fragment of the molecule.

The infrared and mass spectra for the photoactive Step-2 product are given in Figure 5. The FT-IR spectrum shows a nitro peak at 1525 cm^{-1} , amide carbonyl peak at 1637 cm^{-1} , and O-H peak at 3300 cm^{-1} . In addition, the intense azide peak at 2121 cm^{-1} indicates that the product retains its photoactive capabilities. The mass spectrum shows the protonated molecular ion peak at 394.2.

The UV/Visible absorption spectra shown in Figure 6 indicate the wavelength range for photoactivation of the linker molecule. The spectrum on the left corresponds to the azide starting material, with maximum absorbance in the ultraviolet range. The spectrum on the right corresponds to the product, showing maximum absorbance in the ultraviolet range at about 265 nm as well as an absorbance in the visible range centered at 470 nm which gives the molecule its deep orange color.

Figure 7 gives the FT-IR spectrum of the Step-3 ester product, showing a C-O peak at 1100 cm^{-1} , the ester carbonyl peak at about 1700 cm^{-1} , and the O-H peak at 3350 cm^{-1} . In the Figure 8 mass spectrum, the molecular ion peak includes one atom of sodium as illustrated by the structure drawing. The crown ether may have formed due to sodium atoms in the buffer solution associated with liquid chromatography injection.

Discussion

Yields from all reaction steps were quite low. Difficulties were encountered in trying to purify the products from Steps 1 and 3. A change of reaction conditions was tried for Step 2, with the yield increasing only slightly.

The Step-1 product was found to be very water soluble, as was the starting dipropylamine. Therefore, separation of amines using controlled-pH extraction was

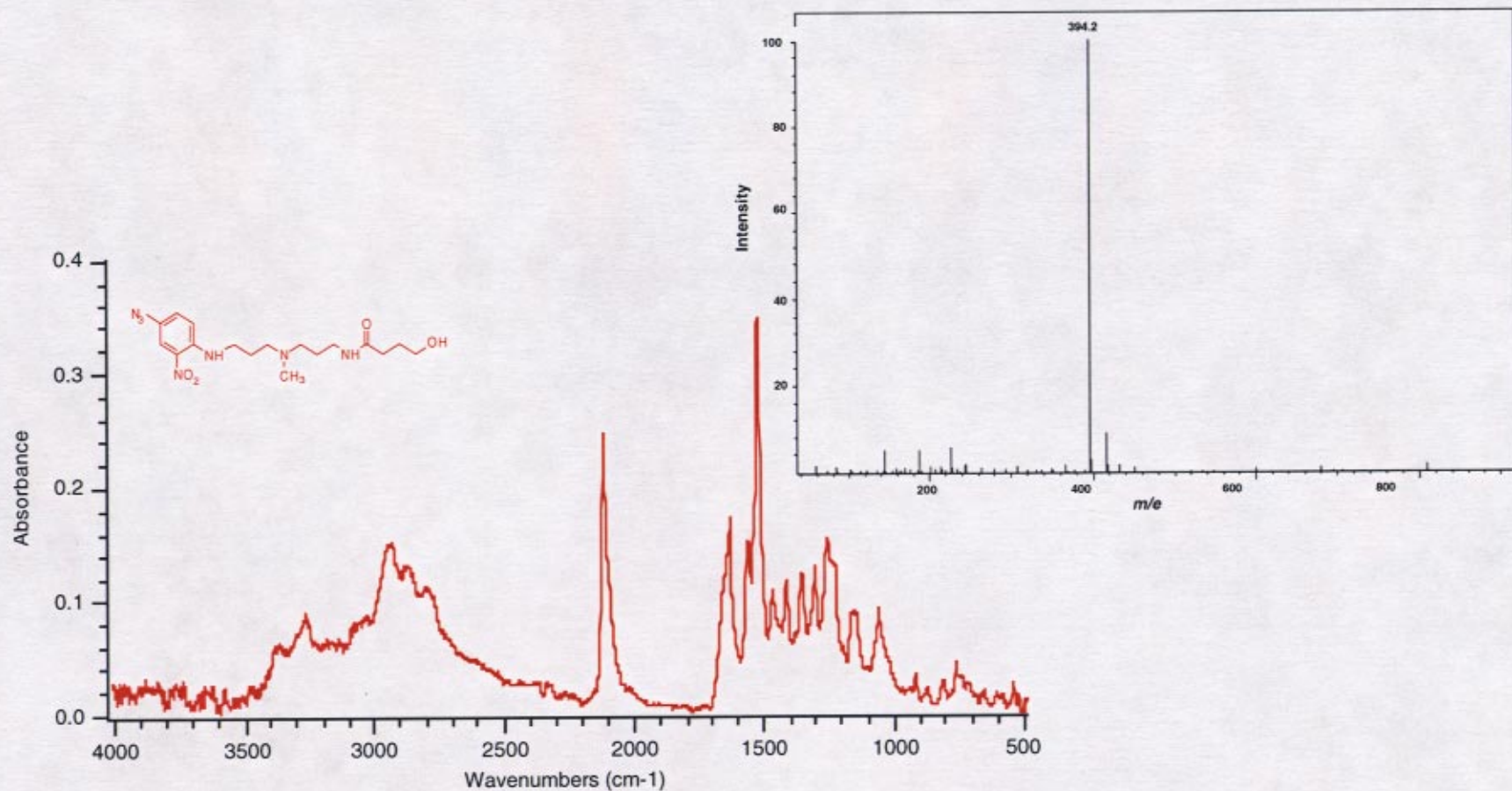


Figure 5. The FT-IR and mass spectra of the photoactivatable linker segment. The FT-IR spectrum shows a nitro peak at 1525 cm⁻¹, the amide carbonyl peak at 1637 cm⁻¹, and O-H peak at 3300 cm⁻¹. The intense azide peak at 2121 cm⁻¹ indicates that the molecule should be photoactive. The mass spectrum gives the protonated molecular ion peak at 394.2.

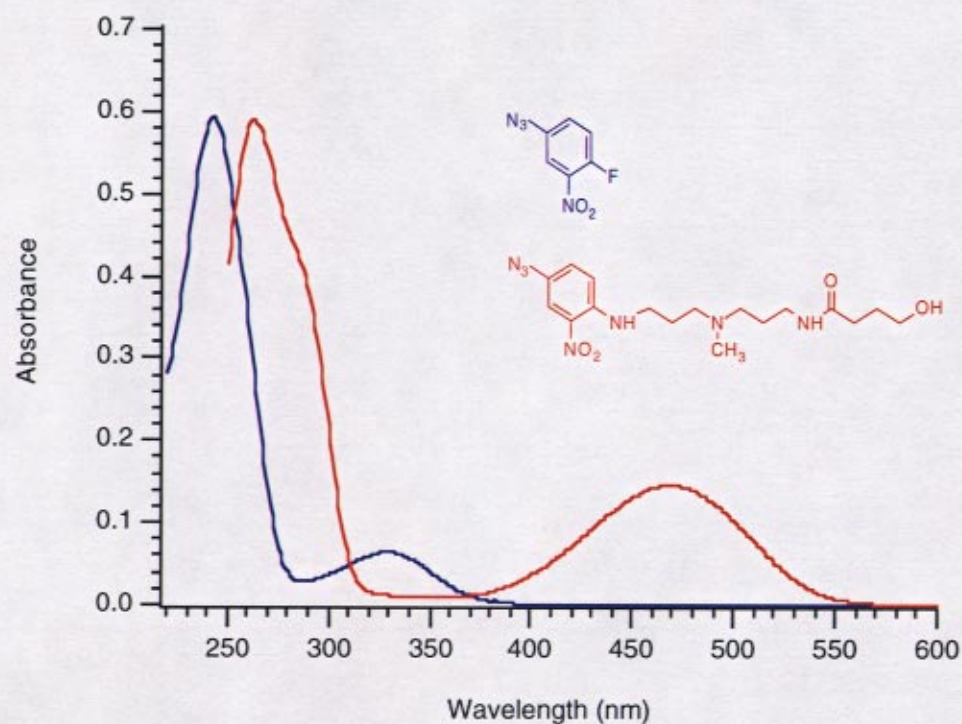


Figure 6. The UV/Visible absorption spectra showing the wavelength range for photoactivation of the linker. The spectrum on the left shows a maximum absorbance of the azide starting material in the ultraviolet range. The spectrum on the right shows a maximum absorbance centered at 265 nm for the Step-2 product. The absorption centered at 470 nm in the visible range gives the molecule its dark orange color.

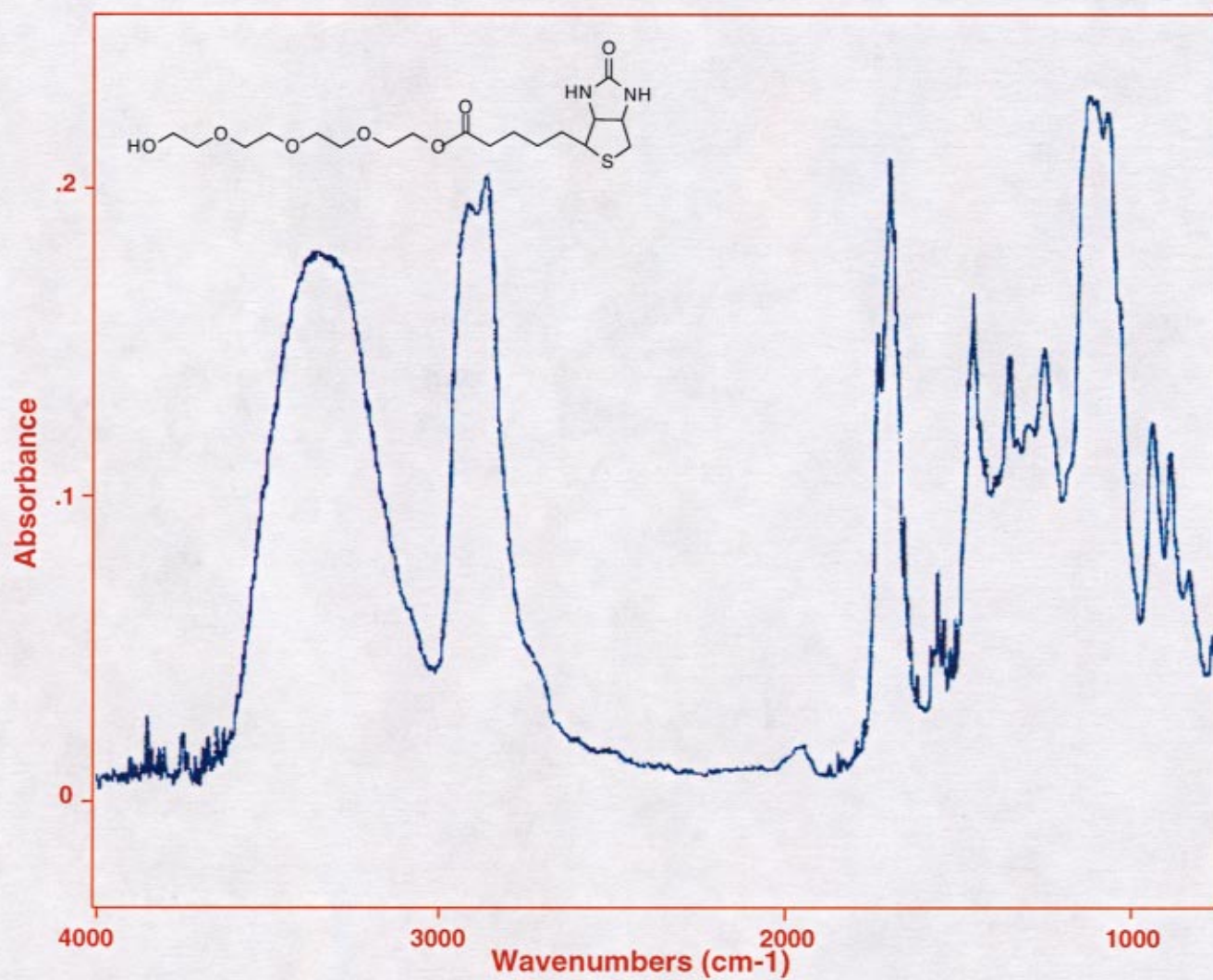


Figure 7. The FT-IR spectrum of the Step-3 ester product. It shows a C-O peak at 1100 cm⁻¹, the ester carbonyl peak at about 1700 cm⁻¹, and a hydroxyl peak at 3350 cm⁻¹.

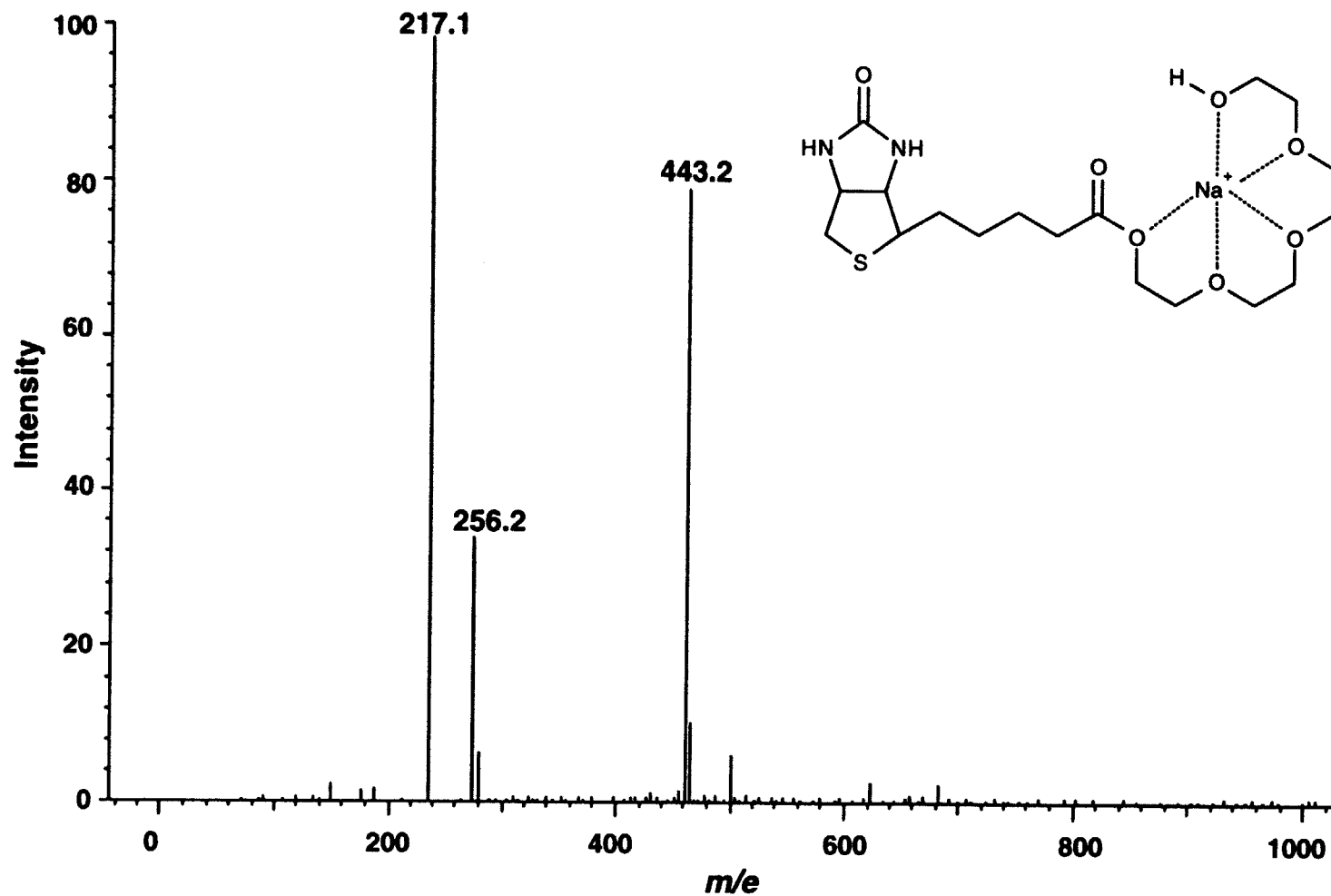


Figure 8. The mass spectrum of the biotin segment of the linker. The peak at 443.2 corresponds to the Step-3 product which has formed a crown ether structure by incorporating a sodium ion from the buffer solution used for liquid chromatography injection of the sample.

not possible. The amines also would not separate on silica thin-layer plates with any solvent system tried.

With vacuum distillation, the excess dipropylamine was readily removed. However, the remaining product would only partially distill due to high boiling point. As the volume of remaining product decreased, distillation stopped as the residue overheated and turned dark brown. In addition, the distilled product was found by thin-layer chromatography to have at least two components which did not separate.

The impure product can be used successfully in the Step-2 reaction. However, it may be possible to increase the yield and purity of the product by trying alumina chromatography, alone or in combination with distillation.

The Step-2 reaction was run originally in dichloromethane as solvent, with a yield of only 24.6%. Because the reaction produces HF, it was felt that the H⁺ ions might be protonating the amino end of the starting amide material and stopping the forward progress of the reaction. Therefore, the reaction was run again in absolute ethanol as solvent, with triethylamine added to capture the protons. The reaction did not proceed any more quickly and so was allowed to run longer, giving a yield of 34.9%.

Because the reaction time seemed to make a difference, it is recommended that the reaction be run under less dilute conditions. This would more closely replicate the reaction reported by Forster et al.² It is also possible that the impurity of the starting amide or impurities in the azide contribute to low yield.

Light conditions were being tested for the Step-2 reaction. Because maximum absorption by the product occurs in the ultraviolet range with lesser absorption in the blue range of visible light, we decided to reduce exposure to direct visible light by working with the fluorescent lights off in the hood but to take no other precautions.

As shown in Figure 5, the azide section of the linker seems to have retained its photoactivatable capacity.

The Step-3 product could not be separated by extraction. However, it separated reasonably well on silica thin-layer plates, so a silica column was used for purification. The product proved to be polar enough that it did not elute well, even with a high percentage of methanol in the eluting solvent. Therefore, it is recommended that an alumina column be tried, or if necessary, distillation.

The remaining steps of the synthesis will involve the attachment of each linker segment to the central silicon atom. In Step 4, reaction conditions need to be determined so that di-substitution of the biotin segment on the silane does not occur. Afterward, the Step-5 reaction should be reasonably straightforward.

Upon successful synthesis of the linker, it must be tested to show that it is capable of photoactivation. In addition, the linker must demonstrate that it can carry a biomolecule into biotin-avidin affinity chromatography and can be cleaved in aqueous conditions to release the biomolecule.

Conclusions

The conclusions drawn from this project can be summarized as follows:

- ❑ Steps 1-3 of the synthesis plan have produced the desired product.
- ❑ Steps 1 and 3 need improvement of the purification process.
- ❑ Step 2 could be tried under less dilute conditions to increase yield.
- ❑ Light conditions for the Step-2 reaction allowed the product to remain photoactive.
- ❑ Reaction conditions need to be determined for Step 4 so that di-substitution can be avoided.
- ❑ After completion of synthesis, the linker must be tested to determine its photoactivatable and reversible capabilities.

Acknowledgments

I am appreciative to Dr. Ken Bogen for enabling me to work at Lawrence Livermore National Laboratory on this synthesis. Dr. Kevin Langry has been especially helpful as the collaborating chemist who has supervised my work and answered many questions. I am grateful to Lynn Wilder for assistance with preparation of figures for the report.

References

1. Lin, W.-C.; Morton, T. H. *J. Org. Chem.* **1991**, *56*, 6850-6856.
2. Forster, A. C.; McInnes, J. L.; Skingle, D. C.; Symons, R. H. *Nucleic Acids Res.* **1985**, *13*, 745-761.
3. Hassner, A.; Alexanian, V. *Tetrahedron Lett.* **1978**, *46*, 4475-4478.

Experimental and Computational Approach to VOC Transport in Ground Water

Kari Fox

Lawrence Livermore National Laboratory
Livermore, California 94550

December, 1996

Prepare in partial fulfillment of the requirements of the Science and Engineering Research Semester under the direction of Fredric Hoffman, Research Mentor, in the Lawrence Livermore National Laboratory.

* This research was supported in part by an appointment to the U.S. Department of Energy Science and Engineering Research Semester (hereinafter called SERS) program administered by LLNL under Contract W-7405-Eng-48 with Lawrence Livermore National Laboratory.

Abstract

The object of this study is to evaluate the physical and chemical retardation processes that impede cleanup in low organic carbon aquifers, and to develop new remediation strategies that allow for minimal time and cost of cleanup. Innovative laboratory column and diffusion experiments were performed to measure the transport mechanisms of retardation, diffusion, and tortuosity for four volatile organic compounds (VOCs) commonly found in ground water. Resolution of problems with experimental methods is in progress. Experimental results are used in a computational model that numerically describes our conceptual model.

Introduction

The aquifers beneath the Lawrence Livermore National Laboratory (LLNL) have been contaminated by volatile organic compounds (VOCs) from World War II solvent discharges. The current method of remediation being employed is Pump and Treat, where the contaminated water is pumped out, treated, and pumped back in. The contaminants, however, are not being pumped out with the ground water. They are staying in the aquifer, a process called retardation, to not only prolong the time, but also increase the costs of cleanup. A better understanding of contaminant transport mechanisms (advection, mechanical dispersion, molecular diffusion, and retardation) will help minimize the time and costs of cleanup.

The objective of this project is to develop new remediation strategies. To accomplish this goal, experimental, computational, and conceptual models are united. Approaches included:

- performing laboratory experiments to reduce uncertainty in values for tortuosity (Ω), effective diffusion (D^*), and retardation (R).
- developing a computational model and testing the results through comparisons with field evidence

Results include improved parameterization and a new method to test alternative remediation techniques.

Methods

To avoid complexities in the experiments, while preserving aquifer conditions, ideal laboratory conditions were used. A low organic, fine grained, well sorted sand was used in the experiments. Past SERS students had discovered a thin layer of clay coats the sand grains (Manz, 1996). To see this clay's effect on retardation, we washed the clay from the sand and performed experiments with washed and unwashed sand. Four VOCs commonly found at LLNL were selected as contaminants: trichloroethylene (TCE), tetrachloroethylene (PCE), carbon tetrachloride (CCl_4), and chloroform ($CHCl_3$). These contaminants were prepared at stock concentrations that simulate concentrations found at the LLNL site (300ppb).

There are four dominant contaminant transport mechanisms: advection, mechanical dispersion, molecular diffusion, and retardation. Advection is the contaminant is being transported by the velocity of the groundwater. Mechanical dispersion is also velocity dependent, and is basically the branching effect of contaminant as it moves around the solid objects. Molecular diffusion is not velocity dependent, and is also a branching effect seen, but on the molecular scale. Diffusion seems to occur from areas of high concentration to areas of low concentration. Retardation is the slowed movement of the contaminant compared to that of the flowing water. Tortuosity is a measure of how tortuous the path of the contaminant molecules is around the solids in the flow path.

Column Experiment

The Column experiment (Fig. 1) measures retardation under advective-flux conditions. Contaminated water is pumped through two packed and saturated sand columns, one containing washed and one containing unwashed sand. Influent and effluent concentrations are measured and the velocity of the water being pumped is noted. The relationship between the velocity of the contaminant and the velocity of the water is evident and is effectively retardation. When the concentration of the effluent reaches the concentration of the influent, clean deionized water is pumped through the column to simulate a cleanup. When effluent

concentration reaches 0, the pumps are switched off and the experiment is done.

Values for concentration and corresponding sampling times are entered into a computer modelling program (CXTFIT, one-site model) which fits the data to a curve and formulates a value for the retardation coefficient.

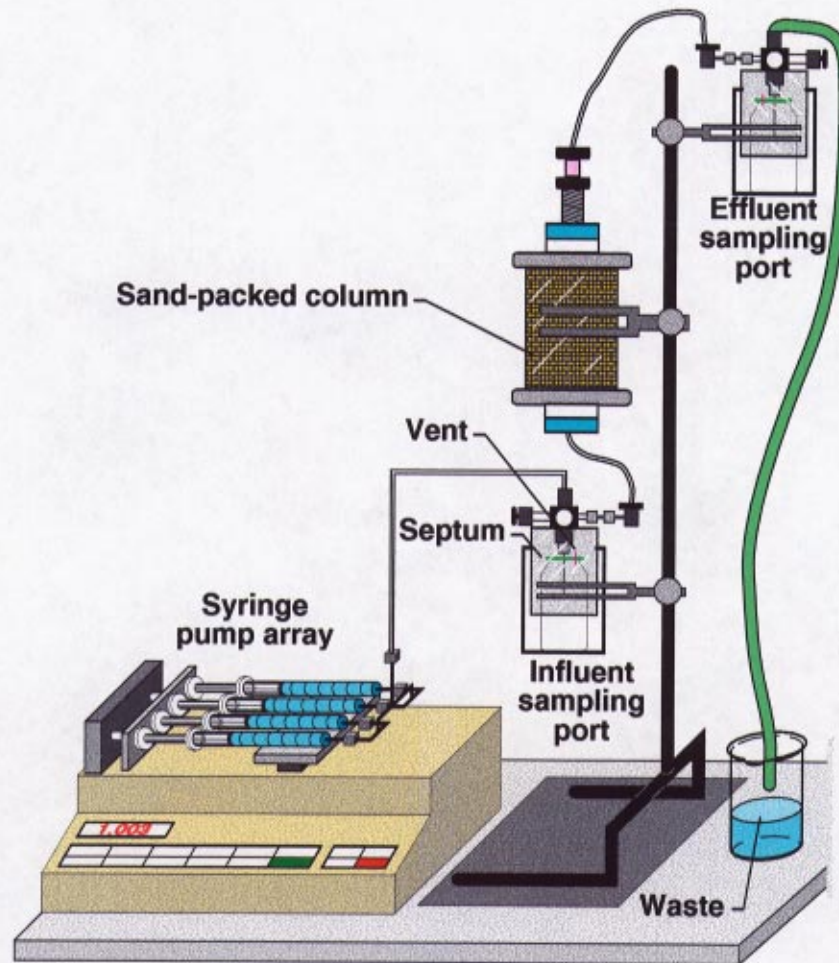


Fig. 1 The Column experiment measures retardation under advective-flux conditions

Diffusion Experiment

The diffusion experiment (Fig. 2) measures retardation under diffusive flux conditions. Contaminated water is passed over the tops of twenty packed and saturated vials. Ten vials contain washed sand, and ten contain unwashed sand. There is a glass plate over the tops of the vials to minimize volatilization. Velocity in the vials is zero, so the only transport mechanism that can account for mass in the vials is diffusion. After two weeks, the vials are removed and analyzed for VOC mass.

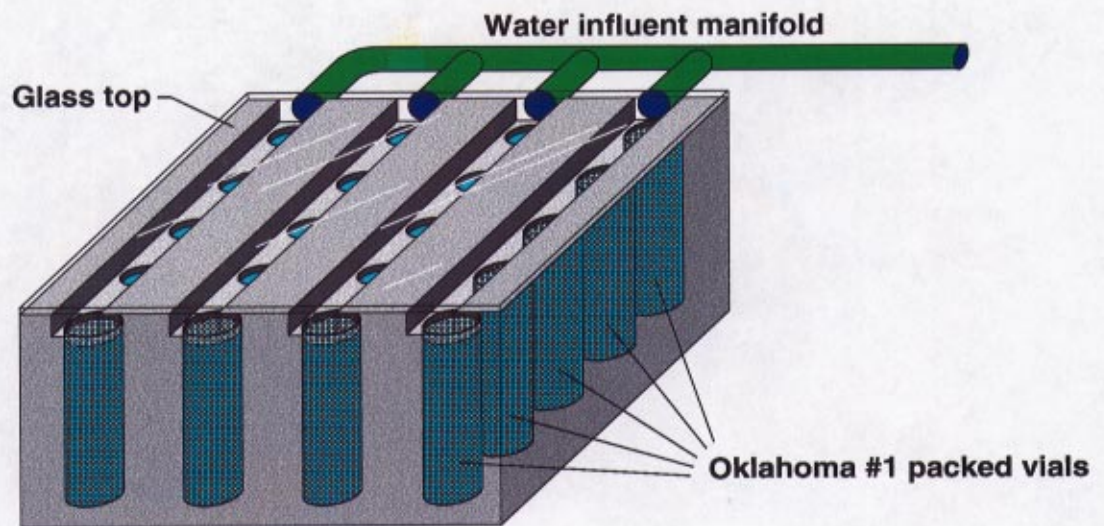


Fig. 2 The Diffusion experiment measures retardation under diffusive-flux conditions

The mass reported from the chemical laboratory is used in the error function equation to solve for tortuosity (Ω). We solve for D^* in this equation and then solve for Ω by dividing D^* by D_w .

$$C_{(x,t)} = C_o \cdot \operatorname{erfc} \frac{x}{2\sqrt{D^* t}}$$

$$D^* = D_w \cdot \Omega$$

- C = concentration at time t and location x
- C_o = initial concentration
- D^* = effective diffusion coefficient
- D_w = diffusion coefficient in water
- Ω = tortuosity coefficient

Values for D_w were obtained from a literature search. Approximately twelve different methods of calculating this value was analyzed with an average difference of 20% between the extreme end members. After careful investigation, it was noted that the Hayduk-Minhas Correlation (1992) seemed the most accurate and recent of these methods. Values for D_w (cm^2/sec) were calculated using this method (see below) and then used in the above equation.

$$D_w = 1.25^{-8} \cdot (V_b^{-0.19} - 0.292) \cdot T^{1.52} \cdot \mu_w^e$$

$$e = \left(\frac{9.58}{V_b^{-1.12}} \right)$$

D_w = diffusion coefficient in water (cm²/sec)

V_b = molar volume at boiling point of solute (cm³/mol)

T = temperature (Kelvin)

μ_w = viscosity of water (cP)

Effective tortuosity (w) is defined as Ω/R . Since w is a property of the geologic media, it is constant in our experiments and should not change between each VOC. However, Ω should, as each contaminant has a different retardation coefficient. It was found from a previous experiment (Manz, 1996) that Chloroform is not retarded ($R=1$). So by a simple relationship, the retardation of the other VOCs can be calculated as shown below.

If:

$$\omega = \frac{\Omega_{CHCl_3}}{R_{CHCl_3}} \quad \text{and} \quad \omega = \frac{\Omega_{VOC}}{R_{VOC}}$$

Then:

$$\Omega_{CHCl_3} = \frac{\Omega_{VOC}}{R_{VOC}} \quad \text{since} \quad R_{CHCl_3} = 1$$

By substitution:

$$R_{VOC} = \frac{\Omega_{CHCl_3}}{\Omega_{VOC}}$$

Results and Discussion

Results are shown in Table 1. Clay plays an important retarding role. Clays have a negative charge to them and are hydrophobic. The VOCs are non polar and are also hydrophobic. Since neither of these two components binds preferably with water, they will bind together in a process called sorption. The more hydrophobic they are, the more likely and stronger they will bind, and the greater the degree of retardation. Solubility is effectively a means of measuring hydrophobicity by an inverse relationship. The higher the solubility, the more likely it will stay in aqueous solution, the less it will sorp to the clay, and the less it will be retarded. This inverse relationship between solubility and retardation is evident in the column data (Table 1). It is also clear from the column data that the unwashed sand has a higher retardation factor than the washed sand, indicating that the presence of clay does play a role in increasing the retardation of VOCs. The clay in our experiments accounts for approximately 0.25% by weight of the column, up to 30% of the surface area, and up to 50% of the retardation (Manz, 1996).

The Diffusion experiment data, however, is not so ideal. We believe this is because our ability to do chemical analyses greatly exceeds our ability to pack the vials so that tortuosity (w) is uniform throughout. Since we are computing retardation based on tortuosity, a high experimental error in the tortuosity leads to a high error in the retardation values. So the difference in retardation between the unwashed and washed sand is insignificant compared to the high experimental error associated with these values.

Chemical	Column R unwashed	Column R washed	Diffusion R unwashed	Diffusion R washed	Ω unwashed	Ω washed	Dw (cm ² /sec)	Solubility (mg/L)
CHCl ₃	1.00	1.00	1.00	1.00	0.256	0.211	1.15E-05	8200
TCE	1.09	1.06	1.27	0.83	0.202	0.256	1.05E-05	1100
CCl ₄	1.11	1.07	1.03	0.91	0.248	0.232	1.03E-05	800
PCE	1.33	1.26	1.24	1.09	0.206	0.194	9.38E-06	150

Method	Bulk Density	Porosity
Column	1.80	0.32
Diffusion	1.78	0.325

Dw = Diffusion Coefficient
in water

Table 1 Results from Column and Diffusion experiments

Experimental Resolutions

Experimental problems need to be resolved before continuing with this project. Unreasonably low masses are being reported from the chemical analysis laboratory. Resolutions are being made to accommodate three possibilities:

- temperature control
- sampling methodology

Temperature control is not maintained in the laboratory. With sampling such sensitive VOCs, it is imperative to have constant temperature. Sampling techniques have become a major source of error in our experiments. An experiment was conducted to measure the concentration of samples taken at different volumes and different sampling times to estimate the most effective sampling method. It is seen that the method of sampling greatly affects the resulting concentrations and that we need to improve our design. Fig. 3 and 4 show results of this experiment.

Small sampling volumes are a problem to overcome. A 1 ml sample is acquired in a 40 ml container. Each drop then must travel the distance of approximately 3 inches from the plumbing to the bottom of the container. The VOCs will tend to diffuse out of solution into the head space of the vial. The seals between the top of the vial and the experimental apparatus are not air tight. The gaseous VOCs can then travel out of the head space and out into the laboratory, giving a low VOC concentration for the collected sample.

Fig. 3 shows this negative correlation between volume and relative concentration.

Linked with sample volume is the another hurdle, long sampling time. With the low flow rates that are used (0.5 ml/hr) it is necessary to leave the sample for a period of 30 min to collect a 1 ml sample. From Fig. 4, a negative trend is seen between relative concentration and time of sampling. This figure also shows that the standard deviation also decreases with increasing sampling time. This is thought to be due to the fact that the longer the sampling time, the longer the VOCs have to equilibrate with the air. This equilibration decreases not only the standard deviation, but also the accuracy.

The main problem is being able to sample a small volume at a low flow rate without losing the volatiles. We have made a temporary solution to influent sampling. Instead of taking many measurements from our apparatus and averaging to an influent concentration, a 1 ml aliquot is simply taken straight out of each syringe before it is hooked up to the apparatus. This concentration is then used as the influent concentration. All analyses for the diffusion experiment used 270 ppb for the influent concentration.

Conceptual model

Figure 5 shows a diagram representing a simplification of the conceptual model proposed by Fredric Hoffman (1996). There is a high concentration of VOCs in the source area, and a low concentration in the

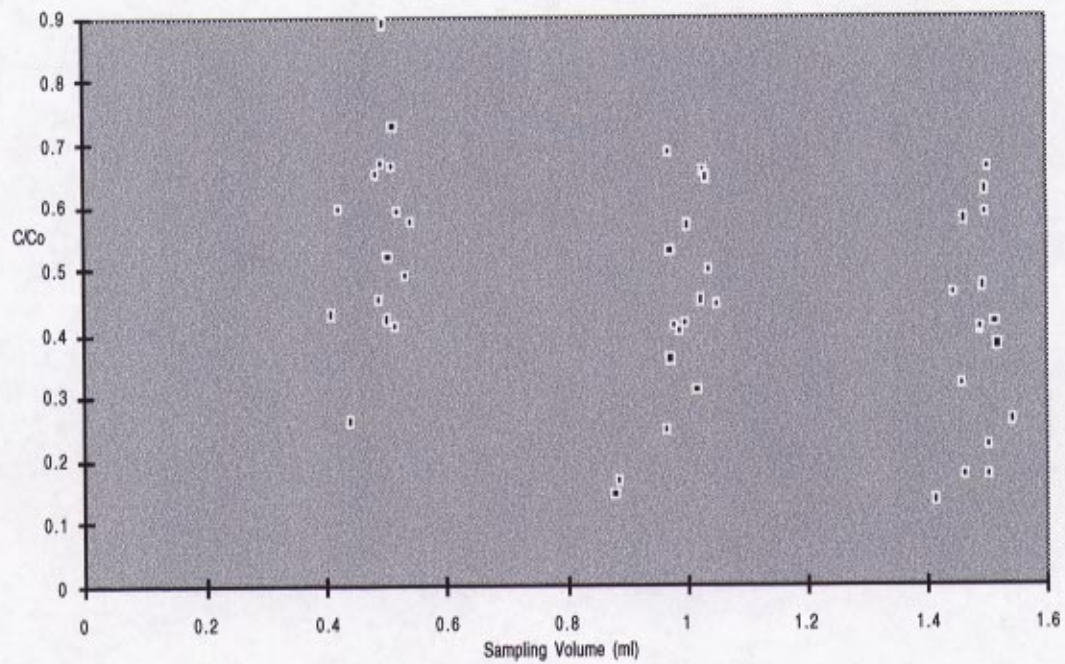


Fig. 3 Lower concentrations are measured with increasing volume

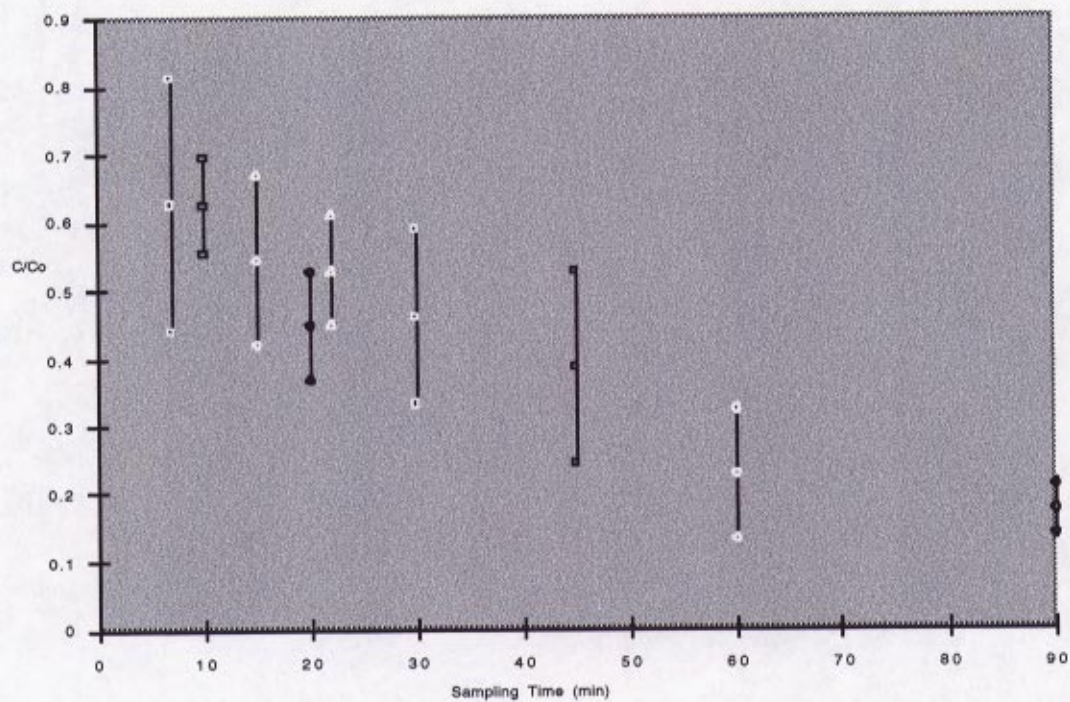


Fig. 4 Concentration with error bars are plotted against the length of sampling time. Lower concentrations with smaller standard deviations are measured with increasing sampling time

distal areas. Beneath the water table, there is flowing ground water. Two geologic mediums are represented here, zones of high hydraulic conductivity (HK) and zones of low hydraulic conductivity (LK). Hydraulic conductivity is a measure of the ease in which an aqueous solution can pass through a porous media. An example of a HK material would be gravel or sand, and an example of a LK material would be silt or clay. The main transport processes in HK zones are advection and dispersion. In the LK zones, however, velocity is essentially zero, so the only transport mechanism is molecular diffusion (orders of magnitude slower than advection or dispersion).

The contaminants in the HK regions of the source area diffuse quickly into the LK regions, and also advect down gradient into the distal areas. In the LK zones, however, there is no advection, so the contaminants do not get transported to the distal areas. The contaminants in the HK regions of the distal areas simply do not have enough time to diffuse into the LK regions.

Extraction wells are placed and the remediation technique of Pump and Treat begins. A guard well is placed down gradient of the source area to isolate the source area from the distal area. This guard well pumps out any contaminant that gets advected from the source area, as well as cleans up the distal areas. The HK zones rapidly clean up in both the source and distal areas.

Diffusion occurs from areas of low concentration to areas of high concentration. Now that the HK zones have low concentration, back diffusion of contaminants occur, where contaminants diffuse out of the LK

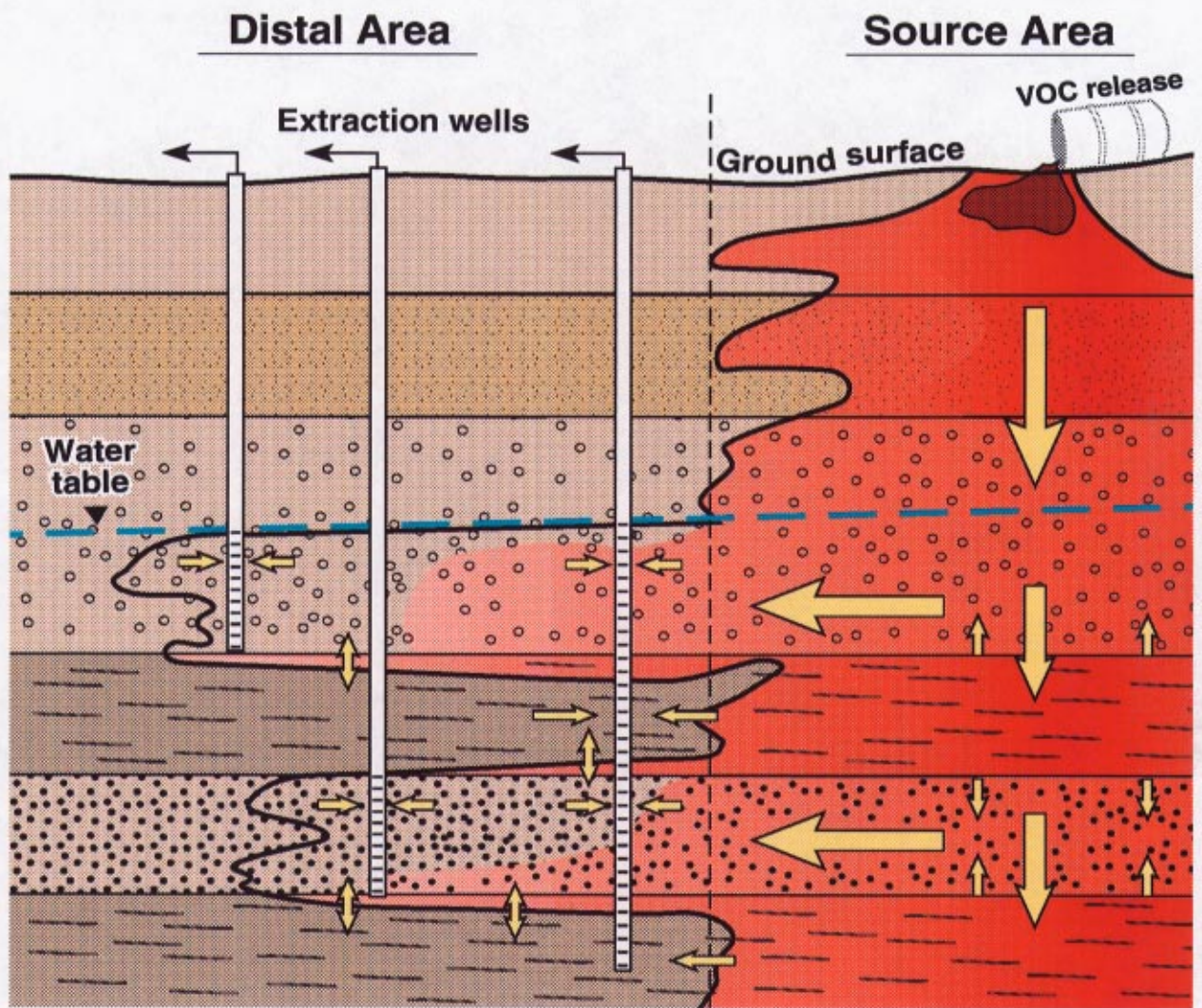


Fig. 5 Conceptual model showing contaminant transport path

and back into the HK. The HK zones in the source area are again pumped and flushed clean, but are resupplied by the LK zones to keep concentration levels in the HK above the Maximum Contamination Limit (MCL) of 5 ppb. This back diffusion is the mechanism that leads to long times to cleanup of source areas and in turn increased costs of cleanup.

Beginnings of the Computational Model

The one-dimensional Advection-Dispersion Equation (ADE) describes our conceptual model:

$$R \frac{\partial C}{\partial t} = -V \frac{\partial C}{\partial x} + D \frac{\partial^2 C}{\partial x^2}$$

R = Retardation factor

C = Concentration

V = Velocity

D = Hydrodynamic Dispersion

We will try to successfully model this equation using an adaptive grid finite element modeling tool called PDEase. This model will incorporate parameters of R , D^* , and Ω , estimated for the laboratory, into the equation. We hope to evaluate the rate at which VOCs diffuse out of LK zones and into HK zones during cleanup.

Our approach is unique in that it divides D into its separate components of molecular diffusion and mechanical dispersion. Previous work modeling this equation has ignored molecular diffusion as it is so small compared to advective and dispersive processes. In our case, molecular

diffusion plays a vital role in the transport of contaminants and cannot be ignored.

Fig. 6a represents field data that was obtained from the Treatment Facility A source area. This data is pleasingly similar to the results of our computational model (Fig. 6b). This similarity is significant in that we can now be confident that our computational model accurately simulates the subsurface contaminant flow beneath LLNL, and we can begin to add complexities into the model.

Conclusions

Our results show:

- high sensitivity of retardation to the presence of clay
- a new method to test alternative remediation techniques and
- parameterization and validation of the computational model using LLNL source - area cleanup data
- that LK zones can act as contaminant sources to HK zones for many years after the initiation of pump and treat cleanup

Continuing Research

Although we have made huge progress in understanding the subsurface contaminant transport at LLNL, research is still needed to:

- improve our experimental methods for more accurate results

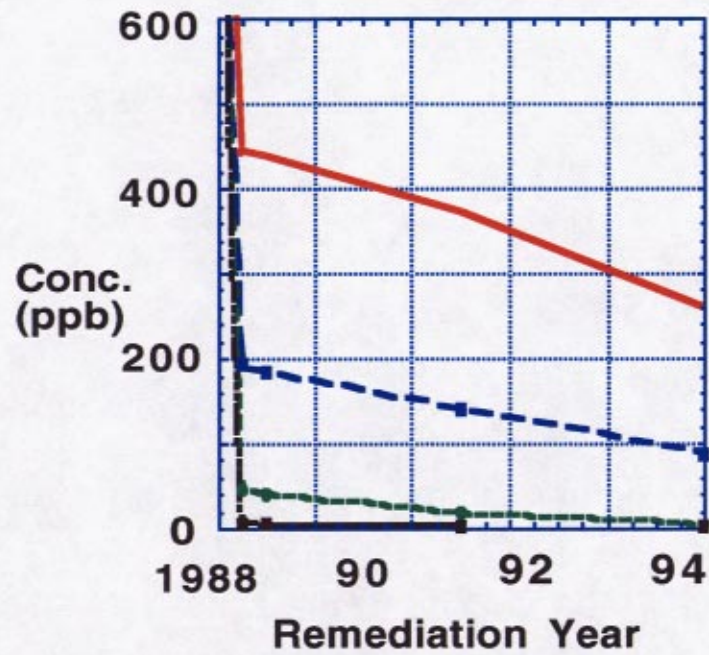


Fig. 6a PDEase idealized TFA Remediation Simulation

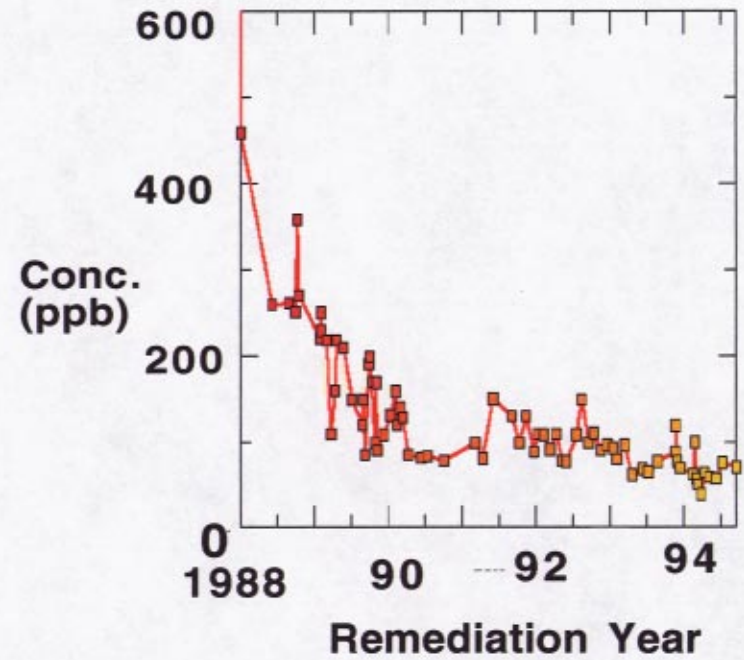


Fig. 6b LLNL TFA Pump and Treat Remediation Data

- further investigate of the chemical interactions that affect sorption of VOCs onto solid surfaces
- perform diffusion experiments into different aquifer materials to provide a more accurate simulation of the geologic heterogeneity of LLNL
- evaluate various pump and treat remediation strategies using the computational model
- continually revise the conceptual model to account for new experimental or computational results.

It is important to understand the behavior of VOCs in a heterogeneous geologic environment in order to inspire new technologies for cleanup.

Acknowledgements

Special Thanks to Fredric Hoffman for all his support, patience, and guidance throughout the entire project, to Said Doss and Eric Brown for their unending enthusiasm and support in the construction and direction of the computational modeling effort, to Kim Bair and Brian Manz for their experimental breakthroughs and hard work, and to Marina Jovanovich for her superb chemical analysis skills.

References

Hayduk, W and B.S. Minhas. April, 1982. "Correlations for Predictions of Molecular Diffusivities in Liquids". *Canadian Journal of Chemical Engineering*. v 60

Hoffman, F. 1996. "A New Conceptual Model and Remediation Strategy of VOCs in Low Organic Carbon Unconsolidated Sediments". Submitted to *Ground Water* Preprint UCRL-JC-125199, Lawrence Livermore National Laboratory, Livermore California.

Manz, B. 1996. "Retardation and Diffusion of VOCs in Ground Water"
Printed in Papers for Lawrence Livermore National Laboratory Science and Engineering Research Semester.

**EVALUATING THE SEWER SATELLITE STATIONS FOR FUTURE
ALTERNATIVES**

Charity Hayden

Norwich University

**Lawrence Livermore National Laboratory
Livermore, California 94550**

20 December 1996

Prepare in partial fulfillment of the requirements of the Science and Engineering Research Semester under the direction of Robert Vellinger, Research Mentor, in the Lawrence Livermore National Laboratory.

*** This research was supported in part by an appointment to the U.S. Department of Energy Science and Engineering Research Semester (hereinafter called SERS) program administered by LLNL under Contract W-7405-Eng-48 with Lawrence Livermore National Laboratory.**

If this paper is to be published, a copyright disclaimer must also appear on the cover sheet as follows:

By acceptance of this article, the publisher or recipient acknowledges the U.S. Government's right to retain a non-exclusive, royalty-free license in and to any copyright covering this article.

SEWER SATELLITE STATIONS

ABSTRACT

Unauthorized releases of contaminants into the sanitary sewer during the 80's led the City of Livermore Sewage Treatment Plant to request additional monitoring measures. Corrections proposed by Lawrence Livermore National Laboratory (LLNL) included sewer satellite stations to identify instantaneous or chronic sewer spill sources.

The purpose of my project is to perform a technical evaluation of these stations functionality and their current applicability. A quantification of past operational findings will be used as a basis for the assessments.

Ten sewer satellite stations were built, beginning in 1989, in response to historical problems with site discharges. The initial concept for these was to perform spill traceback by locating the source of a spill which could have an environmental impact or cause damage to the Livermore Water Reclamation Plant.

Stations that are evaluated to be beneficial to LLNL in monitoring spills or illicit discharges may have to be moved, repaired or upgraded. This project will graph the historical operations of the satellites and from the graph develop criteria for future practices. Operational parameters and equipment for a reliable trace back system will be proposed.

INTRODUCTION

All wastewater generated by LLNL is routed through a sewer drainage system to a common point at building 196 (B196), located in the northwest corner of LLNL. The wastewater is then discharged from B196 to the City of Livermore's sewer collection system and then to the Livermore Water Reclamation Plant (LWRP). In the 1980's there were two releases of contaminants into the sanitary sewer:

- '84, Ni release from Sandia
- '86, Ni and Cr release from Hazardous Waste Management

Both of these releases were diverted at the LWRP but spills such as these can cause a considerable amount of damage to the treatment plant. For example pumps could be damaged and organisms needed for waste treatment die from an acidic flow.

In response to the city of Livermore's request for corrective measures LLNL proposed the implementation of: Sewer satellite stations, Sewage diversion, Upgrade of B196, and Monthly reports. In 1988 modifications of B196 were finished. Sewer Satellite Station (SSS) drawings were also completed in 1988 and by 1989 the first five stations were constructed. Five additional stations were completed by 1991.

There are eight drainage basins making up the sanitary sewer drainage system at LLNL (see Appendix A). The monitoring station locations are significant because they are located to capture discharges isolating each basin. This creates the quickest breakdown of the lab for spill trace back. There is also one SSS located to monitor Sandia National Laboratory wastewater and another station isolates Hazardous Waste Management discharges (HWM).

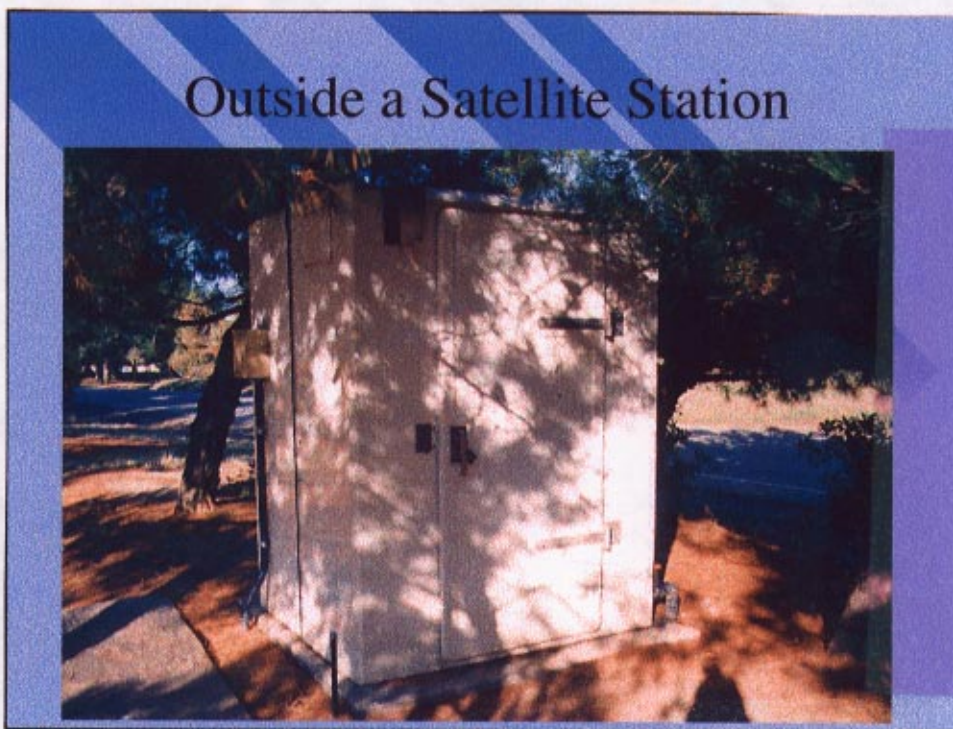


Figure 1

OBJECTIVES

My project was to evaluate these stations to see if they have been successful in tracing back spills. I needed to know their current operational status and the condition of each station. Since there are only 3 running now, due to problems I will be describing to you shortly, I needed to dig into the history to see how they worked in the past. This project will graph the historical operations of the satellites and from the graph develop criteria for future practices. Lastly, operational parameters such as pH and temperature will be proposed along with equipment for a reliable trace back system.

EXISTING SYSTEM EVALUATION

Each sewer satellite station is a weatherproof, locked shelter measuring approximately 5 ft by 5 ft by 6 ft which houses a Manning refrigerated sampler (see Figure 1). Because of the size of the stations, it is extremely difficult to move around and many technicians have ended up with back pain as a result of continuous strain. Each station also has potable water, electrical power, lighting, ventilation, fans, heater, and a floor drain connected to the sanitary sewer system.

A polyvinyl chloride (PVC) pipe connects the station to the manhole that is to be monitored. Inside the pipe is tubing, one end of which is connected to the sampler, the other end to a weighted strainer that is submerged in the sewage flow.

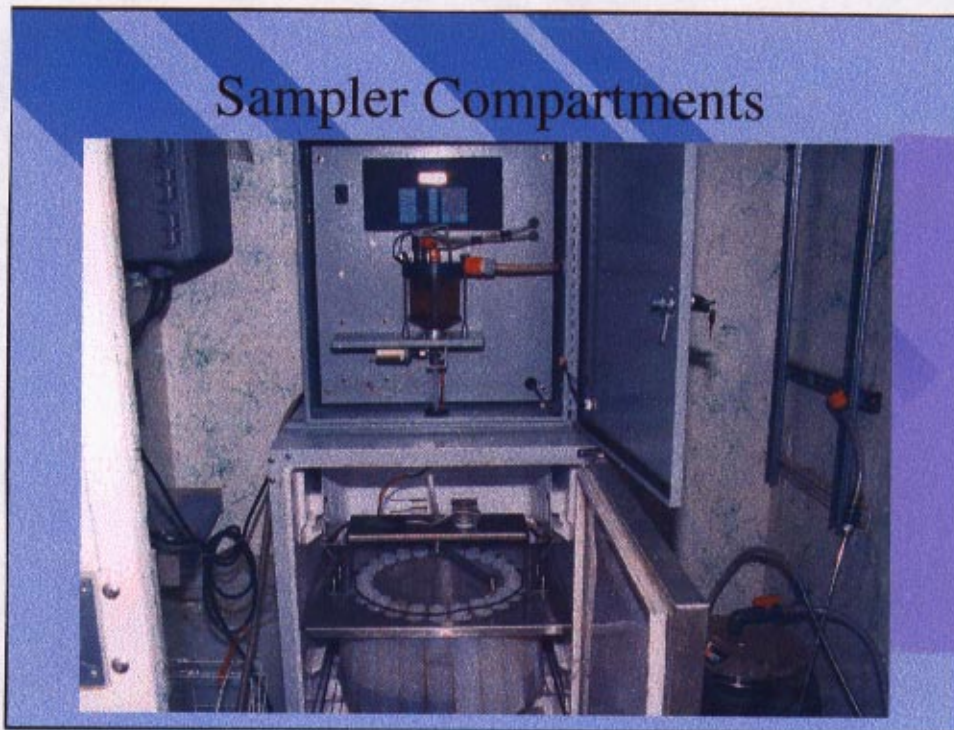


Figure 2

The Manning sampler has two major assemblies, "upper" and "lower". The upper assembly holds the controller. The lower base unit is refrigerated and contains the sample measuring and distribution mechanisms, a circular bottle rack containing 24 sampling bottles (1,000 mL each), and a vacuum pump that draws the sample from the sewer pipe (see Figure 2).

On weekdays the sampler collects eight, 50 mL samples per bottle at the rate of one sample every 15 minutes therefore, because of dilution, a representative sample is not likely. At this setting it takes two hours to fill one sample bottle and 48 hours to fill the 24 bottles in the sampling carousel. On Friday, the sampling frequency is changed to once every 30 minutes to accommodate the extra day. At this setting it takes 72 hours to fill 18 of the 24 bottles. Maintenance on the stations is required on Monday, Wednesday and Friday. This provides the best coverage of releases, requiring no maintenance during off work hours.

Stations were visited to check inventory and operational conditions of the SSS. Physical characteristics were noted and logbooks, which are located in each station, were collected for thorough review.

A checklist of Inventory, shown in Figure 3, was prepared. Itemized inventory of equipment, samplers and refrigerators was taken in each station. The operational status of heaters, fans, lights, and running water was determined. Structural conditions of stations were recorded and a checklist of problems was created while visiting the stations.

Checklist of Inventory

FIGURE 3										
SEWER SATELLITE STATIONS										
CHECK LIST OF INVENTORY										
					SATELLITES					
EXISTING EQUIPMENT	40B	51A	53A	69A	86B	125C	163A	177E	185F	231A
	green	red	red	red	red	red	green	red	red	green
MANNING SAMPLER	YES	RUNNING	NO	YES	RUNNING	NO	RUNNING	YES	NO	YES
WATER HOSE	YES	YES	YES	YES	YES	YES	YES	YES	YES	YES
SAMPLING CONTAINERS	YES	YES	NO	YES	YES	NO	YES	NO	NO	YES
SAMPLING SUCTION	YES	WORKS	NO	YES	WORKS	NO	WORKS	NO	NO	YES
FRIGERATOR	YES	RUNNING	NO	YES	RUNNING	NO	RUNNING	YES	NO	YES
ELECTRIC HEATER	YES	WORKS	WORKS	WORKS	WORKS	YES	YES	WORKS	WORKS	YES
EXHAUST FAN	RUNS	WORKS	WORKS	WORKS	WORKS	WORKS	RUNNING	WORKS	WORKS	RUNS
5 GALLON PLASTIC JUG	YES	YES	YES	YES	YES	YES	NO	YES	YES	NO
FLASHLIGHT	NEW-RUNS	YES	YES	NO	YES	NO	NO	NO	NO	NO
SAFETY GLASSES	YES	YES	YES	YES	YES	YES	YES	NO	YES	YES
FACE SHIELD	YES	YES	YES	YES	YES	YES	YES	YES	YES	YES
PINE OIL	YES	YES	YES	YES	YES	YES	YES	YES	YES	YES
PHISOHEX	YES	YES	YES	YES	YES	YES	YES	YES	YES	YES
TOOLBOX	NO	YES	NO	NO	YES	YES	YES	NO	NO	NO
MANUALS	YES	YES	NO	NO	YES	NO	YES	NO	NO	YES
FIELD LOG BOOK	YES	YES	YES	YES	YES	YES	YES	NO	YES	YES
PEN	NO	YES	YES	YES	YES	YES	YES	YES	YES	YES
KAY-DRYS	YES	YES	NO	YES	YES	YES	YES	YES	YES	YES
LATEX GLOVES, LONG	NO	1-OLD	NO	1-OLD	1-OLD	NO	NO	NO	1-OLD	1-OLD
DISPOSABLE GLOVES	NO	YES	NO	YES	YES	NO	YES	YES	YES	NO
MANHOLE HOOK	YES	TWO	NO	YES	YES	YES	TRUCK-FENCE	YES	YES	NO
2 EXTRA 1000 ML BOTTLES	YES	YES	NO	YES	YES	NO	YES	NO	NO	NO
GARBAGE CANISTER	YES	YES	NO	YES	YES	YES	YES	YES	YES	YES
LOCK ON DOOR	YES	YES	YES	YES	YES	YES	YES	YES	YES	YES
VENT PIPE	YES	YES	YES	YES	YES	YES	YES	YES	YES	YES
OUTSIDE LIGHT	TIMER?,	? BULB	?	?	?	?	PHOTO SENSOR	WORKS	?	?
INSIDE LIGHT	WORKS	WORKS	BURNT OUT	WORKS	WORKS	YES	WORKS	YES	YES	WORKS
TOILET BRUSH	YES	YES	YES	YES	YES	YES	YES	YES	YES	YES
BACKFLOW PREVENTER	YES	YES	YES	YES	YES	YES	YES	YES	YES	YES
YELLOW TAG WITH STRING	YES	YES	YES	YES	YES	YES	NO	YES	YES	YES
CONCRETE PLATFORM	YES	YES	NO	NO	YES	NO	NO	NO	YES	NO
4" PVC OPEN PIPE DRAIN	YES	YES	YES	NO	YES	NO	NO	NO	YES	NO
9X9" DRAIN GRATE	NO	NO	NO	YES	NO	YES	YES	YES	NO	YES
VACUUM GREASE	YES	YES	YES	YES	YES	YES	YES	NO	NO	YES
PAINTED FLOOR	NO	NO	YES	YES	NO	YES	YES	YES	NO	YES
RUNNING WATER	YES	YES	YES	YES	YES	YES	YES	YES	NO	YES

Logbooks located in the SSS describe historical and current operating conditions. Important dates such as: initial start up; equipment and operational problems; spill response activities; repairs; equipment replacement; and operational shut down are logged. LLNL annual Environmental Reports confirmed the dates in the logbooks when samples were collected.

An interview questionnaire, shown in Figure 4, was prepared. Interviews with individuals who have worked with the satellite stations have provided insight on the history of the stations and perspectives on past installation, operational reliability, and ergonomic problems. The following people were interviewed: Shari Brigdon, David Castro, Paul Dickinson, Charlene Grandfield, Allen Grayson, Marion Heaton, Jennifer Larson, Renee Needens, Duke Ramsey, Duane Rueppel, and Bob Williams. Interviewing the people involved with the satellite stations not only answered many questions, but also directed me to valuable sources where documented data could be found. Questions answered included, "Do you know when the monitoring stations were first installed?"

Drawings for the stations were completed in 1988 and by Fall of 1989 the first five stations were constructed. Five additional stations were completed by 1991. Stations were put in five at a time because there were limited end of year funds.

Have the stations been effective in their original purpose? There are no records indicating that the satellites have ever done what they were initially built for (tracking down the source of a spill). One sample was collected from a SSS after the 1991 zinc alarm although five satellite stations were on-line by 1989 (20% capacity). Only three out of ten satellite stations (30%) had samples when chrome was detected in 1992 and when arsenic was detected in 1993. One explanation is that faulty technology made this an unrealizable goal. Do advances in technology now allow this goal to be realized? More development is required to overcome these particular problems. My alternatives identify the best solutions, with current technology, to realize the original goal. Should the goal: spill trace back be the same today, knowing what we know now? Should we negotiate to discontinue these systems altogether, since there is no added benefit?

EXPLANATION OF SAMPLING PROBLEMS

Some of the most common problems associated with the wastewater flow include: a dry sewer, clogging of the strainers and draw distances (see Figure 5). Other problems causing downtime with the samplers include: faulty fill sensor; pinch valve not functioning; ball sticking; stepper or rotator motor replacement; chamber and air leaks; power, logic, or circuit board burnt out; and new or replacement sampler installation.

Checklist of Inventory

FIGURE 3										
SEWER SATELLITE STATIONS										
CHECK LIST OF INVENTORY										
										SATELLITES
EXISTING EQUIPMENT	40B	51A	53A	69A	86B	125C	163A	177E	185F	231A
	green	red	red	red	red	red	green	red	red	green
MANNING SAMPLER	YES	RUNNING	NO	YES	RUNNING	NO	RUNNING	YES	NO	YES
WATER HOSE	YES	YES	YES	YES	YES	YES	YES	YES	YES	YES
SAMPLING CONTAINERS	YES	YES	NO	YES	YES	NO	YES	NO	NO	YES
SAMPLING SUCTION	YES	WORKS	NO	YES	WORKS	NO	WORKS	NO	NO	YES
FRIGERATOR	YES	RUNNING	NO	YES	RUNNING	NO	RUNNING	YES	NO	YES
ELECTRIC HEATER	YES	WORKS	WORKS	WORKS	WORKS	YES	YES	WORKS	WORKS	YES
EXHAUST FAN	RUNS	WORKS	WORKS	WORKS	WORKS	WORKS	RUNNING	WORKS	WORKS	RUNS
5 GALLON PLASTIC JUG	YES	YES	YES	YES	YES	YES	NO	YES	YES	NO
FLASHLIGHT	NEW-RUNS	YES	YES	NO	YES	NO	NO	NO	NO	NO
SAFETY GLASSES	YES	YES	YES	YES	YES	YES	YES	NO	YES	YES
FACE SHIELD	YES	YES	YES	YES	YES	YES	YES	YES	YES	YES
PINE OIL	YES	YES	YES	YES	YES	YES	YES	YES	YES	YES
PHISOHEX	YES	YES	YES	YES	YES	YES	YES	YES	YES	YES
TOOLBOX	NO	YES	NO	NO	YES	YES	YES	NO	NO	NO
MANUALS	YES	YES	NO	NO	YES	NO	YES	NO	NO	YES
FIELD LOG BOOK	YES	YES	YES	YES	YES	YES	YES	NO	YES	YES
PEN	NO	YES	YES	YES	YES	YES	YES	YES	YES	YES
KAY-DRYS	YES	YES	NO	YES	YES	YES	YES	YES	YES	YES
LATEX GLOVES, LONG	NO	1-OLD	NO	1-OLD	1-OLD	NO	NO	NO	1-OLD	1-OLD
DISPOSABLE GLOVES	NO	YES	NO	YES	YES	NO	YES	YES	YES	NO
MANHOLE HOOK	YES	TWO	NO	YES	YES	YES	TRUCK-FENCE	YES	YES	NO
2 EXTRA 1000 ML BOTTLES	YES	YES	NO	YES	YES	NO	YES	NO	NO	NO
GARBAGE CANISTER	YES	YES	NO	YES	YES	YES	YES	YES	YES	YES
LOCK ON DOOR	YES	YES	YES	YES	YES	YES	YES	YES	YES	YES
VENT PIPE	YES	YES	YES	YES	YES	YES	YES	YES	YES	YES
OUTSIDE LIGHT	TIMER?,	? BULB	?	?	?	?	PHOTO SENSOF	WORKS	?	?
INSIDE LIGHT	WORKS	WORKS	BURNT OUT	WORKS	WORKS	YES	WORKS	YES	YES	WORKS
TOILET BRUSH	YES	YES	YES	YES	YES	YES	YES	YES	YES	YES
BACKFLOW PREVENTER	YES	YES	YES	YES	YES	YES	YES	YES	YES	YES
YELLOW TAG WITH STRING	YES	YES	YES	YES	YES	YES	NO	YES	YES	YES
CONCRETE PLATFORM	YES	YES	NO	NO	YES	NO	NO	NO	YES	NO
4" PVC OPEN PIPE DRAIN	YES	YES	YES	NO	YES	NO	NO	NO	YES	NO
9X9" DRAIN GRATE	NO	NO	NO	YES	NO	YES	YES	YES	NO	YES
VACUUM GREASE	YES	YES	YES	YES	YES	YES	YES	NO	NO	YES
PAINTED FLOOR	NO	NO	YES	YES	NO	YES	YES	YES	NO	YES
RUNNING WATER	YES	YES	YES	YES	YES	YES	YES	YES	NO	YES

LLNL Satellite Monitoring Stations
History of the Stations

Interview Questionnaire

Name:

Title:

When did you begin working with the satellite monitoring stations?

What do you see as the purpose of the satellite monitoring stations?

Do you know when the monitoring stations were first installed? Why were they first installed? What was the rationale behind the installation? What were the other options being considered?

What parameters were being tested during your involvement with the satellite monitoring stations? If sample parameters were added or deleted, please explain why.

Where were the samples analyzed once collected? Who reviewed the analytical results?

Were or are there problems you can think of? Location of the monitoring stations with regards to the manholes has been identified as one problem. Do you agree?
- Why or why not?

What were/are the positive aspects of using the satellites (if any)?

Who did you work with during your involvement with the satellite stations?

How many stations are currently in use?

Would it be beneficial, in your opinion, to use these stations again? If not in their current capacity, what changes would be necessary?

These new values showed longer distances than previously thought and since the samplers were programmed to the old distances this caused the pump to give up pulling a sample too soon therefore getting a small sample or no sample.

The pinch valve regulates the volume of sample taken . By pinching the tube while a sample is being pulled and then releasing the sample into the sample bottle, there is a safety feature in case the pump overfills the vacuum chamber. A ball, much like a ping pong ball, floats in the sample-collection chamber. If the chamber fills up too high the ball gets pushed up and sometimes gets stuck in the inlet.

ESTHETICS VS. ECONOMICS

In 1989 there was a problem with esthetics. Site and Planning stated that the stations would be unsightly if they were placed near the manholes they were sampling. It is no longer economically possible to operate the stations at these locations. Logbooks have documented considerable damage due to the distance a sample has to be pulled. Samplers run continuously, 24 hours a day, 7 days a week.

Logbooks showed that samplers that are closer to the manholes, such as 125C, require fewer repairs and replacement of parts and in turn less maintenance. Satellite stations housing samplers 60 to 130 feet away from the manhole, such as 177E, show significantly more failures in parts, causing downtime and approximately 2 extra hours of maintenance per sampler per week.

Manning sampling equipment has the power to lift a distance of 19 ft. All of our samplers are well under this distance, however, the maximum horizontal distance the samplers can pull without causing immature ware on the motor is 95 ft. Therefore, it is recommended that all samplers currently located further than 95 ft from the manhole be moved to this distance or closer, in order to maximize the life of the equipment. These stations include 163A, which is 114 ft. away from the manhole it is monitoring, and 53A which is located 132 ft away from the manhole. If moved, replacement costs will decrease. However, replacement costs would not be cheaper if it cost ten thousand dollars to move each station.

GRAPHING THE INFORMATION

A quantification of past operational findings will be used as a basis for the deciding the operational fate of these systems. Historical operations of the satellites have been graphed and from this graph criteria developed for future practices. A graph showing the entire operational history of the stations can be found in Appendix D. Operational status during the first full operational year

Satellite station 40B had problems in April. A new sampler was being installed because the old one was shorting out and many times the pick up tube was clogged. No samples could be taken in November and December because of problems with the compressor.

All previous logbooks were thrown out when they were full so an accurate evaluation for stations 51A and 86B is impossible. However, information has been predicted by averaging the number of months samplers in other stations operated in 1993. Since other samplers were off-line about two months out of the year, February and March were randomly selected as non-operational periods for 51A, and November and December were selected for 86B.

During 1993 a bad pump forced 53A off-line in January and February. In March and again in August, 69A had problems with clogging. A new sampler was installed in 125C in January and February. 177E had problems with the fill sensor during the month of June.

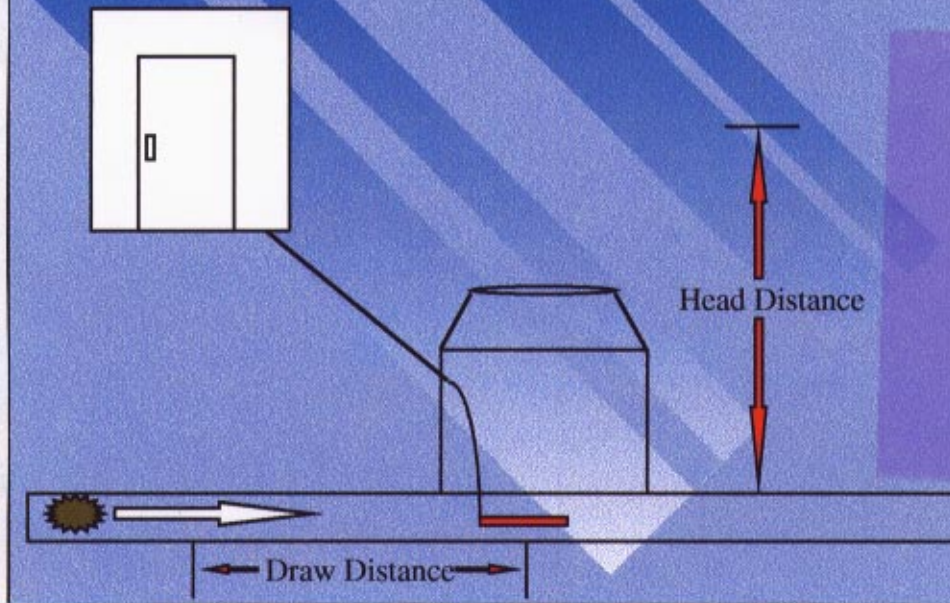
Over this year the operation the sampling equipment looks good because a lot of effort by trained technicians went into keeping these stations working properly. A trained technician would need 20 hrs/wk for routine maintenance and six additional hrs/wk for problems. It takes a trained and experienced technician to know how to trouble shoot. Maintenance times were reviewed with the technicians and Duane Rueppel, technical support group leader. Assumptions made in reviewing maintenance times and manpower hours for ten satellite stations include proper cleaning and upkeep of the equipment along with disinfection and use of appropriate personal protective equipment. All 1993 maintenance and manpower calculations can be found in Appendix E

EVALUATIONS OF PORTABLE MONITORING EQUIPMENT

Portable monitoring equipment was recommended and purchased for pH spill trace back and possible use in future monitoring stations. Sampling equipment was purchased to continuously monitor pH and collect a sample when triggered by pH events below 5.0 or above 10.0. The equipment purchased includes, two portable samplers with two pH probes and one refrigerated sampler with a pH probe and a flow meter. All equipment was checked upon arrival.

The following monitoring locations were selected. The portable samplers were assembled, programmed, and placed in manholes 87B and 286A, where they monitored pH for one week. The flow conditions at these two manholes were adequate but it was found that the design of the probe caused a tremendous amount of debris hang-up and clogging of the sewer pipe line. Down-loading information from the sampler to a laptop is possible, but was not done while the samplers were in place. The refrigerated sampler will be placed in SSS 177E. Station 177E is downstream of Hazardous Waste Management.

Problems Associated with Flow



Clogging is usually caused by a dry sewer. When paper products catch on the pick up tube and block the flow a sample can not be collected. Fill sensors operate the sampling by sensing when enough sample has been taken and shutting off the motor. When the fill sensors are not calibrated correctly the motor is worn out by continually trying to pull a sample. The sensors are very sensitive to moisture and therefore if there is a leak in the system the sensors will not work. They are calibrated according to head height. Past head height estimates were found in the "Procedure on Satellite Station Maintenance" (Appendix B) Values were checked in the field and recalculated using the "Sanitary Sewer Manhole and Lift Station Coordinates" drawing (Appendix C). Revised values are presented in the table below.

Manhole #	Draw (ft)	Head ₁ (ft)	Head ₂ (ft)
40B	85	5.8	10.3
51A	45	4.3	9.3
53A	132	6.8	7.4
69A	56	5.1	8.3
86B	76	6.1	5.5
125C	8	4.9	9.04
163A	114	11.7	8.5
177E	85	8.6	9.4
185F	40	4.1	7.6
213A	75	5.8	11.2

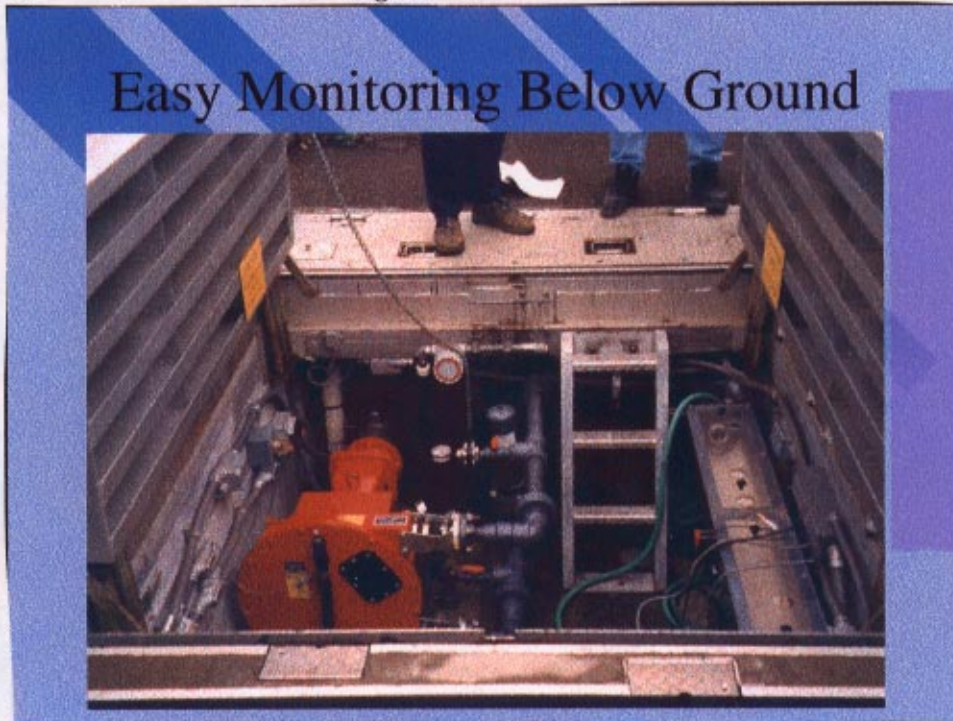
1- Head from "Procedure on Satellite Station Maintenance"

2- Head from "Sanitary Sewer Manhole and Lift Station Coordinates"

COMPARING FACILITIES

East Bay Municipal Utility District (EBMUD) was visited to discuss sewer sampling equipment. The practicality of pumping, using a parastatic pump, and monitoring the stream in a channel where pH, conductivity, and ORP probes could be placed, was discussed with Dave McMullen and Mike Walton, two Wastewater Control Inspectors. Several pictures were taken of this system (see Figure 8). The pump, channel, and all of the equipment, were in a vault approximately four feet below ground level. No confined space permit would be needed.

Figure 8



Other equipment discussed included an ISCO model 1640, liquid level sampler actuator which enables and disables a sampler when the contact detects flow. This equipment is to aid in sampling during low flow situations. Another very interesting improvisation was the use of a water bottle and duct tape to create a bowtie whereby a probe could float and accommodate several water levels.

They have a system much like our sewer satellite system which they call QMS (Quality Monitoring Stations). Seven stations were constructed four years ago. One field inspector, 20 hours per week was needed to maintain their system. This is comparable with our system, which requires 26 hours per week for 10 stations. Problems with grease, grit, and paper clogging the pick up lines, the tremendous cost burden and the fact that the stations were extremely time consuming, forced EBMUD to abandon the system. Due to these findings, monitoring the sewer instead of sampling is recommended for LLNL. Not only will monitoring eliminate the problems associated with sampling but it will also maintain spill trace back capabilities of the system.

A portable QMS is being developed which can monitor several parameters at the same time. A Campbell Scientific wiring panel, which can be triggered by cell phone to download readings, sits inside.

One problem with the system above is the telemetry lines. They have poor data transfer. Signals are often interfered and probes send false signals when fouled. This will be followed up with Ted Mayer a representative of Sharman Inc., who has spoken of the successful use of plastic manhole covers as an alternative/solution to these type of problems.

These systems look well thought out and impressive. Designing and installing an entire vault system would be over \$100,000. However, a down-scaled, trial model is highly recommended for LLNL. Answers to the transmitting problems may be found if LLNL and EBMUD work together.

FURTHER STUDY

Can stations be used to perform research testing on new monitoring technologies and instrumentation?

Would there be a significant time advantage to triggering the sewer diversion facility from stations 51A or 86B?

Can monitoring data be transmitted back to the environmental analyst's desktop for rapid response? With proper equipment data transfer is possible by phone lines or packet radios. A supervisory control and data acquisition system, otherwise known as SCADA, uses packet radios to monitor wastewater stations.

Can alarm notification be made to pager or voice-mail?

ALTERNATIVES

What makes sense for LLNL is a monitoring system instead of a sampling system because not only will monitoring eliminate the problems associated with sampling but it will also maintain spill trace back capabilities. Costs and funds available play a big role in what will be done in the future.

Employee awareness is an effective tool, in source minimization, but there will always be people who make mistakes. There is no additional benefit to increasing employee awareness when 99% of the employees know about proper disposal procedures. Education must continue, but it must be done in conjunction with satellite monitoring in order to trace back spills when someone is careless.

Flow rate and pH are the only parameters that will be continually monitored due to the soiling characteristics of the wastewater being monitored. Dissolved oxygen may be implemented in one or two stations to see if there are any relationships between a decrease in dissolved oxygen and pH. Historically, other parameters, such as temperature, show no large fluxuations, and therefore do not need to be monitored.

The following are not recommendations. These are all of the possible alternatives, good and bad. Each of the five were analyzed for installment costs and yearly maintenance.

1) Install 6 monitoring vaults and 4 portable

- year 1
 - » 2 trial models = \$200 k
 - » 20 hrs/week to maintain = \$25 k for the first year
- year 2
 - » 4 more vaults = \$400 k
 - » 40 hrs/week to maintain = \$50 k for the second year
- year 3
 - » 4 portable monitors = \$80 k
 - » 40 hrs/week to maintain = \$50 k for the third year to life

Total for this system is approx. \$800 k and yearly maintenance would be \$50 thousand. Designing and installing a vault system, like EBMUD, would be extremely costly. However, a down-scaled, trial model is highly recommended. The model would be made using equipment and supplies already at the lab. This would keep costs down while still testing the alternative.

The following three alternatives would not solve any of the problems mentioned.

2) Place 4-6 sampling stations on line.

30 hrs/week to maintain = 40 k / year

3) Maintain the 3 stations that are now sampling

- 20 hrs/week to maintain = 25 k / year

4) Stop all satellite sampling

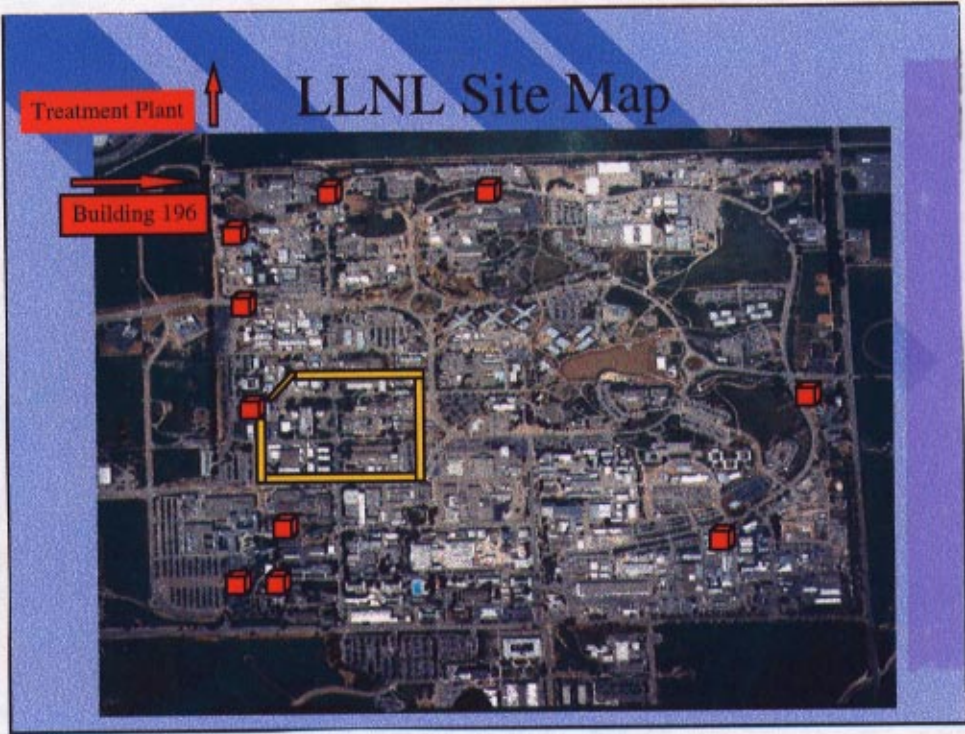
Regulatory drivers would intervene therefore this would only be an alternative to use as a transition stage between systems.

5) Place probes to monitor pH, in manholes and run the power lines and data up to the ten existing stations where the data could then be sent automatically, via radio, to a computer.

- probes can monitor pH, DO, temp., conductivity.
- cost 2K each to install = 20 k installation
- 30 hrs/week to maintain = 40 k / year
- Total = 20 k to install, 40 k / year to maintain

This alternative is recommended because: it is cost wise; it monitors the wastewater, therefore there are no problems associated with sampling; and, it maintains spill trace back capabilities.

Appendix A



Appendix B

EMP-SW-SSM-R

SATELLITE STATION MAINTENANCE

Prepared by: Brian Balke 4/5/93
Brian Balke date
Environmental Analyst, WGMG

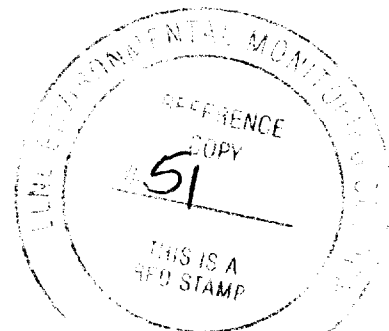
Reviewed by: Paul Dickinson 4/6/93
Paul Dickinson date
Environmental Technician, TSG

Renee Needens 4-6-93
Renee Needens date
Environmental Technician, TSG

Approved by: William G. Hoppes 4/7/93
William G. Hoppes date
Group Leader, WGMG

Rebecca A. Failor 4/7/93
Rebecca A. Failor date
Section Leader, EMS

Lucinda M. Garcia 4/7/93
Lucinda M. Garcia date
Quality Assurance Coordinator, EMS



1. PURPOSE

This procedure describes tri-weekly maintenance activities at the satellite sewer-monitoring stations.

2. DISCUSSION

Ten satellite sewer-monitoring stations, ranging from the south side of the Laboratory to its northwest corner, collect sewage samples from LLNL's sewer system. In the advent of an inadvertent introduction of contaminants, the appropriate samples are analyzed in order to permit a possible traceback to one of the various laboratory operations (see Attachment A for locations of satellite sewer-monitoring stations).

5 locations
set-up with
data com.
line + pH
cabling

CURRENT SATELLITE SEWER-MONITORING STATION LOCATIONS			
General Location	Manhole Number	Draw (ft)	Head (ft)
B231 North	40B	85	5.8
West of B190	51A	45	4.3
West Gate Dr and Ave A	53A	132	6.8
South of T1677	69A	56	5.1
East of B191	86B	76	6.1
North of 391	125C	8	4.9
South of B319	163A	114	11.7
T5226 North	177E	85	8.6
West of Visitor's Center	185F	40	4.1
B113 Northwest	231A	31	5.8

→ to Ground level
14"

Each satellite sewer monitoring station is equipped with a Manning 6900 Stationary Priority Contaminant Sampler, which is housed in a weatherproof, locked shelter measuring approximately 5 ft by 5 ft by 6 ft. Each station has a plumbed potable water supply, electrical power, lighting, ventilation, fans, heater, and a floor drain that is connected to the sanitary sewer system.

A buried, 1.5-inch polyvinyl chloride (PVC) pipe connects the station to the manhole that is to be monitored. Inside this pipe is a half-inch tygon hose, one end of which is connected to the sampler, the other end to a weighted strainer that is submerged in the sewage flow.

The 6900 Sampler has two major assemblies, "upper" and "lower". The upper assembly includes the controller. The lower base unit is refrigerated and contains the sample volume measuring and distribution assemblies, a circular bottle rack containing 24 sampling bottles (1,000 mL each), and a vacuum pump that draws the sample from the sewer pipe. On weekdays the samplers collect eight 50 mL samples per bottle at the rate of one sample every 15 minutes. At this setting it takes two hours to fill one sample bottle and 48 hours to fill the 24 bottles in the sampling carousel. On Friday, the sampling frequency is changed to once every 30 minutes to accommodate the extra weekend day. At this setting it takes 72 hours to fill 18 of the 24 bottles. Maintenance on the stations is required on Monday, Wednesday and Friday. This provides the broadest possible coverage of releases from facility operations, without requiring maintenance during nonwork hours.

If the monitoring equipment at Building 196 (Reference 1) detects the presence of contaminants in LLNL sewage, the WGMG analyst who is assessing the alarm will, if necessary, require that samples be submitted for analysis to aid in determining the time and place at which the release occurred (see Reference 2). Since sewage may take as long as three hours to travel from the point of release to Building 196, quite often the bottle currently being filled is not the bottle that should be

submitted for analysis. This document does not cover the procedure for acquiring the sample that is to be submitted for analysis; that procedure is described in Reference 3.

In addition to daily maintenance, on a monthly basis the sample bottles are changed and the measuring chamber cleaned. See Section 6.4.

A Manning 6900 Operation and Service Manual (Reference 4) is available at each satellite station.

3. REFERENCES

1. EMP-SW-AR, *Sewer Alarm Response*
2. EMP-SW-SID, *Sewer Spill Source Identification*
3. EMP-SW-SAS, *Sewer Satellite Station Alarm Sampling* **READ**
4. TN Technologies INC., *Installation and Operation Manual for the 6900 Stationary Priority Contaminant Sampler*
5. EMP-QA-DC, *Document Retention*

4. DEFINITIONS

Bottle Stay: When the sample bottles are hanging from the bottle plate, this large rubber O-ring pulls the bottle bodies into a compact bundle.

Bottle Plate: Plate with 24 mounting holes for positioning the 1,000 mL sample bottles relative to the distribution assembly.

Distribution Assembly: Located by two guide plates on the top of the bottle plate. An assembly consisting of a transparent measuring chamber with a scale (in milliliters) for reading the sample volume; a sensor for determining when the measuring chamber is filled to the desired volume; and a filler spout that sequences the sample stream to the sample bottles. During operation, the distribution assembly rests on the bottle plate. During sampling or maintenance, it is lifted away, and set on the brackets located in the refrigerator above the bottle plate.

Pinch Valve: AC solenoid driven pinching device. Closes off the sample tube allowing a vacuum to be applied to the measuring chamber. Allows sample to pass to the filler spout when sampling sequence is completed.

Power Switch: Controls connection to A/C power.

Refrigerator Subassembly: A refrigerated area containing the bottle rack with 24 sample bottles (1,000 mL each) and the distribution assembly.

Reserve Bottles: Last two filled bottles in the rack. Because of the direction of sewage flow, sampling at a station occurs prior to monitoring at B196, these bottles are set aside to allow trace-back of spills that passed the satellite station just before maintenance was started.

Filler Spout: Channels the sample to the proper bottle.

Sampling Volume: Determined by a mechanical adjustment to the siphon spiral in the measuring chamber. It is set to 50 mL.

Slide rack; Frame to hold the bottle plate when it is pulled out of the refrigerator; the weight of the bottle plate is supported via the slide rack by a triangular brace that rests against the lower inside edge of the refrigerator cabinet. Stored inside the shelter exterior to the sampler.

Stepper Motor: Rotates the filler spout to the next bottle.

5. RESPONSIBILITIES

5.1. WGMG ENVIRONMENTAL ANALYST

The WGMG (Water Guidance and Monitoring Group) Environmental Analyst is responsible for establishing the operating parameters of the sampling stations (sample frequency and volume). The Analyst also coordinates acquisition of alarm samples from the satellite stations, including the identification of locations and sampling times of the bottles to be collected.

5.2. TSG ENVIRONMENTAL TECHNICIAN

The TSG Environmental Technician is responsible for proper maintenance of the satellite stations, and for the physical collection of the samples.

5.3. WGMG GROUP LEADER

The WGMG Group Leader is responsible for ensuring that sufficient resources are allocated to allow maintenance to be completed in a timely fashion.

5.4. EMS SECTION LEADER

The EMS Section Leader is responsible for ensuring that sufficient resources are allocated to allow maintenance to be completed in a timely fashion.

6. PROCEDURE

Note: Occasional failures of the sampling equipment, or mishaps in the handling of samples, can result in the exposure of personnel to raw sewage. According to Hazards Control Industrial Hygienists, exposure to sewage is not a significant health hazard if reasonable hygienic steps are taken. When performing the procedures described below, gloves and other personal protective equipment should be worn. Exposed personnel should wash with disinfectant soap (PhisoHex soap, kept in Satellite Station 163A). If clothes become soaked with sewage, personnel should shower and change into clean clothing, and the soiled clothing should be washed as soon as possible.

6.1. PREOPERATION CHECKS AND PROGRAMMING

Equipment Required:

Face Shield (Stock catalog #4240-58220)
Kay-drys (Stock catalog #7999-63447)
Latex gloves, long (Stock catalog #8415-41567 and 77)

6.1.1. Prior to standard operation of the 6900 Sampler, preoperation checks and tests are to be performed using the procedures in Reference 4, pages 1-1 through 1-16.

6.1.2. The configuration and program parameters for the sampler will be established by the Environmental Analyst.

6.1.2.1. The configuration parameters are described on page 2-8 and 2-9 of Reference 4. The settings should be:

- 6.1.2.1.1. OP = 2
- 6.1.2.1.2. PLEP = 24
- 6.1.2.1.3. PH0 = 6
- 6.1.2.1.4. PH1 = 150
- 6.1.2.1.5. PH2 = 13
- 6.1.2.1.6. PH3 = 8
- 6.1.2.1.7. PHLL = 1
- 6.1.2.1.8. PE = 1
- 6.1.2.1.9. PL = 2
- 6.1.2.1.10. PPPP = 0000

6.1.2.2. The program parameters should be as follow.

6.1.2.2.1. Program the Single Time Interval for 15 minutes (page 2-14 of Reference 4).

6.1.2.2.2. Select eight (consecutive) samples per bottle (page 2-19 of Reference 4).

6.1.3. The sample volume should be adjusted to 50 mL. Follow the procedure on page 1-17 of Reference 4. The sampler is manufacturer designed for a 100 mL minimum sample. Therefore, to achieve a 50 mL sample volume, the outer sleeve of the purge tube must be pulled down 0.25" from the top of the chamber (in violation of step 2 on page 1-17) and the sleeve must be rotated so that the slit in the slit tube is completely covered. After the sampler is re-assembled, a sample should be taken to confirm the sample volume; the maximum allowable sample volume is 60 mL.

6.2. MAINTENANCE

Equipment Required:

Face Shield (Stock catalog #4240-58220)
Kay-drys (Stock catalog #7999-63447)
Latex gloves, long (Stock catalog #8415-41567 and 77)
Manhole hook (available from the Pipe Shop)
Pen
Pine Oil
Portable road barrier or traffic cones (available from Plant Engineering laborers)

When performing maintenance or collecting samples from sewer satellite stations, proper hygiene requires use of a face shield and long latex gloves.

As necessary the Environmental Technician must empty satellite stations trash cans while making maintenance rounds. The trash is to be put in large plastic bags such as those used by LLNL janitors, and the bags disposed of in any LLNL garbage dumpster.

Note: Always consult the alarm printout in Room 200 of Building 196 before performing routine maintenance. If an alarm has occurred since previous maintenance, notify the Environmental Analyst to determine which samples are to be saved when bottles are drained during routine maintenance. See reference 3 for alarm sampling instructions.

6.2.1. Unlock the shelter and open the door

6.2.2. Put on long latex gloves and plastic face shield.

6.2.3. Open the door on upper (control) assembly and use the ON/OFF toggle switch to turn the power off.

6.2.4. If the manhole is situated in the middle of a street or other traffic zone, use the portable road barrier or cones to block the road in the direction of approaching traffic. Using the manhole hook, remove the manhole cover. Clear debris from sampling line and then replace the manhole cover. Remove the road barrier or cones.

6.2.5. Open the door on the lower (refrigerator) assembly. Mentally note the position of the filler spout (see step 6.2.8 and 6.2.9). Lift the distribution assembly off of the bottle plate, and set it on the brackets located in the refrigerator above the bottle plate.

6.2.6. Attach the slide rack to the two pins at the front of the refrigerator. Set the foot of the slide rack on the lower inside edge of the refrigerator housing. Pull the bottle plate forward onto the slide rack.

6.2.7. Enter the date, time, and your initials in the field logbook stored in the satellite station. Inspect each bottle for total volume, abnormal sample coloration and condition of sample. Record any deviant conditions in the field logbook as well as the position of the filler spout.

6.2.8. Remove the bottle stay.

6.2.9. Drain the two reserve bottles stored in the bottom of the refrigerator. Remove the last two filled bottles from the rack. Cap the bottles: use the cap labelled "2" on the last bottle that was filled (the bottle that the filler spout was positioned over when the sampler was turned off). Place the bottles in the bottom of the refrigerator. Because there is a delay between sampling at a station and monitoring at B196, these bottles are set aside to allow trace-back of spills that passed the satellite station just before maintenance was started.

6.2.10. Remove each bottle from the bottle plate and empty the contents into the floor drain. Thoroughly flush the bottles (including the old reserve bottles), using the garden hose that is located outside the shelter. Thoroughly rinse the exteriors of the bottles.

6.2.11. Spray pine oil on the bottle plate and interior of the lower (refrigerator) assembly (including door panel, shelf, and floor of unit), and thoroughly rinse. Thoroughly rinse the satellite station floor.

Note: Take extreme care not to douse the stepper motor, located above the filler spout. Use of excess water will cause premature failure of this part.

6.2.12. Return the bottles to the bottle plate, being certain to put the bottle labeled "START" at the front of the bottle plate. Use the old reserve bottles to complete the set. Wrap the bundle with the bottle stay. Slide the bottle plate back into the refrigerator. Remove the slide rack and return it to its storage location inside the shelter exterior to the sampler.

6.2.13. Restore the distribution assembly to its operating position on the bottle plate. Manually rotate the filler spout counter-clockwise until it is positioned to dispense into the first bottle to the right of the "START" bottle.

6.2.14. Use the ON/OFF toggle switch to turn the sampler power on. Press the TIME button. Enter 00:15 hours on Monday and Wednesday and 00:30 hours on Friday. Press the ENTER button. Press the MULTI SAMPLE button. Enter 08. Press the ENTER button. Press the START button and then the TEST CYCLE button; a sample should be taken automatically. Check for proper functioning of the sampler. Proper functioning means that the:

- Sample filler spout advances to the "START" bottle.
- Sampler purges intake line with pressurized air.
- Pinch valve closes.
- Measuring chamber fills, without bubbles, to the correct volume (50 mL).
- Sample is dispensed to the sample bottle.

If there is a malfunction, switch off the sampler power and initiate repairs (section 6.3).

6.2.15. If the sampler has successfully taken a sample (the first of the eight samples for the "START" bottle), rinse the gloves and dry with Kaydrys. Place refuse in the trash can. Remove face shield and gloves, and store in shelter.

6.2.16. Close and lock the shelter.

6.3. SAMPLER MALFUNCTION

If the sampler does not function properly following maintenance, see Chapter 3 of Reference 4 for helpful troubleshooting and maintenance tips. The TN Technologies service department number and shipping instructions are in Appendix A of Reference 4.

6.4 MONTHLY MAINTENANCE

6.4.1 As necessary, but at least once a month, the measuring chamber is cleaned.

6.4.2. Once a month every sample bottle is removed from the bottle plate and soaked overnight in a chlorine solution at Building 196. The empty bottle plate is filled with previously soaked sample bottles.

7. DOCUMENTATION/QA RECORDS

Field logbooks shall be used to note all maintenance activities. The notes should include (as a minimum) sample location, date and time sampled, identity of the sampler, any difficulties or special circumstances, and the position of the filler spout. All field logbooks shall be archived according to the requirements of Reference 5.

8. ACCEPTANCE CRITERIA

Maintenance will be considered complete and acceptable if:

- The sampler, sample bottles, and satellite station are cleaned adequately to prevent contamination of samples (i.e., no sediments in bottles).
- In order to minimize exposure of personnel to sewage residue, the equipment is cleaned, at the very least, with the frequency and thoroughness described in this procedure.
- The sampler operates properly.
- Maintenance activities have been documented in the field logbook.

9. ATTACHMENTS

Attachment A: Locations of LLNL Satellite Sewer-monitoring Stations

Appendix C

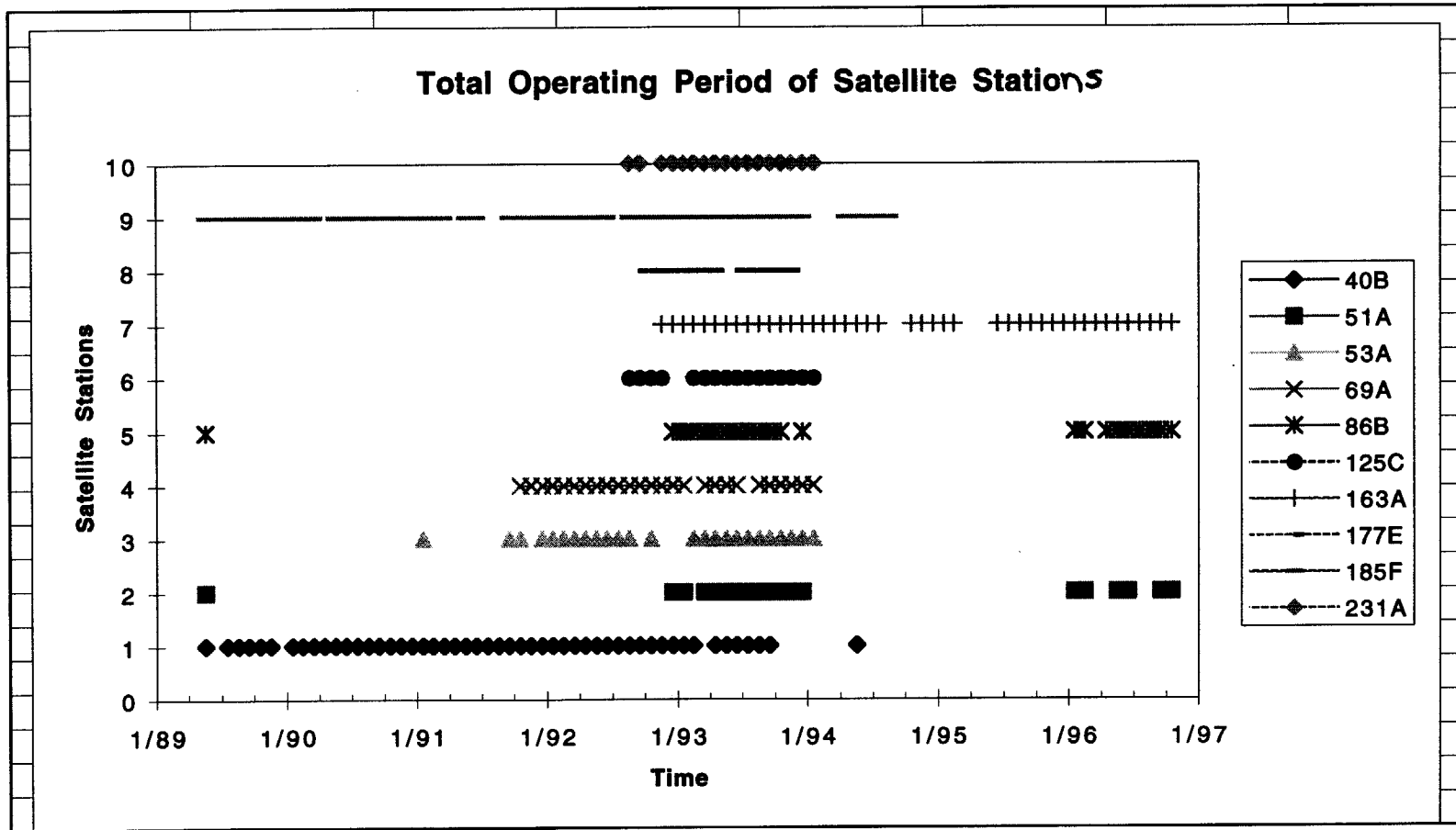
Unable to scan this page

For original report

**call
Reports Library**

x37097

Appendix D



Appendix E

MAINTENANCE

- *assume proper maintenance expected
- *assume personal protective equipment (goggles, gloves) used
- *assume proper disinfection
- *assume proper cleaning and drying of chambers and bottles once a week

Weekly maintenance = Routine Maintenance + Problem Maintenance

Routine Maintenance-

10 stations

check at B196 for alarm	10 min./day
maintenance	15 min./station
travel	10 min./station
total	35 min./station
35 min./station X 10 stations/day = 350min./day	
350 min/day X 3 days/week = 1050 min / week ~ 20 hours/week	

Problem Maintenance-

10 stations

8 hrs/month = 2hrs/wk to maintain 3 samplers
 2 hrs/ wk X 10 samplers/3 samplers ~ 6hrs /week

Weekly Maintenance = 20 hrs + 6 hrs = 26 hours X 1.2 (factor of safety) = 31hrs

Monthly Maintenance = 125 hours

Yearly Maintenance = 1498 hours ~ 1500 hours

Factor in: (holidays / vacations / meetings / sick leave & other)

TOTAL Maintenance = 40 hrs/week

Real-Time Earthquake Warning Using Artificial Neural Networks

Eric Jacobsen

The University of Dayton

**Lawrence Livermore National Laboratory
Livermore, California 94550**

12/20/96

Prepared in partial fulfillment of the requirements of the Science and Engineering Research Semester under the direction of Richard Leach Jr., Research Mentor, in the Lawrence Livermore National Laboratory.

This research was supported in part by an appointment to the U.S. Department of Energy Science and Engineering Research Semester (hereinafter called SERS) program administered by LLNL under Contract W-7405-Eng-48 with Lawrence Livermore National Laboratory.

By acceptance of this article, the publisher or recipient acknowledges the U.S. Government's right to retain a non-exclusive, royalty-free license in and to any copyright covering this article.

Real-Time Earthquake Warning Using Artificial Neural Networks

Eric Jacobsen, University of Dayton

Richard Leach Jr., LLNL Engineering Research Division

Lawrence Livermore National Laboratory
University of California, Livermore, CA 94550

Abstract

This report describes a neural network based earthquake early warning system. The system would estimate the complete time series immediately after the beginning of an earthquake and continuously update the estimate as the earthquake evolves. The estimates could be used to trigger automatic shut off systems or sound alarms before the most damaging shaking occurs.

A set of recorded time-series earthquake signals is prepared. Several signal pre-processing algorithms and neural network architectures are tested to minimize estimation error. The network is trained with a large portion of the available data, while some data is set aside for testing. Successful estimation is determined by the network's performance with the previously unseen data.

Because of recent damaging earthquakes such as Mexico City, Loma Prieta, Northridge, and Kobe, previously unavailable strong-motion recordings are now available. With this new data, we will try to further the research by addressing two important issues.

- Can the neural network be trained to estimate over a wide dynamic range of ground motion including very large (>7.0 MI) earthquakes?
- Can a neural network be trained to provide warning to a network of stations using recorded signals from all the stations as training input, as opposed to using data only from a single site?

Introduction

A short term real-time earthquake warning system based on an artificial neural network (ANN) is being developed. This study is a continuation of previous work, (Leach, 1996). The system is designed to give on the order of a few seconds to a minute of actual warning time before the onset of the most serious shaking in an earthquake. While at first this might not seem like a useful amount of warning time, there are several areas of applicability. First, with a reliable warning of up to a minute, automatic shut off systems could be implemented with this system. Industrial applications might include the shut down of major machinery, computer systems, or reactors in order to minimize damage, lost data, and casualties at the site. Damage and fatalities would also be decreased dramatically with reliable automatic shut off of pipes carrying gas, water, or other hazardous liquids. The system might also trigger warning announcements in schools, hospitals, public areas, and homes.

The science of earthquake warning can be divided into two primary categories of study. The most commonly researched paradigm is that of a distributed network of sensors with a central control center. When an earthquake is detected and determined to be dangerous at one station, the warning can be radioed ahead to sites needing protection along the predicted path of the earthquake. The actual warning time would be the difference between the time it takes the earthquake to propagate from the warning station to the site needing protection, and the time it takes the station to determine that the earthquake is dangerous. Potentially, several minutes of warning might be available. There are several disadvantages to this scheme, however. For one thing, a large distributed network is expensive and difficult to install and maintain. Further, a very fast central computer is necessary to process the large amounts of incoming data from all the

stations. Any delay in processing incoming signals decreases actual warning time. Finally, the problem of determining the severity of an earthquake is a highly nonlinear one. Simple threshold detectors or other linear algorithms might not be reliable enough for such a critical task. Also, actual ground acceleration is highly dependent on the properties of the earth at that point. Powerful waves propagating through hard ground might not set off a warning, while still having the potential to do damage at soft ground sites in its path. For the reverse case, there is the danger of false alarms. For these reasons, the distributed network paradigm of real-time earthquake warning may not be adequate.

An alternate paradigm, one that is the focus of this study, is that of a locally placed earthquake warning system. These smart sensors could be used independently to protect a single site, or as units in a distributed system to increase its performance. For now, only the single site application is considered. A three component accelerometer detects the incoming earthquake and makes an estimate of the incoming ground motion based on the real time data it has received. The actual warning time is the time from when the system makes an accurate estimation of the complete earthquake to when the most severe shaking occurs. Instead of a linear detection algorithm, a neural network is used that has been trained on previous earthquakes from that region. In general, ANNs are good for processing non-linear data such as incoming earthquake signals. Analogous to the type of processing that takes place in our brain, ANN processing is well suited for applications such as pattern recognition and interpolation and extrapolation from incomplete data. By training a network with earthquake distributed both in size and location about a site, we are giving it small pieces of the total puzzle of characterizing an entire region.

The highly non-linear aspect of earthquakes is the result of their being made up of various different kinds of waves, all of which propagate in different ways through varying medium

before recombining at the recording station to make of a single complicated seismogram. For the purpose of our study, we focus on the two prominent types of earthquake waves. The first arriving elastic wave is called the primary (P) wave. This is a compression wave, one which causes the material through which it propagates to move back and forth parallel to the direction of wave travel. This is the fastest type of seismic wave, traveling about 5.5 km/sec through granite (Bolt, 1978). Another kind of wave is the secondary (S) wave. It is a sinusoidal wave in that the material through which it travels moves laterally to the direction of the wave. S waves are inherently slower than P waves, traveling about 3 km/sec through granite (Bolt, 1978). The S waves, however, are the most damaging. They are generally of a lower frequency and cause more ground shaking than P waves. It is the S waves which usually cause most of the damage associated with an earthquake. Utilizing the differences in their respective travel times, we hope to use the information contained in the P arrival to predict the incoming S arrival before it hits the site. Certain characteristics of the P wave including but not limited to maximum acceleration and total energy might be correlated with certain S wave arrivals for a specific region. The adaptive non-linear processing of a neural network can sort through these complex signals to form useful categories for estimation.

DATA GATHERING

One of the primary things I was concerned with during my work on the project was gathering an adequate data set of earthquakes with which to train the neural network. Previously, a large data set of over 400 earthquake seismograms recorded near Landers, California, was gathered and used to train a neural network (Leach, 1996). This data set had a good geographic distribution around the recording station, as well as a fairly good distribution of earthquake

magnitudes, ranging from 2.0 to 5.5 M_L . However, noticeably lacking were any large magnitude earthquakes, those capable of causing severe damage. One of the criteria that we imposed on our sought after data set was that it contain at least a few very large earthquakes. There is a controversy among seismologists as to whether large magnitude quakes are qualitatively different from smaller, more common quakes. While neural networks are known for their powers of extrapolation, it seems reasonable that with a few examples of the large magnitude earthquakes in its training set, an ANN would have an easier time estimating the arrival of a real, strong motion earthquake.

By setting this criteria, however, a big limitation was put on our possibilities. Only in the last ten years or so have many strong motion sensors been in place that were adequate for our research. The region had to be quite seismically active, including several large earthquakes, and the station needed to be in operation for several years if we were to hope to gather a large enough data set. Further, we required the sensors to have a pre-event buffer, in order that the critical first seconds of the quake were not lost due to late triggering of the instrument. Several locations were suggested that might provide us with a large amount of data.

The Kyoshin Net in Japan is a recently installed network of over 1000 strong motion sensors arrayed across the country. Someday this will offer a wealth of training data, but because most of the sensors have been operating less than a year, too few earthquakes have occurred to make any one location desirable for study. In Taiwan, an accelerograph array called SMART2 has been in operation since late 1990 (Beresnev, 1994). Like Japan, this is a very seismically active area and there is much potential for a strong data set from this area. However, at this time the data was unavailable to us.

Another possibility is a strong motion recorder on Adak Island, Alaska. The region has been very active and the sensor has been operating since 1993. There was a very large series of earthquakes and aftershocks in June of 1996. We have not yet pursued locating this data, but it may be available through the Iris Data Management Center.

Several factors contributed to the final decision to use a large data set of earthquakes from the Guerrero region of Mexico (Anderson, 1995). First, there has been an accelerometer array of around 30 stations operating since early 1985. This is by far the oldest array of those we looked at. Further, the very severe Mexico City earthquake of September, 1985 took place in the region and is included in the data set. For the most part, the quality of the recordings is adequate for our purposes. Most but not all of the recordings have the first seconds of shaking intact. Finally, and perhaps most importantly, the data is readily available over the internet from the University of Nevada, Reno at <http://www.seismo.unr.edu/ftp/zeng/GUERRERO/guerrero.html>. The data set includes over 1000 seismograms from over 300 earthquakes in the region. The files are in ASCII format with limited header information. They were converted to Seismic Analysis Code (SAC) format for use. Some of the appropriate header information has been inserted into the files such as recording station latitude, longitude, elevation, and station name. Ideally we would like to include the event latitude and longitude, depth, and magnitude information. This data is available for all earthquakes in the region during the period of recording, however it has not yet been correlated with the actual data files.

After the SAC files were created and some limited header information was included, we individually looked at each three component seismogram to determine its quality. The majority of the recordings were kept for further study, but some were set aside for various reasons. These included poor signal to noise ratio, a very short recording time, or a missing component. There is

still much work to be done preparing the data files for use. Even so, the remaining data was used for some preliminary pre-processing and neural network training studies.

Although there is a large amount of data from the Guerrero network, there is not an overwhelming number of recordings from any one site. On average, each earthquake was only seen by three recording stations. This distribution of the 300 earthquakes among the 30 stations effectively reduces the size of the data set. Because of this, we do not believe that we will have a large enough set from any single station to train a neural network as in the previous study. Instead, due to the limited data, we have shifted our focus slightly and will attempt to characterize the *entire* region. Using the location of the station as an additional input value to the neural network will hopefully allow it to learn different characteristics of different stations and different parts of the region. Then, when testing the data, hopefully the network will identify certain characteristics by which station the signal was recorded on. This problem of characterizing an entire region has never been attempted before and the results should prove interesting.

PRE-PROCESSING

Before a set of seismograms can be used to train a neural network, certain pre-processing steps need to be taken. The primary reason for this is to simplify the job of the neural network by getting rid of extraneous information contained in the signals. Some of the pre-processing algorithms which were performed in the previous study are time series envelope, frequency spectrum envelope, cumulative absolute velocity (CAV), peak ground acceleration (PGA), as well as an estimate of the direction of the incoming earthquake in the form of incidence angle and backazimuth (Leach, 1996). At this point in the current study, only some of these pre-

processing steps have been taken. The time-series envelope and the angle estimates are being used currently. Future plans include frequency spectrum envelopes and perhaps distance from epicenter estimates.

First, Matlab is used to create files of input and output windows. There are several steps and options to this process.

- Each three component record is converted from SAC format.
- The three components are algebraically added together, and an envelope of the resulting signal is made by the equation,

$$e = \sqrt{(x^2 + y^2)} \quad (1)$$

where x is the original signal and y is the Hilbert transform of x .

- The resulting envelope is then normalized by dividing the maximum value into each value of the signal. This retains the shape of the signal while allowing the network to compare earthquakes of different magnitudes.
- Finally, windows of increasing length are made from the beginning of the resulting normalized envelope. About five windows are created, ranging in length from 0.5 seconds to 8 seconds, each starting at the beginning of the earthquake. Each window is composed of 10 equally spaced samples across the window. Also, output windows of 30 seconds are taken across the entire signal. With the shorter windows as input, and the entire signal as output, these windows are used as training data to the neural network. Windows of increasing length are used in order to capture the emerging properties of the earthquake.

These input and output windows are created for each earthquake in the data set. Then the data is compiled into one large training file for use in the neural network training.

NEURAL NET TRAINING

All training and testing was done using software developed here at LLNL. The program 'learn' allows for many variations on neural network architecture and training method. It is based on the conjugate gradient method of reducing errors (Johansson, 1990). The program learns from the data compiled in the training file of the previous section. For each of the input windows, the network is expected to learn the appropriate output waveform. Because of time

limitations, we were not able to produce any successful neural network results. However, work is continuing and it is hoped that results at least as successful as those in the previous study will be found (Leach, 1996).

A successful training session would be one in which the correlation between the actual output waveforms and those given by the network for each of the training examples is on the order of 95% to 98% correlation. Correlation for testing data, those seismograms which the network has not seen previously, may be slightly less. To declare success in the testing of a neural network, this should be relatively high as well ($> 95\%$). One situation when the training appears successful while the testing is not successful occurs when the network memorizes the data. With enough nodes in the network, a neural network will be able to memorize almost any data set. It will perform at almost a 100% correlation level for the training data, yet will flail miserably with earthquakes it has not been trained with. This happens when the network is trained too long. Instead of generalizing to common patterns between the data, those patterns which may be universal to the type of data one is trying to characterize, the network has simply memorized the examples which were presented to it and has lost its ability to generalize.

It is hoped that with further study, both on the pre-processing and the determination of the best network architecture, a high level of success may be found for both training and testing data.

CONCLUSION

Much groundwork has been done to prepare the way for further study on this topic. Building from the previous study, we have built a new data set and developed many of the pre-processing algorithms necessary to prepare it for training in a neural network. Some preliminary results have shown that we are on the right track yet still have much work to do before we have a

successfully trained and tested network. We are continuing work on the project in the hopes of answering the questions posed at the beginning. Can we build on previous work with a data set that includes much larger earthquakes as well as many smaller earthquakes? Also, can we train a network to characterize an entire region, using data from multiple stations, rather than characterizing a single station?

ACKNOWLEDGMENTS

I would like to thank my mentor Richard Leach Jr. for giving me the opportunity to work with this project, Larry Hutching for helping me out with earthquake theory as well as giving me the opportunity to do some field work, and Farid Dowla for his support and teaching me a bit about neural networks. I encourage those of you eager for more knowledge about earthquakes, neural networks, or the integration of both to read the references that taught and inspired me, especially Bolt, Churchland, and Leach.

REFERENCES

- Anderson, J. G., and Q. Chen (1995). Beginnings of Earthquakes in the Mexican Subduction Zone on Strong-Motion Accelerograms. *Bull. Seism. Soc. Am.* 85, 1107-1115.
- Beresnev, I. A., K. Wen, and Y. T. Yeh (1994). Source, path and site effects on dominant frequency and spatial variation of strong ground motion recorded by SMART1 and SMART2 arrays in Taiwan. *Earthquake Engineering and Structural Dynamics*, 23, 583-597.
- Bolt, B. A. (1978). *Earthquakes, A Primer*. W. H. Freeman and Company, San Francisco, CA.
- Churchland, P. M. (1995). *The engine of reason, the seat of the soul: a philosophical journey into the brain*. MIT Press, Cambridge, Mass.
- Hertz J., K. Anders, and R. G. Palmer (1990). *Introduction to the Theory of Neural Computation. Lecture notes Vol. 1., Santa Fe Institute Studies in the Sciences of Complexity*. Addison-Wesley, Menlo Park, CA.
- Johansson, E. M., F. U. Dowla, and D. M. Goodman (1990). Backpropagation Learning for Multi-Layer Feed-Forward Neural Networks Using the Conjugate Gradient Method. *Lawrence Livermore National Laboratory report UCRL-JC-104850*. Livermore, CA.
- Leach, R. R., F. U. Dowla (1996). Earthquake Early Warning System using Real-time Signal Processing. *Lawrence Livermore National Laboratory report UCRL-JC-123270*. Livermore, CA.
- Lomnitz, C. (1994). *Fundamentals of Earthquake Prediction*. Wiley, New York.

Identifying Barriers and Facilitators to Curriculum Reform*

Erin Kraut

Saint Mary's College of California

Lawrence Livermore National Laboratory
Livermore, California 94550

December 20, 1996

Prepare in partial fulfillment of the requirements of the Science Engineering Research Semester under the direction of Richard Farnsworth, Research Mentor, in the Lawrence Livermore National Laboratory.

*This research was supported in part by an appointment to the U.S. Department of Energy Science and Engineering Research Semester (hereinafter called SERS) program administered by LLNL under Contract W-7405-Eng-48 with Lawrence Livermore National Laboratory.

If this paper is to be published, a copyright disclaimer must also appear on the cover sheet as follows:

By acceptance of this article, the publisher or recipient acknowledges the U.S. Government's right to retain a non-exclusive, royalty-free license in and to any copyright covering this article.

Abstract

The purpose of this study is to review and synthesize the research literature referring to barriers and facilitators to implementing new curriculum and instructional techniques. The methodology consisted of an extensive literature search of the ERIC database and the MELVYL database. There was also an Internet search to locate titles and references to original sources. Several research reports on schools attempting to implement new curriculum programs and/or instructional techniques were examined.

Results from the review identified ten conditions that appear to facilitate successful implementation: 1) leadership, 2) teacher empowerment, 3) professional development, 4) guidelines, 5) embrace problems, 6) program monitoring, 7) district support, 8) resources, 9) incentive programs, 10) information dissemination. Successful schools implemented at least five of the conditions concurrently.

The major consensus is that successful reform requires established goals and a vision, fundamental pedagogical changes and time. Changes that take place over time must be inclusive and tied to established goals.

Identifying Barriers and Facilitators **to Curriculum Reform**

by
Erin Kraut

Curriculum reform is one objective of our educational system in the 20th century. Changes must be made in our educational system in order to meet the demands of our changing social and economic structure (Thompson, 1994). Our students must be prepared to compete in a scientific and technological workforce that requires the ability to learn, think critically and creatively, problem solve, and work as a member of a team (NRC, 1996; National Commission on Excellence in Education, 1983). These skills will allow our nation to remain competitive in the international marketplace. (NRC, 1996)

The publication of A Nation at Risk in 1983 sparked a new wave of reform efforts. This document was a warning to the American people that our place as world leaders in industry, science and technology is being threatened by our indifferent educational performance and standards (National Commission on Excellence in Education, 1983, pg. 1).

Support from the National Governors Association, the National Education Goals Panel and the National Science Teachers Association (NSTA) led to the development of the National Science Education Standards (1994). A major goal of the Standards is to ensure scientific literacy upon high school graduation by changing the way teachers teach and changing the way students learn.

The implementation of programs aimed at altering teachers and students' roles in the classroom is a long, complex process. The purpose of this study is to review and synthesize the research literature referring to the barriers and facilitators to implementing new curriculum and instructional techniques.

Methodology

The methodology consisted of a literature search of the ERIC database and the MELVYL database. MELVYL consists of a catalog of books for UC and California State Libraries, a catalog of periodical titles for UC and academic libraries of California, journal article information, abstracts, and text in major subject areas and Internet access to databases and systems across the world. There was also an Internet search to locate titles and references to original sources. The keywords used to locate pertinent articles were curriculum development, educational change, resistance to change, curriculum problems, teacher influence, program effectiveness, program evaluation and program development. The criteria for selecting research articles required that schools in the study were attempting to implement new curriculum programs and/or instructional techniques. The articles also had to determine whether the reform efforts were successful. Successful implementation was determined by whether the objectives of the program were met. Research reports on schools attempting to implement new curriculum programs and/or instructional techniques were examined. Findings were summarized from 10 case studies, 12 research articles and 15 best practice articles.

Data

Although most of the schools examined were implementing programs in line with the Standards, it is important to note that this research review does not deal with the types of curriculum being implemented. This study examined the implementation approach schools used with new curriculum programs, not curriculum content.

Only one review of research on curriculum reform was located (Butt, 1984). The articles Butt reviewed were published after the unsuccessful reform efforts of the 60's and 70's, but prior to the reform efforts that began subsequent to the release of A Nation at Risk. Butt's findings suggest that successful reform requires (a) mutual understanding and agreed upon changes between those trying to implement change inside the classroom (teachers) and those imposing change from outside the classroom

(curriculum developers, administrators, etc.), (b) a holistic, school based approach to change, (c) focus on teacher beliefs and resistance through professional development, training and support, (d) agreed upon goals, objectives and efforts to meet them, (e) commitment and continuity over time, (f) curriculum implementation must become a research process, (g) change in supervisory relationships. The findings in this review are similar to what Butt found in 1984.

Three Key Factors to Successful Curriculum Reform Efforts

The findings in this review can be summarized into three key factors to successful reform efforts. The three factors are establishing goals, making fundamental pedagogical changes and giving reform efforts adequate time to make an impact on teaching methods and student performance. The factors are discussed in detail as follows.

Goals/Vision

There must be established goals and a vision for change (Hansen, 1989). Reformers must have agreed upon goals regarding student and/or teacher outcomes and changes must be tied to these goals. Establishing goals coordinates reform efforts and assists everyone to move in the same direction. Goals also act as a motivator for change when participants in reform efforts view them as worthwhile and attainable (Kelly & Protsik, 1996;).

Fundamental Pedagogical Changes

When schools are attempting to implement new curricula programs it is important to acknowledge teacher beliefs, attitudes and feelings. For example, in referring to mathematics..."It is the teacher who establishes the classroom learning environment and the instructional activities for students. It is the teacher who communicates an attitude toward, and a vision of, mathematics and helps students construct their mathematical understanding." (Mumme & Weisglass, 1988). Change ultimately occurs at the classroom level through the interaction of student and teachers in new, productive ways (Honig, 1988).

Teacher beliefs and attitudes have a strong influence on curriculum implementation. As stated by Olson (1981), teachers tend to translate intended curricula to match their beliefs. They deal with change depending on how they define their role in the classroom and the role of their students. They allocate time to various curricular content due to their attitudes towards the subject matter and the amount of enjoyment they experience teaching it (Cronin-Jones, 1991).

Olson's case study (1981), of teacher influence in the classroom shows how teachers translate the concepts of innovative programs into a form that reflects their concern to keep their influence in the classroom strong. The teachers could not move from their familiar "high influence" teaching methods (lectures, seat work, firm control over direction of lesson) to the "low influence" teaching methods of the new curriculum (discussion lessons, student seminars, social debates) (Olson, 1981, pg. 266)

Bruckerhoffs study of the Cleveland Problem Solving Infusion Project (PSIP) (1995) reported that teachers negative, destructive attitudes towards the school system and curriculum hindered successful implementation (Bruckerhoff, 1995, pg. 10). Teachers felt that the curriculum had little to do with the districts course of study and doubted the goals of the project would be met. Lack of support from the school administration added to teachers resistance to develop and implement the intended curriculum.

Although teacher attitudes and behavior created resistance to the implementation of PSIP (Bruckerhoff, 1995, pg 3), the blame cannot be put sole on the teachers. Reformers must be careful of the word resistance. It often masks the real problems of implementation (diffuse objectives, lack of technical skill, insufficient resources). Fullan & Miles (1992) state that "Change does involve individual attitudes and behaviors, but they need to be framed as natural responses to transition, not misunderstood as resistance" (Fullan/Miles, 1992, pg 14).

Mistaking slow progress as resistance is the downfall of many reform efforts. This concepts leads to the third key factor of successful reform - time.

Time

Crosswhite (1989) states "Enduring change comes slowly and deliberately -- more through evolution than through revolution (Crosswhite,1989, pg 7). The downfall of many reform efforts is that new programs are not given adequate time to work (Smith, 1993). When reformers do not see immediate, positive results they quickly move on to another proposed solution. Successful reform efforts take patience, persistence and time - a period of years, not months. (Anderson, 1994; Jacobs, 1989; Parker, 1991)

These three key factors for success, 1) goals, 2) fundamental pedagogical changes and 3) time, are attainable when certain conditions are present in curriculum reform plans. The research review identified ten conditions which have a positive affect on curriculum reform efforts. The most successful schools implemented several of these conditions at once. The ten conditions are (a) leadership, (b) teacher empowerment, (c) professional development, (d) guidelines, (e) embrace problems, (f) monitoring/assessment, (g) district support, (h) resources, (i) incentive programs, (j) information dissemination.

It is important that these conditions be implemented concurrently. In their policy document, AAAS (1989) state "Piecemeal reform measures beget piecemeal effects, if any" (AAAS, 1989, pg. 156) The book goes on to state that reform efforts must be inclusive and changes be compatible so as not to cancel each other out (AAAS, 1989, pg 157).

Bruckerhoff's study (1995), indicated that non-inclusive efforts was one attributing factor to the failure of the Cleveland PSIP. Cleveland teachers were expected to implement a new form of curriculum, but changes were not made to the system to make the curriculum implementation successful (Bruckerhoff, 1995, pg. 6). The most appropriate use of the PSIP instruction required that students do work in the math lab, but taking students to the math lab took up a considerable amount of time. The 40 minute class periods

made it nearly impossible to use the PSIP instruction. As a result, teachers preferred to stay in their classroom and use the available resources, which were not necessarily the most appropriate for PSIP (Bruckerhoff, 1995, pg. 10).

In 1990, Kentucky passed the Kentucky Education Reform Act (KERA) which has had an impact on all areas of the Kentucky education system (David, 1994). All ten conditions are found in the KERA implementation model (Kelley & Protsik, In Press).

In most cases, successful schools did not implement all ten conditions listed above. However, most of the successful schools implemented a similar grouping of conditions. Some of the conditions appear to facilitate change more than others. These conditions can be broken down into three levels, based on the degree in which they appear to facilitate change, as shown in table 1.

The conditions will be discussed in detail and findings from the review of research will be used to support the level of importance they play in successful implementation. Foremost, it is important to establish what constitutes successful implementation.

Table 1. Condition Levels

Critical Level	Moderate Level	Low Level
<p>Conditions in this level were found in most of the successful schools. Absence of these conditions constitute barriers to successful implementation.</p>	<p>Conditions in this level were found in many successful schools. Absence of these conditions can create resistance to successful implementation, but are not necessarily barriers within themselves.</p>	<p>Conditions in this level were found in some successful schools. Absence of these conditions appear to have no affect on successful implementation.</p>

One determining factor of success is that the program be implemented in its intended form. However, absolute success is determined by whether the goals and desired outcomes of the project are met. In some cases this means that the program should *not* be implemented in its intended form. Sometimes changes need to be made in order to ensure that desired outcomes are met. Michael Fullan refers to this as the mutual adaptation perspective, changes take place as a result of adaptations made by users as they work with new programs (Fullan, 1991 pg. 38) This will be discussed in more detail in the section dealing with program monitoring.

Critical Level Conditions

Guidelines/Goals

Mohrman, Robertson, & Wholstetter (1995), state that it is very important at the beginning of any project that specific guidelines regarding project outcomes are established. Using district, state, and national guidelines to focus reform efforts provides direction and boundaries for new curriculum and instructional techniques.

In the case of the Cleveland Problem Solving Infusion Project, the goal was to make math curriculum consistent with NCTM Standards. However, the intended curriculum did not match up with district guidelines. The lack of alignment between district and curriculum guidelines discouraged teachers from developing and using the new curriculum. Teachers risked losing their jobs if they did not comply with the districts competency based learning strategy (Bruckerhoff, 1995).

Aligning changes within texts, tests, technology and teacher development improve the chance for successful reform . "School, district, state and higher education leadership can coordinate these key factors in a teachers repertoire to enhance rather than combat one another" (Wiske & Levinson, 1992, pg. 8).

Teacher Empowerment

Empowering teachers to make decisions regarding curriculum, budget, personnel, and staff development is an important element to successful reform (Jacobs, 1989; Johnston, 1995; Elmore, McCarthy & Peterson, 1996). Decision making develops a sense of ownership, and this makes teachers more likely to implement new curriculum (Saranchuck, 1995). Successful programs give teachers the flexibility to make decisions regarding curriculum content and delivery (Policy Studies Associates, 1994; Hansen, 1989).

In their policy document, Project 2061, AAAS assert that teachers are less willing to implement new curriculum programs if they feel they are being forced upon them "...reform cannot be imposed on teachers from the top down or the outside in" (AAAS, 1989, pg. 155).

Cleveland teachers had to deal with the tight limits placed on them by local principles regarding curriculum decisions. Teachers were discouraged from developing and implementing the intended curriculum and instead, were pressured to follow the objectives of the official course of study. This caused anger and frustration among the teachers over empowerment issues. One teacher explained

"The administration is beating up on teachers for failing kids. Some principles demean teachers who consistently hold high standards and threaten these same teachers with lower evaluations. So, we keep two records: one we use for teaching and one we turn in to keep our jobs" (Bruckerhoff, pg 7).

Teachers need to understand how important their role is in creating change. A true sense of empowerment can mean the difference between a successful and unsuccessful program.

Professional Development

Professional development involves workshops on a variety of subjects as well as collaboration opportunities. Teachers and administrators are

involved in the planning and implementation of the most successful professional development activities.

Professional development is an essential component of curriculum reform efforts, yet most districts do not provide necessary funding for such activities "...advocates have yet to make an argument compelling enough to spark such an investment." (Cornett & Gaines, 1995)

There are three basic reasons why workshops should be held: (a) instruct teachers how to use new curriculum. Teachers must be well prepared and instructed for new content and approach if a program is going to be implemented in its intended form; (b) to give teachers an understanding of the theory behind the curriculum development. Teachers are more likely to implement a new program as its intended, if they understand why the curriculum was developed and the function each lesson plays (Saranchuck, 1995); (c) to increase teacher professionalism. If teachers are expected to take on new roles in the classroom they must acquire new skills to do so (Johnston, 1995). It is important for administrators to understand this and give teachers the support and training they need to make the expected changes. (Bondy, 1994).

Professional development does not work as a one time event (Elmore, McCarthy & Peterson, 1996). The consensus is that successful curriculum implementation takes a minimum of three to five years of extensive workshops (Wiske & Levinson, 1992). Understanding develops with time and repeated encounters with ideas (Saranchuck, 1995).

In their study of teachers implementing the NCTM Standards, Wiske & Levinson (1992) found that teachers who were most comfortable integrating the Standards and pedagogy were those who participated in extensive staff development and coaching. They also participated in guided inquiry of mathematics (instead of just being told), observed successful teachers, and practiced new methods under observation and coaching by experienced colleagues. (Wiske & Levinson, 1992, pg.11)

Collaboration opportunities are important when it comes to making any type of change. Teachers, parents, administrators, curriculum developers, and mentors need to communicate with each other to understand where obstacles lie and how best to overcome them. Sharing problems and successes with a new program leads to new ideas and keeps participants motivated to continue (Leiberman & Miller, 1990).

Providing release time, stipends and convenient scheduling for teachers increases the success rate of professional development activities (Mumme & Weisglass, 1988; Mohrman, Robertson & Wohlstetter 1995; Bondy, 1994).

Leadership

An essential component of successful curriculum reform is strong, consistent leadership (Bondy, 1994). Changes in administration pose a constant threat to project success. Strong administrative support provides stability and continuity to a new project which collapses when principles are transferred in the midst of restructuring efforts (Policy Studies Associates, 1994). Fullan and Miles (1992), indicate other characteristics of a good administrative leader such as 1) providing teacher support (Smith, 1993), 2) creating a safe environment for change and 3) encouraging teachers to take risks for the sake of change (Fullan/Miles, 1992).

Embrace problems/take risks

Fullan & Miles (1992) use the term "implementation dip" to remind reformers that things will go wrong before they go right. It is important to understand and address this issue or frustration will hinder successful implementation. The most successful schools embrace problems, take risks and develop good coping skills such as tracking and monitoring problems and making structural changes to find solutions (Elmore, McCarthy & Peterson, 1996). "It is important to make a commitment to change and not be afraid to take the necessary risks" (Policy Studies Associates, 1994).

Implementation problems of reform efforts can make policy makers and practitioners view reforms as too complex or ambitious for schools to

accomplish. But if implementation efforts are seen as an opportunity to focus on capacity problems and make improvements, there is a greater chance for success.

Program Monitoring

Analyzing and understanding problems leads to solutions. Monitoring a program over time is the only way to identify problems and make changes accordingly (Jacobs, 1989). Each school has different structure, needs and problems which means there is not a program that will fit the needs of every school. Therefore, it is important that schools use the mutual adaptation perspective - assess whether the desired outcomes/objectives are being met and make changes based on these assessments (Fullan, 1991, pg. 38).

Flexibility and constant evolution was a key factor to the success of schools participating in schoolwide projects "...summary plan is fluid and can be changed totally or in part when it no longer meets the needs of all students" (Policy Studies Associates, 1994).

Supporting Conditions at the Moderate Level

District Support

In most cases, district support is not so much a facilitator for reform, but its absence can pose barriers. In other words, real change occurs at the school level, when the district does not hinder reform efforts. The best district support is in the form of school-based management. States and districts can support reform efforts by giving schools the freedom to make decisions regarding budget, curriculum and personnel (Bondy, 1994).

One example of the district being a barrier was in the Cleveland school district. The district chose interviewees when positions were open and the schools conducted the interviews. There were three open positions and the district sent three people to be interviewed. This left the school with no choice of flexibility over staffing (Bruckerhoff, 1995).

Another way in which districts can hinder reform efforts is through student assessment measures. If standardized tests required by the district (to

assess student achievement and teacher performance) are not aligned with new curriculum programs, teachers must choose what content to use in the classroom. If teachers choose to spend less time covering the content found in the standardized tests, it could result in poor student test performance which reflects poorly on teachers and could result in teacher transfers, close supervision, or being fired. In many cases, standardized tests required by school districts discouraged teachers from implementing new curriculum. "...assessment currently constitutes a gaping hole in the fabric of curricular change." (Wiske & Levinson, 1993)

New curriculum requires new assessment measures. The focus of Kentucky's reform strategy is to align assessment and curriculum. Kentucky replaced its old standardized testing program with a new assessment approach, the Kentucky Instructional Results Information System (KIRIS). KIRIS consists of multiple choice items, performance evaluations, open-ended items and portfolio sections developed in conjunction with the state curriculum framework. The hope is that school-developed curricula will be based on these state-level measures. The reform is structured so curriculum and assessment will mesh.

Some teachers participating in KERA felt that the district did not define curriculum content well enough to prepare students for the KIRIS assessment. Others felt that the assessment caused an overly focused instructional program which gave teachers less curriculum flexibility. These factors contributed to the stress teachers and principals experienced due to the KIRIS assessment measures. (Kelley & Protsik, 1996).

Findings in Cox's study (1983) of external and local facilitators show that the clusters of activity formed by local facilitators (district personnel) seem to be a critical component of successful school improvement efforts. The study contradicts other findings that districts are not facilitators for change, since many schools were successful without the assistance of local facilitators (Johnston, 1995). However, schools in other studies that did not have local facilitators were able to form similar "clusters of activity" through

other means such as strong leadership and motivated staff (Mohrman, Robertson & Wohlstetter, 1995). Therefore these studies suggest that successful reform is attainable without district support as long as other conditions are present within school reform strategies.

Resources

When resources are defined as curriculum materials, these do not appear to be a big factor in successful reform efforts. In most cases, the necessary resources were provided as part of the new curriculum package. If certain resources were not available, successful schools found creative ways to use the resources they had.

In some cases resources do play a big role in successful reform efforts. For example, if a school is trying to integrate the use of technology into their lesson plan then it is necessary to have computers and the appropriate software. Resources are also important when they are seen in terms of money and time. However, these tend to be resources which schools usually do not have control over and must learn to accommodate. For example, providing more time and money for professional development would increase success rate of reform efforts (Hanson, 1989). Yet many schools have managed successful professional development activities without such luxuries.

Supporting Conditions at Low Level

Information Dissemination

It is important to stay motivated in the midst of reform efforts as they can be frustrating and tiring. One way to do this is by keeping those involved updated on progress. Disseminating information on changes taking place at the school keeps parent and community informed (Bondy, 1994).

Disseminating information about changes due to reform efforts can help keep support coming from parents and the community. It is important that parents and the community understand what changes are taking place, since they are often concerned when they see classroom activities that differ from their own experiences (Fullan/Miles, 1992).

Information Dissemination does serve a valuable purpose, but it does not appear to play a big role in successful curriculum reform. Not many schools in the review put time, money or energy into information dissemination system. Successful schools that did disseminate information were also implementing several other conditions (Kelley & Protsik, In Press).

Incentive Programs

Teacher incentive programs do not appear to have a big impact on curriculum reform. Incentive programs may work well in some cases, but the studies examined show that the incorporation of incentive programs did have a big impact on whether programs were implemented successfully (Kelley & Protsik, In Press; Cornett & Gaines, 1994). Rewarding teachers can increase motivation but is not a solution in itself (Cornett & Gaines, 1994).

In Kelley and Protsik's study (In Press), teachers who were offered bonuses for improved student outcomes did not even believe that funding would come through. Fear of sanctions and the threat of failure were found to be more motivational than the promise of salary increase or bonuses. In most cases teachers were motivated by public recognition and student achievement.

Wohlstetter's study of conditions which support high performance, shows that principals at successful schools recognized improved performance on a regular basis. They used "pats on the back", notes of appreciation, and "thank you" lists and luncheons to acknowledge achievement.

These findings are not meant to suggest that increased salary or bonuses should not be part of reform efforts. Increased teacher professionalism is part of a successful reform package and that includes higher salaries for teachers (Honig, 1988).

Discussion

It appears that the reform efforts that began in the early 80's are beginning to have an impact. Over and over again best practice states that successful reform takes time. We learned from mistakes made in the reform efforts of the 60's and 70's (top down) and we've taken a new approach (School-based management, bottom up). After 13 years we have a lot farther to go but we have defiantly made progress. We've established guidelines necessary for change and have success stories based on that criteria. It's been documented that it takes a minimum of three to five years of intensive workshops for teachers to increase the success rate of a program being implemented in the classroom. Is it not unlikely that other aspects of change could take 10-20 years to see results? As Fullan states we must give the reform efforts time and not mistake slow progress for resistance or failure (Fullan, 1991).

References

- American Association for the Advancement of Science (AAAS) (1989). Project 2061: Science for All Americans. American Association for the Advancement of Science, Washington DC.
- Anderson, R. (1995). "Curriculum Reform Dilemmas and Promise". *Phi Delta Kappan*, (1995): 33-36.
- Bondy, E. (1994). Building Blocks and Stumbling Blocks. Three Case Studies of Shared Decision Making and School Restructuring. National Center for Restructuring Education, Schools, and Teaching, New York, NY.
- Bruckerhoff, C. (1995). "School Routines and the Failure of Curriculum Reform". Paper presented at the Annual Meeting of the American Educational Research Association, 1995.
- Butt, R.L. "Curriculum Implementation, Classroom Change and Professional Development: The Challenge for Supervision." Paper presented at the Annual Meeting of the Canadian Society for the Study of Education, 1984.
- Cornett, L. & Gaines, G.F.(1994). *Reflecting on Ten Years of Incentive Programs*. Atlanta: Southern Regional Education Board.
- Cox, P.L. "Inside-Out and Outside-In: Configurations of Assistance and their Impact on School Improvement Efforts." Paper presented at Annual Meeting of the American Educational Research Association, 1983.
- Cronin-Jones, L. (1991). Science Teachers Beliefs and their Influence on Curriculum Implementation: Two Case Studies. *Journal of Research in Science Teaching*, **28**, 235-250
- Crosswhite, F. Joe. "NCTM Standards for School Mathematics: Vision for Implementation," *Arithmetic Teacher* 37, November (1989): 55-60.
- David, J.L. (1994). School-Based Decision Making: Linking Decisions to Learning. Third-Year Report to The Prichard Committee.
- Dwyer, D.C. & Ringstaff, C. & Sandholtz, J. (1990). "The Evolution of Teachers Instructional Beliefs and Practices in High-Access-to-Technology Classrooms". Paper presented at meeting of the American Education Research Association.
- Elmore, R. & McCarthy, S. & Peterson, P.L. (1996). Learning from School Restructuring. *American Educational Research Journal*, **33**, 119-153
- Fullan, M. (1991). The New Meaning of Educational Change. Teachers College Press, New York, NY.
- Fullan, M. & Miles, M. "Getting Reform Right: What Works and What Doesn't," *Phi Delta Kappan*, June (1992): 745-752.

Hansen, K. (1989). "The Anatomy of 'Restructuring': Strategies for Re-Forming American Education." The Northwest Regional Educational Laboratory.

Honig, B. (1988). The Key to Reform: Sustaining and Expanding Upon Initial Success. *Educational Administration Quarterly*, **24**, 257-271

Jacobs, H.H. (1989). "Design Options for an Integrated Curriculum." In *Interdisciplinary Curriculum: Design and Implementation*, edited by H.H. Jacobs, pp13-24. Alexandria, Va: Association for Supervision and Curriculum Development.

Johnston, S. (1995). Curriculum Decision Making at the School Level: Is It Just a case of Teachers Learning to Act Like Administrators? *Journal of Curriculum and Supervision*, **10**, 136-154

Kelley, C. & Protsik, J. (In Press). Risk and Reward: Perspectives on the Implementation of Kentucky's School-Based Performance Award Program. *Educational Administration Quarterly*.

Leiberman, A. & Miller, L. (1990). "The Social Realities of Teaching." In *Schools as Collaborative Cultures: Creating the Future Now*, edited by A. Leiberman. Bristol, Pa.: Falmer Press.

Mohrman, S., & Robertson, P.J., & Wohlstetter, P. (1995). Generating Curriculum and Instructional Innovations Through School-Based Management. *Educational Administration Quarterly*, **31**, 375-404

Mumme, J. & Weissglass, J. (1988). "Improving Mathematics Education through Site-Based Change: Preliminary Report." Paper presented to the ICME Theme Group on the Profession of Teaching at ICME VI, Budapest, Hungary, 1988.

Olson, J. (1981). Teacher Influence in the Classroom: A Context for Understanding Curriculum Translation. *Instructional Science*, **10**, 259-275

National Commission on Excellence in Education. (1983). *A Nation at Risk: The Imperative for Educational Reform. A Report to the Nation and the Secretary of Education* United States Department of Education

National Research Council (1996). *National Science Education Standards*. National Academy Press, Washington, DC.

Parker, R. "Implementing the Curriculum and Evaluation Standards: What Will Implementation Take?," *Mathematics Teacher* 84, no. 6 (1991): 442-449, 478.

Policy Study Associates (1994). *An Idea Book for Educators: Implementing Schoolwide Projects*. Prepared for the U.S. Department of Education.

Saranchuk, R. (1995). "The Assessment-Curriculum Relationship: Participants Views of its Consequences on School Curriculum and Classroom Practices." Paper presented at the annual meeting of the American Educational Research Association.

Smith, W. (1993). "Teachers' Perceptions of Role Change through Shared Decision Making: A Two-Year Case Study." Paper presented at the Annual Meeting of the American Educational Research Association.

Thompson, J. (1994). Systemic Education Reform. ERIC Digest, Number 90.

Wiske, M. & Levinson, C. (1993). "How Teachers are Implementing the NCTM Standards". *Educational Leadership*, **50**, 8-12.

ABSTRACT

Mapping Genes on Chromosome 19

Sheila Lawrence

In order to increase the utility of the physical map of chromosome 19, more genes need to be isolated along the entire length of the chromosome. The purpose of my project is to define several Expressed Sequence Tags (EST's), which are portions of genes, and then further characterize them. Eleven cDNA clones chosen from the databank of the I.M.A.G.E. Consortium were initially hybridized to high density filters containing cosmid clones, and positive signals were verified by PCR. Four clones were chosen for further characterization by sequencing and Northern Hybridization to determine mRNA size and tissue specificity. The results are the addition of four EST's to the Human Genome databank, which will increase the resolution of the physical map of chromosome 19. Also, isolation of full length cDNA clones for two of these clones was attempted using the GeneTrapper positive selection system. The genes in this study were previously undiscovered. By characterizing them, more was learned about their position on the chromosome as well as their role and function based on sequence homologies.

MAPPING GENES ON CHROMOSOME 19*

Sheila Lawrence

Auburn University

**Lawrence Livermore National Laboratory
Livermore, California 94550**

12/18/96

Prepare in partial fulfillment of the requirements of the Science and Engineering Research Semester under the direction of Greg Lennon, Research Mentor, in the Lawrence Livermore National Laboratory.

***This research was supported in part by an appointment to the U.S. Department of Energy Science and Engineering Research Semester (hereinafter called SERS) program administered by LLNL under Contract W-7405 with Lawrence Livermore National Laboratory.**

If this paper is to be published, a copyright disclaimer must also appear on the cover sheet as follows:

By acceptance of this article, the publisher or recipient acknowledges the U.S. Government's right to retain a non-exclusive, royalty-free license in and to any copyright covering this article.

INTRODUCTION

The Human Genome Project is an international effort to try to understand the 3 billion base pairs of DNA in the human genome. This project has long-range implications for studying human genetic diseases, and will affect every aspect of health care in the future from diagnosis to treatment of diseases.

The three goals of the Human Genome Project are to construct linkage maps of polymorphic markers of the entire human genome, build a physical map of overlapping cloned fragments that cover the entire genome, and accurately sequence the entire genome. Beyond gaining knowledge of genes, the Human Genome Project will improve understanding about genetics and biology. Data from this project will also improve understanding of other organisms (1).

There are between 50,000 to 100,000 genes in the human genome. Chromosome 19 comprises about 2% of the total genome, and is being studied at Lawrence Livermore National Laboratory (2). Eleven cDNA clones were chosen for this study, which came from two regions of chromosome 19 containing undiscovered genes responsible for causing strokes and cleft palate.

MATERIALS AND METHODS

HYBRIDIZATION Probes were made using a PCR product labeled with ^{32}P -dCTP. DNA or RNA is denatured and bound to a nylon membrane. When a single stranded PCR product labeled with ^{32}P is put into a solution containing the membranes, the probe hybridizes with the bound DNA or RNA. After removing non-specifically bound radioactivity, signals are detected using phosphor screen technology.

Southern Hybridization is when the probe is bound to denatured DNA. High density filters containing overlapping cosmids, whose order on chromosome 19 is already

known, were hybridized to the probes in order to learn more about the location of the DNA. Positive signals were identified and later verified by PCR.

Northern hybridization is when the probe is hybridized to RNA. RNA from eight different human tissues is denatured and run on a gel, where it is separated on the basis of size. The RNA is then transferred to a nylon membrane and hybridized to the probe. This step gives information about the size of the full length mRNA and about tissue specificity (3).

PCR VERIFICATION The Polymerase Chain Reaction allows for a large scale amplification of DNA between two unique primers. Three steps (denaturation, primer annealing, and DNA synthesis) are carried out at different temperatures from a range of 50-95 C. The process of PCR was enhanced by the discovery of the thermostable DNA polymerase found in the bacteria *Thermus aquaticus*, which has increased the specificity, yield, and length of PCR products (4).

PCR was needed to verify the positive signals from the hybridizations to the high density filters which contain DNA from overlapping cosmids. Single pass sequence data from the 5' and 3' ends of all the clones was available from the I.M.A.G.E. Consortium database, and primer pairs were designed from the 3' sequence data. The PCR products were typically about 100-200 base pairs in length. Template DNA was available from each cosmid. The reaction was run on a 1% agarose gel stained with ethidium bromide, and positive signals were determined.

SEQUENCING Sequencing determines the linear order of nucleotides in a DNA molecule. The Sanger method, also known as dideoxy chain termination, was used in these experiments. A polymerase chain reaction generates a nested set of fragments in which the terminating nucleotide contains a fluorescent dye label. The fragments are then run in a polyacrylamide gel which allows for nucleotide resolution. The fluorescent dye label, which is different for each of the four nucleotides, is read linearly (1).

Transposon facilitated sequencing was used in these experiments. The Ty1 transposon was used, which randomly inserts itself into a target plasmid. Thus, a known priming site is introduced next to unsequenced regions (5). Unique primers are located on both ends of the transposon, which allows sequence analysis in both directions from the insertion point.

DATA BASES FOR BLAST AND BROWSER Browser is a LLNL computer database that takes the data obtained in the PCR verifications and matches the contig with a specific location on the chromosome. This determines the position of a particular cDNA.

The BLAST (Basic Local Alignment Search Tool) database compares a known query sequence to all other known sequences. Data obtained from BLAST was used in two ways. First, the data was used to find other I.M.A.G.E. Consortium cDNA clones that came from the same gene. Also, results from BLAST searches often give the first clues about protein function based on sequence homologies to other proteins.

GENE TRAPPER Gene Trapper is a positive selection system used to isolate cDNA clones from cDNA libraries. Primers are chosen from within the known cDNA sequence and biotinylated. During the Gene Trapper process, the biotinylated primer (which hybridizes to the complementary cDNA) binds to the streptavidin protein which is attached to paramagnetic beads. The beads are recovered, the attached DNA is removed, and *E. coli* cells are electroporated with the recovered DNA. Two methods- PCR and hybridization- were used to screen colonies obtained from the selection.

Clone #	Clone ID	Vector	Vector Primers	GenBank 5' end	GenBank 3' end
1	110079	pT7T3D-pac	T7/T3	T85246	T89203
2	129665	pT7T3D-pac	T7/T3	R16683	R16684
3	133631	pT7T3D-pac	T7/T3	R28560	R28356
4	150897	pT7T3D-pac	T7/T3	H03518	H03436
5	195990	pT7T3D-pac	T7/T3	R92659	R91402
6	249681	pT7T3D-pac	T7/T3	H85735	H85452
7	26233	lafmid BA	DM1/DM2	R12452	R37338
8	44452	lafmid BA	DM1/DM2	H05435	H05436
9	51368	lafmid BA	DM1/DM2	F06304	Z39207
10	74025	BS SK-	T7/T3	T48255	T48256
11	80516	BS SK-	T7/T3	T64632	T64489

Clone #	Insert Estimate in Data Base (Kb)	Insert Estimate based on PCR	Position (cM)	Disease
1	0.872	1.2	87.20	stroke
2	0.612	0.7	325.62	cleft palate
3	0.948	0.8	325.62	cleft palate
4	1.047	1.8	89.70	stroke
5	1.908	1.6	87.60	stroke
6	not available	0.3	81.60	stroke
7	1.269	1.1	331.12	cleft palate
8	1.821	0.9	325.62	cleft palate
9	not available	1.1	87.1	stroke
10	0.704	1.8	333.56	cleft palate
11	0.592	1.8	87.65	stroke

Figure 1 Information obtained for all clones including clone ID in the I.M.A.G.E. Consortium database, vector, vector primers, GenBank account numbers for 5' and 3' ends, insert size as estimated by Washington University, insert estimate based on PCR using vector primers, estimated position along chromosome 19 based on radiation hybrid mapping by the Whitehead Institute, and disease gene region of chromosome 19.

		Vector	DM1/DM2	Restriction Sites	3' Primers
1	Northern Hybridization	pT7T3D-Pac	DM1/DM2	EcoRI/PacI	110079f
110079	PCR with Gene Trapper Libraries				110079r
2	Northern Hybridization	pT7T3D-Pac	DM1/DM2	EcoRI/PacI	129665f2
129665	PCR with Gene Trapper Libraries				129665r2
	Gene Trapper				
8	Northern Hybridization	lafmid BA	T3/T7	HindIII/NotI	44425f
44452	Sequencing				44425r
	PCR with Gene Trapper Libraries				
	Gene Trapper				
9	Northern Hybridization	lafmid BA	T3/T7	HindIII/NotI	51368f
51368	PCR with Gene Trapper Libraries				51368r

Figure 2 Information obtained for the four clones studied in further detail including steps taken for further analysis, vector, vector primers, restriction sites on both ends of the insert, names of working primers within the 3' single pass sequence region, optimal PCR temperature, PCR size, Rmap location based on hybridization verification, page where data can be found in notebook, full length mRNA size based on Northern hybridization, and tissue specificity based on Northern hybridization

1	55	211	869	39	3.0	heart, brain, lung	
110079					6.0	skeletal muscle,	
						placenta, liver,	
						kidney, pancreas	
2	55	137	591	51	1.4	heart, placenta,	
129665					3.0	skeletal muscle,	
					5.0	kidney, pancreas	
8	55	126	1141	37	not available	not available	
44452			591				
			367				
			859				
9	55	106	ab39h1	50	4.0	heart, brain, lung	
51368					5.0	skeletal muscle,	
						placenta, liver,	
						kidney, pancreas	

Figure 2, cont.

ANALYSIS AND RESULTS

Of the original eleven clones that were analyzed in these experiments, four were analyzed further. All clones used in this study came from two regions of chromosome 19 which are known to contain undiscovered disease genes responsible for causing strokes and cleft palate. Information obtained for all eleven clones can be found in Figure 1, which includes ID numbers, vector information, and size and distance estimates. The four clones that were studied in further detail (clone ID #'s 110079, 129665, 44452, 51368) were chosen because there were working PCR primers with an estimated size of 100-200 base pairs within the 3' end chosen from the original single pass sequence. Information about these clones concerning primers and PCR conditions can be found in Figure 2.

The first clone, 110079, is a very rare cDNA. It's sequence from the 5' and 3' ends, when compared to all sequences in the BLAST database, was not similar to any other cDNAs. This clone mapped to Rmap 869. This clone was also used for transposon sequencing. Because of the small insert size (about 870 bp), clones obtained from the transposon experiments were first analyzed by PCR. Five clones should contain transposons that landed within the insert, and sequencing of these clones has been attempted. The Northern hybridization showed expression in all tissues (heart, brain, placenta, lung, liver, skeletal muscle, and pancreas) with full length mRNA sizes of approximately 3.0 and 6.0 kb. When primers within the known 3' end sequence were used with eight Gene Trapper libraries, results showed many different sized bands in all libraries. Thus, this clone was not a good candidate to be used in the Gene Trapper experiments.

The second clone, 129665, mapped to Rmap 591. There were many copies of this cDNA in the BLAST database. Because of the small size of this clone (about 600 bp), sequencing was not attempted. The full sequence is already known since single pass sequence data is available for both the 5' and the 3' ends of the insert. Northern hybridization showed tissue specificity, and there were bands in the lanes for heart,

placenta, skeletal muscle, kidney, and pancreas. The Northern also showed that the mRNA has sizes of 1.4, 3.0, and 5.0 kb. This clone was used in the Gene Trapper experiments using the testis cDNA library. Clones were analyzed by hybridization of a probe labeled with ^{32}P -dCTP, and 10 of the 17 positive clones are in the process of being analyzed further. These clones were chosen on the basis of size, which is estimated to be about 1.4 kb and is consistent with a band seen on the Northern hybridization.

The third clone, 44452, was mapped to four Rmaps (1141, 591, 367, and 859) after positive signals from the hybridizations were verified by PCR. The Northern hybridization for this clone was not successful and lanes were streaked. This clone may have a repetitive element because of the results of the Northern hybridization and because it mapped to four Rmaps. Sequencing of this clone (approximately 1800 bp) has been attempted. The brain cDNA library for the Gene Trapper selection system was used to obtain a full length clone. Clones were screened by PCR, and four positive clones were found. The insert size of the clones obtained from Gene trapper is estimated to be about 2.7 kb. Further analysis of these clones has not yet been completed.

The fourth clone, 51368, mapped to a cDNA ab39h1. Based on Northern hybridizations, this clone is present in all tissues tested (heart, brain, placenta, lung, liver, skeletal muscle, kidney, and pancreas) and has a full length estimates of 4.0 and 5.0 kb. PCR using the eight Gene Trapper libraries did not yield any positive signals, so this clone was not a good candidate for using the Gene Trapper system.

BIBLIOGRAPHY

1. Los Alamos Science, *The Human Genome Project* (1992) Los Alamos National Laboratory, Los Alamos NM.
2. Ashworth, A. K. *et al.* (1995) *Nature Genetics*. 11, 422-427.
3. Maniatis, t., Fritsch, E.F. & Sambrook, J. (1982) *Molecular Cloning: A Laboratory Manual* (Cold Spring Harbor Lab., Cold Spring Harbor, NY).
4. Saiki, R.K., Gelfand, D.H., Stoffel, S., Scharf, S. J., Higuchi, R., Horn, G. T., Mullis, K. B., Erlich, H. A. (1988) *Reports*. 487-491.
5. Devine, S. E., Boeke, J. D. (1994) *Nucleic Acids Research* 22, 3765-3772.

Optimization of the Biodegradation of Trichloroethylene

Tina Legler

University of Wisconsin - Stevens Point

Lawrence Livermore National Laboratory
Livermore, California 94550

December 18, 1996

Prepared in partial fulfillment of the requirements of the Science and Engineering Research Semester under the direction of Joanne Horn, PhD., Research Mentor, in the Lawrence Livermore National Laboratory.

*This research was supported in part by an appointment to the U.S. Department of Energy Science and Engineering Research Semester (hereinafter called SERS) program administered by LLNL under Contract W-7405-Eng-48 with Lawrence Livermore National Laboratory.

ABSTRACT

As an interim step towards optimizing the biodegradation of trichloroethylene (TCE) by methanotrophic bacteria, the lowest concentration of methanol that could support cellular growth and yet not inhibit TCE degradation needed to be determined. Population growth and TCE degradation rates were determined by analyzing growth curves and gas chromatograph assays. The data from these analyses showed that at concentrations of 0.001% methanol, cultures continued to grow, and TCE degradation was comparable to rates displayed in the absence of methanol. Although all data analysis is not yet complete, these results suggest that it will be possible to support a bacterial culture on methanol, while allowing TCE degradation to occur.

Introduction

Bacteria that can grow on methane as their sole source of carbon and energy are known as methanotrophs, one group of which are members of the genus *Methylosinus*. Recently, methanotrophs have attracted interest because of their ability to degrade the widespread ground water pollutant trichloroethylene (TCE).

Currently there are several environmental and physiological factors that will inhibit the ability of bacteria to degrade TCE in the environment. One of the most significant problems is that the biodegradation of TCE creates unstable products that inactivate cellular enzymes. Thus, to sustain TCE degradation, cells must be supplied with a growth substrate. *Methylosinus* will grow on methanol, however this substrate competitively inhibits the enzyme that oxidizes TCE, soluble methane monooxygenase (sMMO). Thus, to achieve optimal TCE degradation, a balance must be maintained between providing sufficient growth substrate and minimizing its inhibitory effects on the TCE degradation process. Through our research we found that significant degradation is possible in the presence of low concentrations of methanol, and cell growth is supported at these same concentrations.

Materials and methods

Bacterial Growth Curves. *Methylosinus trichosporium* OB3b and *Methylosinus sporium* strains were grown from ATCC cultures 35070 and 35069 respectively. Cultures were grown in Higgins nitrate minimal salt medium (Park *et al.*, 1991) in 8 oz. amber bottles topped with mini-inert valves (Dynatech, Inc.) to allow gassing of the cultures while minimizing gas loss. 100 ml of air were removed before bottles were injected with 50 ml of methane and 50 ml of air. Cultures were incubated at 30 degrees Celsius, and agitated at 300 rpm. In separate experiments methanol concentrations of 0.1%, 0.01%, and 0.001% were added to determine the growth rate of the strains. Growth was monitored by taking periodic cell counts from a

Coulter Counter, or optical densities from a spectrophotometer, over a three to four day period. Bacterial growth rates were plotted showing the relationship of the cell density to the time of incubation. (Figures 1-4 show representative examples of growth curves generated.)

Trichloroethylene degradation assays. TCE degradation assays were conducted in 4.0 ml, 15X45mm septum vials containing in a 0.5 ml reaction; 25mM MOPS, 5mM MgCl₂, 20mM formate, 0.3 mg cells (dry weight) of methane or methanol grown cells, and varying concentrations of methanol (25mM, 2.5mM, 0.25mM). 500 nM of TCE was added, and samples were then immediately incubated 5 minutes, 30 degrees Celsius, 170-180 rpm in a water bath. 30 ul of headspace samples were collected at 5 minute intervals and analyzed by gas chromatography (Hewlett Packard 5890 Series II gas chromatograph).

Presentation and Discussion of Data

Over a 72 hour time period, both strains showed an increase in cell number in all concentrations. *Methylosinus trichosporium* OB3b showed an increase of 1.30E+08 cells/ml in 0.1% methanol, 1.40E+07 cells/ml in 0.01% methanol, and 1.13E+07 cells/ml in the 0.001% methanol concentration. *M. sporium* increased 5.21E+08 cells/ml in 0.1% methanol, 1.88E+08 cells/ml in 0.01% methanol, and 1.32E+08 cells/ml in 0.001% methanol (Fig. 1 and 2). Absorbency readings correlated with the cells/ml counts, showing an increase in optical density in all concentrations of methanol in both strains (Fig. 3 and 4).

TCE degradation assays showed that the presence of high concentrations of methanol will inhibit TCE degradation in methane-grown cells. Figures 5 and 6 are representative graphs showing the effect of different methanol concentrations on the rate of TCE degradation of methane-grown, stationary phase cells. In these figures the most inhibition was seen at 0.1% methanol, showing little to no degradation for either strain. The least inhibition was seen for 0.001% methanol, which correlated almost exactly with the rate for

the positive control, where no methanol was added. Both strains exhibited TCE degradation of 400-500nm TCE/mg dry cell weight between the 5 and 15 minute incubation period. No significant degradation was seen in methanol-grown cells.

Figure 1.

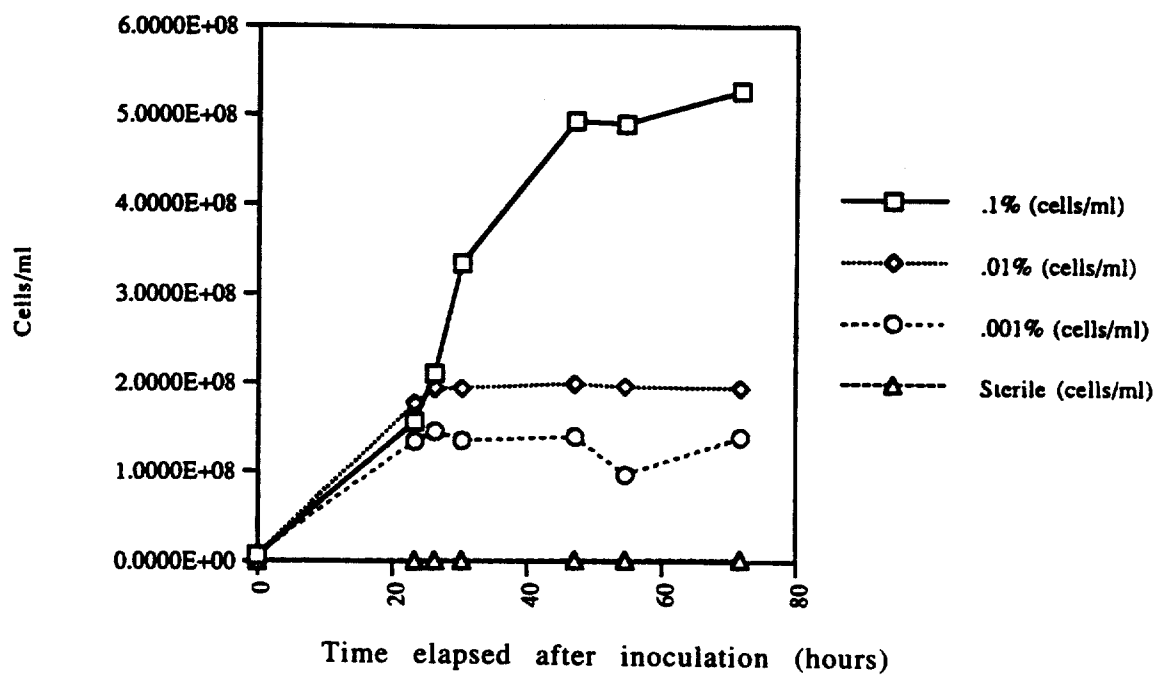
Growth Rates of *Methylosinus sporium* in Methanol

Figure 2.

Growth Rates of *Methylosinus trichosporium* OB3b
in Methanol

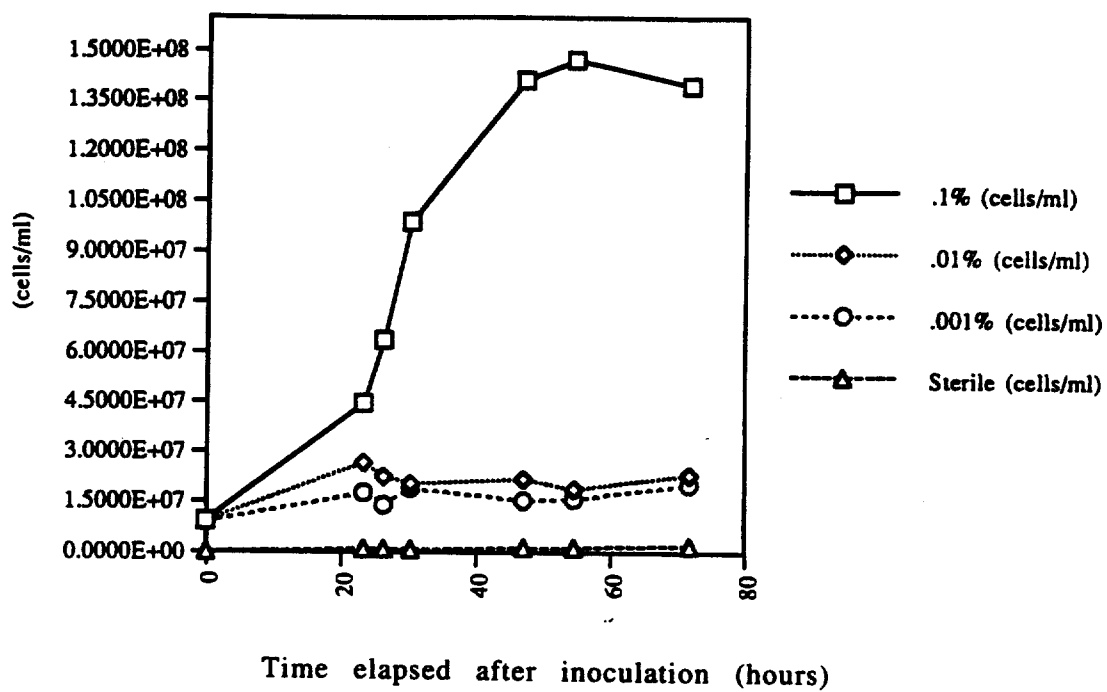


Figure 3.

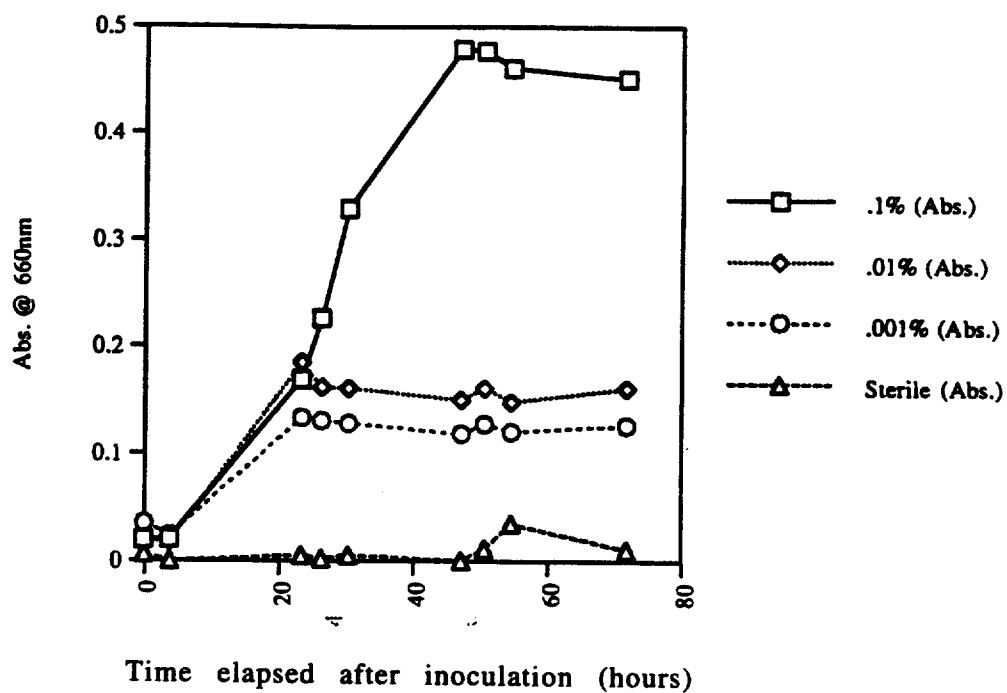
Growth Rates of *Methylosinus sporium* in Methanol

Figure 4.

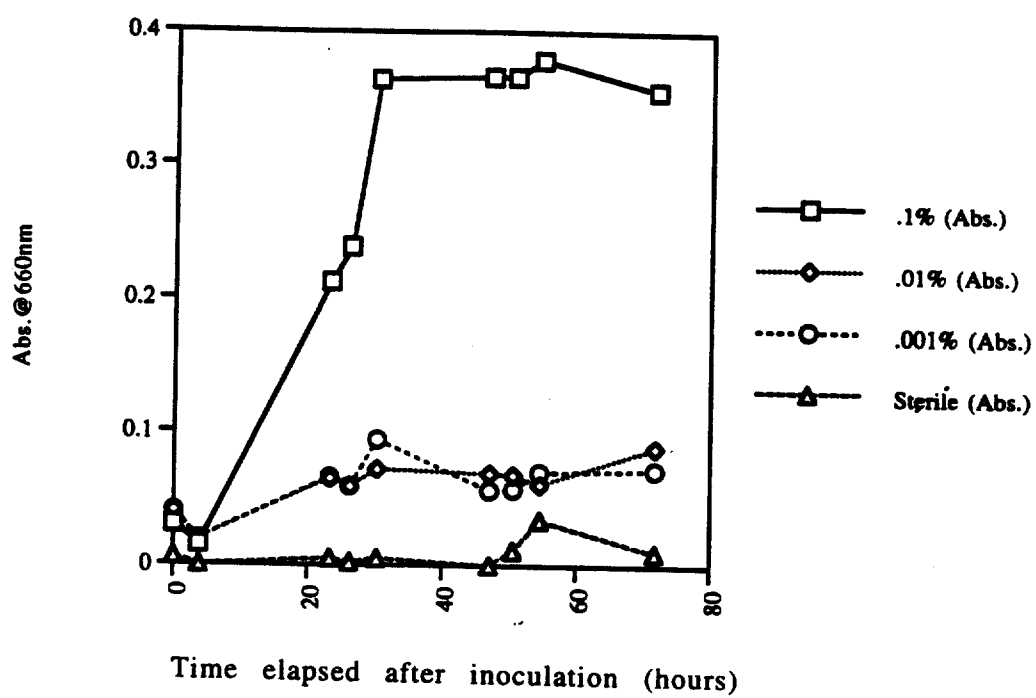
Growth Rates of *Methylosinus trichosporium* OB3b
in Methanol

Figure 5.
Methane-Grown *M. sporium* 35069 (A660=1.118)
Effect of MeOH on TCE Degradation by sMMO

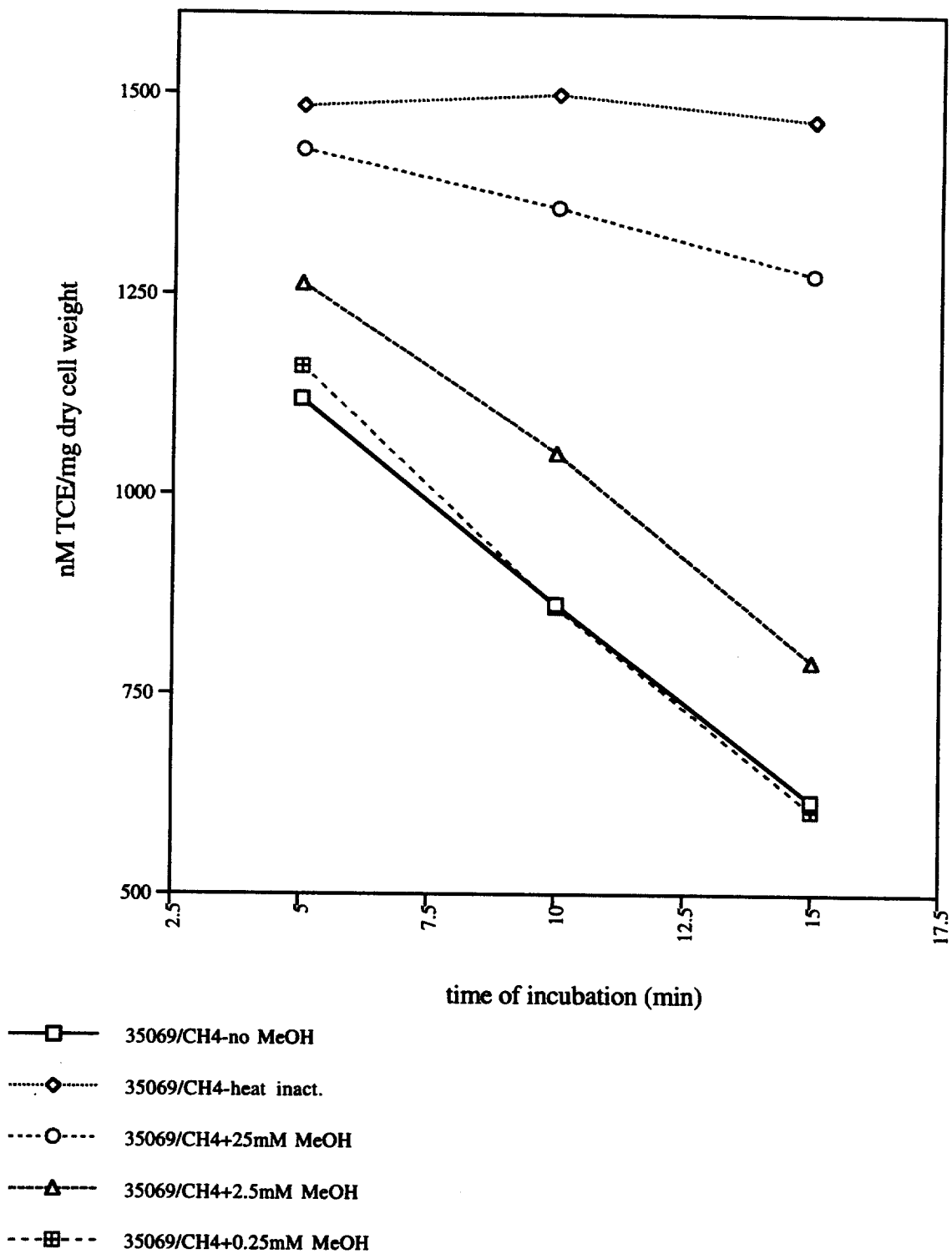
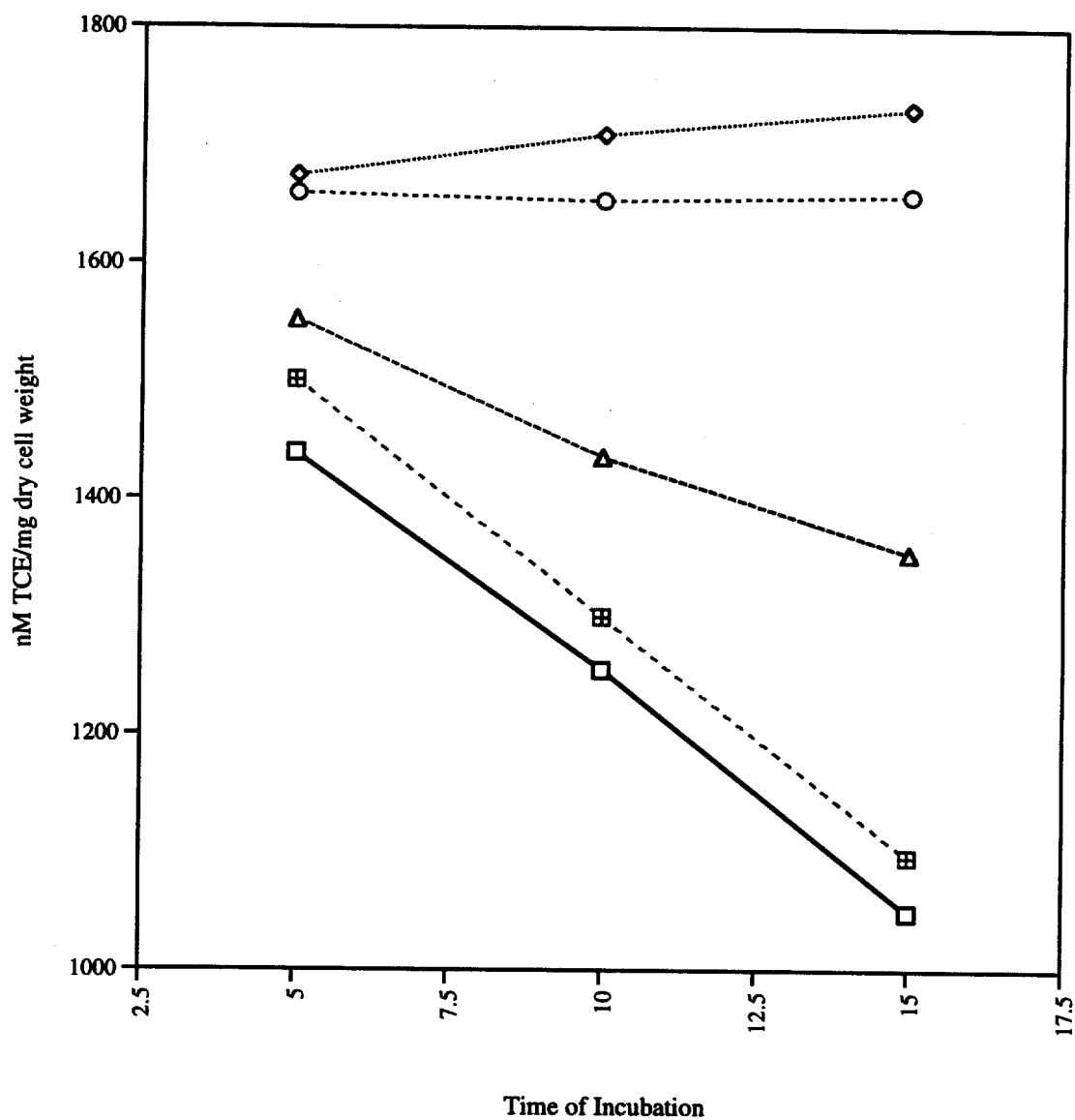


Figure 6.
Methane-Grown *M. trichosporium* 35070 (A660=1.201)
Effect of Methanol on TCE Degradation by sMMO



- 35070/CH4 - no MeOH
-◇..... 35070 - heat inact.
- 35070/CH4 + 25mM MeOH
- - -△- - - 35070/CH4 + 2.5mM MeOH
- 35070/CH4 + 0.25mM MeOH

Analysis of results

Although the highest cell growth was noted in higher concentrations of methanol, significant cell growth still occurred in very low concentrations of methanol, even as low as 0.001%. *M. sporium* appeared to be a better growing strain, reaching greater cell concentrations than *M. trichosporium* OB3b. This occurred not only at corresponding methanol concentrations, but even when comparing *M. sporium* growth in 0.001% versus *M. trichosporium* growth in 0.1% methanol. Gas chromatograph assays showed the inhibitory effects of the presence of methanol on the degradation of TCE. The presence of 0.1% methanol almost completely inhibited the occurrence of any TCE activity, while the presence of 0.001% methanol showed little to no effect on the degradation of TCE.

Conclusions

The significance of these findings shows that low concentrations of methanol can support cellular growth. It also shows that these same low concentrations do not inhibit TCE degradation in the presence of methane-grown cells. Theoretically, once a TCE degrading methanol-grown variant can be isolated, a culture of TCE degrading bacteria could be sustained in a low concentration of methanol, and used in the bioremediation of TCE contaminated ground water.

The data from this research has also led to other useful conclusions. By using two *Methylosinus* strains in our growth and TCE assay experiments, we can compare their activities to determine an optimal species to work with. Because methanol-grown cultures do not exhibit TCE degrading activity, a constitutive mutant that will exhibit TCE degradation after growth in methanol will need to be found. The species we choose to use in order to isolate such a variant will need to exhibit optimal growth and TCE degrading ability. At

this time we are considering *M. sporium* because of its higher growth rate in low concentrations of methanol, and because methane-grown cells show significant TCE degradation even in the presence of these same methanol concentrations. Statistical analysis also reveals that the potential of OB3b to degrade TCE is growth phase dependant, *M. sporium* is not.

Because of the sensitivity of growing *Methylosinus sp.*, growth experiments will continue in order to determine a more precise growth curve for each strain used. Also, further research will be performed to analyze the mechanism of sMMO regulation in methanol.

References and Additional Reading

- Bowman, J.P., and G.S. Sayler. 1994. Optimization and maintenance of soluble methane monooxygenase activity in *Methylosinus trichosporium* OB3b, *Biodegradation*, 5:1-11.
- Brusseau, G.A., H-C. Tsien, R.S. Hanson, and L.P. Wackett. 1990. Optimization of trichloroethylene oxidation by methanotrophs and the use of a colorimetric assay to detect soluble methane monooxygenase activity, *Biodegradation*, 1:19-29.
- Fitch, M.W., et.al. 1993. Phenotypic Characterization of Copper-Resistant Mutants of *Methylosinus trichosporium* OB3b, *Appl. Environ. Microbiol.*, 59:2771-2776.
- Fitch, M.W., G.E. Speitel, Jr., and G. Georgiou. 1996. Degradation of Trichloroethylene by Methanol-Grown Cultures of *Methylosinus trichosporium* OB3b PP358, *Appl. Environ. Microbiol.*, 62:1124-1128.
- Graham, D.W., D.G. Korich, R.P. LeBlanc, N.A. Sinclair, and R.G. Arnold. 1992. Applications of a Colorimetric Plate Assay for Soluble Methane Monooxygenase Activity, *Appl. Environ. Microbiol.*, 58:2231-2236.
- Little, C.D., A.V. Palumbo, S.E. Herbes, M.E. Lidstrom, R.L. Tyndall, and P.J. Gilmer. 1988. Trichloroethylene Biodegradation by a Methane-Oxidizing Bacterium, *Appl. Environ. Microbiol.*, 54:951-956.
- Murrell, J.C. 1994. Molecular genetics of methane oxidation, *Biodegradation*, 5:145-159.
- Park, S., M.N. Hanna, R.T. Taylor, and M.W. Droege. 1991. Batch cultivation of *Methylosinus trichosporium* OB3b:I. Production of soluble methane monooxygenase. *Biotech. Bioengin.*, 38:423-433.
- Phelps, P.A., S.K. Agarwal, G.E. Speitel, Jr., and G. Georgiou. 1992. *Methylosinus trichosporium* OB3b Mutants Having Constitutive Expression of Soluble Methane Monooxygenase in the Presence of High Levels of Copper, *Appl. Environ. Microbiol.*, 58:3701-3708.
- Whittenbury, R., K.C. Phillips, and J.F. Wilkinson. 1970. Enrichment, Isolation, and Some Properties of Methane-utilizing Bacteria, *Journal of Gen. Microbiol.*, 61:205-218.

ABSTRACT

The purpose of this study is to measure the ratio of translocations to pericentric inversions for low-LET radiation and high-LET radiation using fluorescence *in situ* hybridization (FISH). A composite chromosome 1p telomeric region specific probe, a chromosome 1 heterochromatin probe and a pan-centromere probe were developed to identify pericentric inversions. A chromosome 1 paint probe was employed to measure translocations on chromosome 1 as described by Lucas *et al.* (1989, 1992). Translocation frequencies and pericentric inversion frequencies were calculated as described by Lucas *et al.* (1989, 1996).

Translocations are interchromosomal aberrations (breaks in different chromosomes), while pericentric inversions are intrachromosomal aberrations (breaks in the same chromosome). High-LET radiation produces energy depositions that are much closer together (dense) than those produced by low-LET radiation (sparse). Hence, it may be more likely for high-LET radiation to cause multiple breaks in the same chromosome than it is for low-LET radiation. If this is true, then it is expected that the ratio of translocations to pericentric inversions for high-LET radiation will be less than the ratio for low-LET radiation.

Being able to distinguish high-LET radiation will allow for distinction between high- and low-LET radiations by facilitating the measurement of a signature for high-LET radiation.

Pericentric Inversion Frequency for High- and Low-LET Radiation Measured By Fluorescence *in situ* Hybridization (FISH)

**S.W. Oram², F.S. Hill¹, M.J. Cassel¹, and J.N. Lucas¹,
Biol. Biotech. Res. Prog., ¹ Lawrence Livermore National
Laboratory, CA 94550;**

² Biology Dept. Ithaca College, Ithaca, NY 14850

December 18, 1996

Prepare in partial fulfillment of the requirements of the Science and Engineering Research Semester under the direction of Joe N. Lucas, Research Mentor, in the Lawrence Livermore National Laboratory.

* This research was supported in part by an appointment to the U.S. Department of Energy Science and Engineering Research Semester (herein after called SERS) program administered by LLNL under Contract W-7405-Eng-48 with Lawrence Livermore National Laboratory.

If this paper is to be published, a copyright disclaimer must also appear on cover sheet as follows:

By acceptance of this article, the publisher or recipient acknowledges the U.S. Government's right to retain a non-exclusive, royalty-free license in and to any copyright covering this article.

INTRODUCTION

The purpose of this study is to measure the ratio of translocation to pericentric inversions for high-LET radiation and low-LET radiation using fluorescence *in situ* hybridization (FISH). Dicentrics and translocations are interchromosomal aberrations, caused by breaks in different chromosomes (Figure 1); while centric rings and pericentric inversions are intrachromosomal aberrations, caused by multiple breaks in the same chromosome (Figure 2). High-LET radiation produces energy depositions that are much closer together (dense) than those produced by low-LET radiation (sparse). Hence, it may be more likely for high-LET radiation to cause multiple breaks in the same chromosome than it is for low-LET radiation. Therefore, it is expected that the ratio of translocations to pericentric inversions or dicentric to centric rings for high-LET radiation will be lower than the ratio for low-LET radiation. However, dicentrics and centric rings are unstable with time, but translocations and pericentric inversions are stable with time. Measurement of pericentric inversions using FISH have not been reported previously.

Here, a rapid and accurate method for measuring pericentric inversions using FISH is described. The method to measure pericentric inversions employs fluorescent probes generated by degenerate oligonucleotide-primed-polymerase chain reaction (DOP-PCR). Probes consisting of a composite chromosome 1p telomeric region specific probe (labeled green), a chromosome 1 heterochromatin region probe (labeled green) and a pan-centromere probe (labeled red) were developed to identify pericentric

inversions. A chromosome 1 paint probe was employed to measure translocations on chromosome 1 as described by Lucas *et al.* (1989, 1992). A pericentric inversion is made distinct by the position change of the fluorescent signals relative to the chromosome centromere. When the two probes (green) were used in combination with a pan-centromere probe (red), pericentric inversions were easily scored based on an inverted color pattern change among the probes (Figure 3).

Being able to distinguish high-LET radiation will allow distinction between high-LET radiation and low-LET radiation by facilitating a "fingerprint" for high-LET radiation (Brenner 1996).

METHODS AND MATERIALS

FISH ANALYSIS: We used DNA probes specific for the heterochromatin (pUC 1.77) and p arm telomere region (1p36.3) on chromosome number 1 in combination with a pan-centromere probe. The pan-centromere probe was amplified and directly labeled with Tetramethylrhodamine-6-dUTP (Boehringer Mannheim) by DOP-PCR. The pUC 1.77 DNA for the heterochromatin and the p arm telomere DNA were also amplified by DOP-PCR. The telomere and pUC 1.77 probes were then labeled with FluoroGreen (Amersham) in a second round of amplification. Details of the hybridization procedures are as described in Pinkel *et al.* (1986). Briefly, the target metaphase spreads were denatured in 70% formamide/2XSSC at 70° C, dehydrated and air-dried. The directly labeled probes in hybridization buffer (50% formamide/2XSSC, 10% dextran sulfate)

were thermally denatured at 70° C and added to the slides. The cover slips were sealed, and the slides were incubated overnight at 37° C

. After washing, the slides were counter stained with 2,6-diamidino-2-phenylindole (DAPI).

CELL CULTURE: Procedures are as described in Lucas *et al.* (1989). Heparinized whole blood from a healthy male donor was irradiated at ambient room temperature with different levels of high- and low-LET radiation. Absorbed doses to the blood in Gy were obtained from procedure described in Lucas *et al.* (1989). Lymphocytes were separated from whole blood of a healthy male donor by centrifugation through a continuous density gradient formed by mixing whole blood with a commercially available separation medium (Sepracell-MN, Sepratech Co., Oklahoma City, OK). The lymphocytes were stimulated to proliferate with phytohaemagglutinin (0.15 mg/ml). The cells were maintained in suspension cultures in upright T-75 flasks in 50 ml RPMI 1640 medium containing 20% fetal bovine serum. After 48 hours, colcemid was added to the cultures for 4 hours, and metaphase spreads were prepared by the method of Evans *et al.* (1971).

SCORING: For pericentric inversion identification a metaphase spread was scored as normal if green fluorescent domains positioned on opposite sides of a red fluorescent centromere were present on each of the two no. 1 chromosomes. Two kinds of chromosome rearrangements involving chromosome 1p were scored: (1)

Pericentric inversions with one breakpoint in 1p and the other in 1q; these produced a derivative chromosome with a visible change in the color pattern (Figure 3). (2) Centric rings with one breakpoint in 1p and the other in 1q; these produced centric rings with the ring carrying the paracentromeric locus of chromosome 1 and an acentric fragment containing the telomeric locus. All metaphase spreads containing structural aberrations involving 1p were photographed and the scoring was reviewed in conference.

Identification and scoring of translocations using FISH employed the methods of Lucas *et al.* (1992). Only reciprocal translocations were used in determining the translocation frequency.

GENOMIC TRANSLOCATION AND PERICENTRIC INVERSION

CALCULATIONS: Identification and scoring of chromosome exchange aberrations using FISH employed the methods of Lucas *et al.* (1992). The scoring criteria are equivalent to those described by Simpson and Savage (1995) as apparently simple exchange-type painting pattern. Only apparently simple translocations (AST's) were used to calculate F-ratios (Lucas *et al.* 1996). The translocation frequency measured by FISH was scaled to full genome equivalents using the Lucas *et al.* formula (Lucas *et al.* 1992). In brief, the formula relates the translocation frequency measured by FISH, F_p , to the genomic translocation frequencies, F_G , through the fraction of the genome covered by the probes, f_p , as follows:

$$F_G = F_p / (2.05 f_p (1 - f_p))$$

where the genomic conversion factor for chromosome 1 is 0.156.

The FISH measured pericentric inversions, p_i , involving the i th chromosome is proportional to the product of the long (L_i) and short (S_i) arms of the i th chromosome. The total genomic number of pericentric inversion, P , is obtained similarly (Hlatky *et al.* 1992) from the ratio of the product of the long and short arms of the i th chromosome to the sum of products of the long and short arms for the total genome to the product of the long and short arms of the i th chromosome, times the FISH measured pericentric inversions, p_i , involving the i th chromosome: where L_i and S_i are the long and short arms of the i th chromosome.

RESULTS

Table 1 lists the translocation frequencies, pericentric inversion frequencies and F-ratios for both high- and low-LET radiation. For the 2.89 Gy Co-60 gamma irradiation (low-LET radiation), 1966 metaphase lymphocytes were scored. There were 24 pericentric inversions and 140 reciprocal translocations.

The high-LET radiation Iron (Fe-56) study consisted of three different doses and two different types of cells. There were 2110 metaphase fibroblasts scored, resulting in 17 pericentric inversions and 33 translocations. Data for the 0.25 Gy dose consisted of 2727 metaphase lymphocytes, with 5 pericentric inversions and 14 translocations. There were 2142 metaphase lymphocytes scored for the 0.75 Gy dose, with 11 pericentric inversions and 12

translocations. The last group consisting of a dose of 1.25 Gy had 4922 metaphase lymphocytes with 21 pericentric inversions and 32 translocations.

The high-LET radiation Carbon (C-14) study contained 1070 metaphase lymphocytes, resulting in 16 pericentric inversions and 31 translocations.

DISCUSSION

In summary, we have presented a rather simple method for measuring pericentric inversions using FISH. This method requires three DNA probes: a chromosome 1p telomere (green), a chromosome 1 heterochromatin (green), and a pan centromere (red). The three probes represent a color pattern that allows for rapid identification of pericentric inversions.

The F-ratio (reciprocal translocations to pericentric inversions) measured in low-LET (2.89 Gy Co-60 gamma) irradiated lymphocytes was 5.7. This compared to a F-ratio of ~3 for high-LET (0.25-1.25 Gy Fe-56 particles) irradiated lymphocytes demonstrates a decrease in the F-ratio for high-LET radiation. However, the F-ratio for high-LET (3.0 Gy C-14 particles) irradiated human lymphocytes was 6.6. This data suggests no apparent difference between high- and low-LET radiation based F ratios. The Fe-56 particles suggest that high-LET may demonstrate a lower F-ratio than low-LET radiation, although statistical examination of the results have not been performed yet. While the C-14 particles demonstrated a slight increase in F-ratio in comparison to the low-LET radiation. Not all the data for the C-14

and Fe-56 studies has been collected, therefore definite conclusions can not be drawn yet.

Future plans are to finish the C-14 and Fe-56 studies and determine if there is a difference in F-ratios for high- and low-LET radiation.

TABLE 1: Translocation frequencies, pericentric inversion frequencies and F-ratios for high- and low-LET radiation.

<u>Cells</u>	<u>Dose</u>	<u>Trans. Freq</u>	<u>Inv. Freq</u>	<u>F-ratio</u>
<u>High-LET Radiation</u>				
Iron (Fe-56)				
Lymphocytes	0.25	0.071	0.025	2.8
	0.75	0.130	0.041	3.2
	1.25	0.160	0.036	4.1
Fibroblasts	1.25	0.220	0.103	2.3
Carbon (C-14)				
Lymphocytes	3.00	0.820	0.123	6.6
<u>Low-LET Radiation</u>				
Gamma Rays				
Lymphocytes	2.89	0.530	0.083	5.7

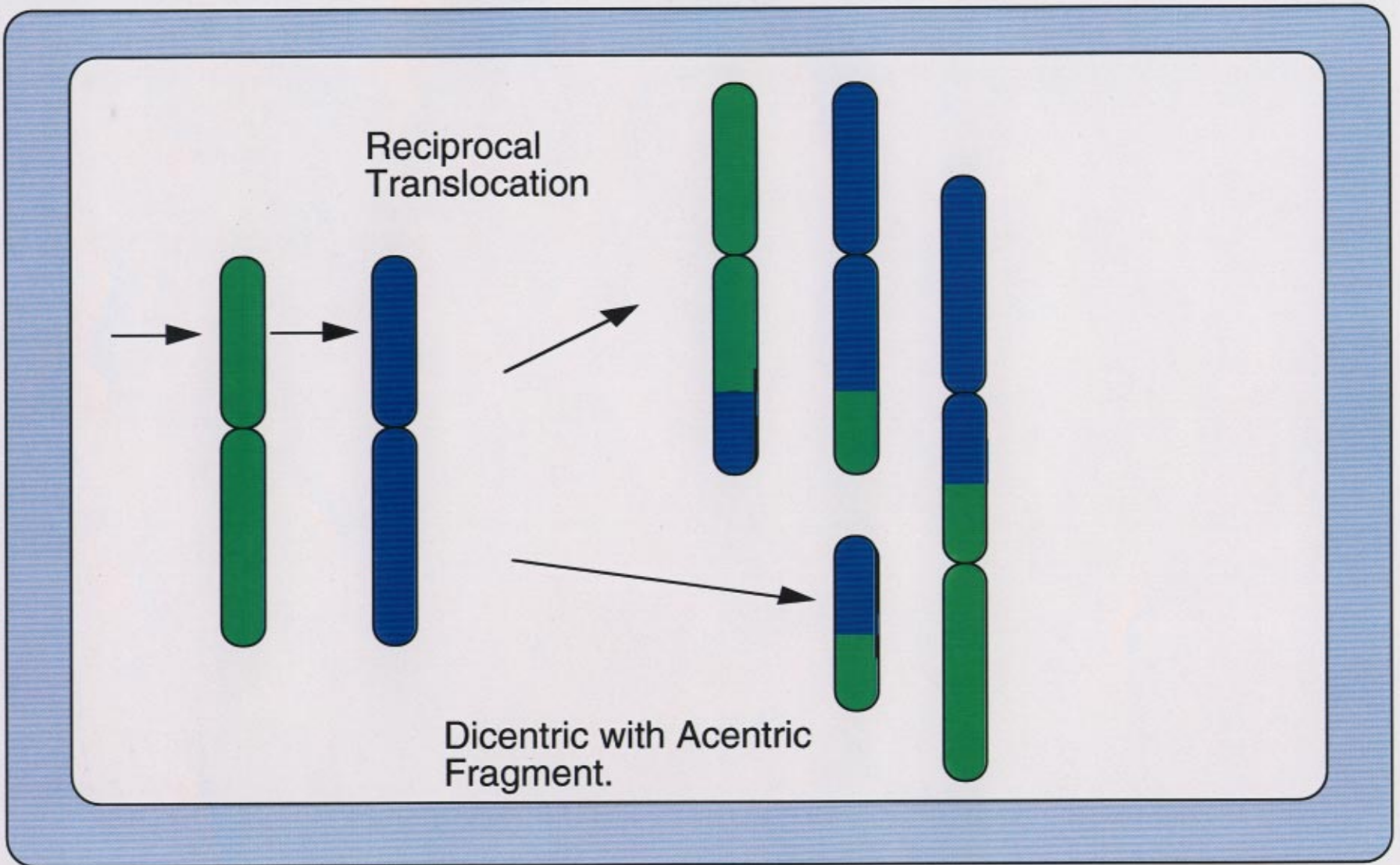


Figure 1: Example of an interchromosomal aberration, resulting in either a translocation or a dicentric.

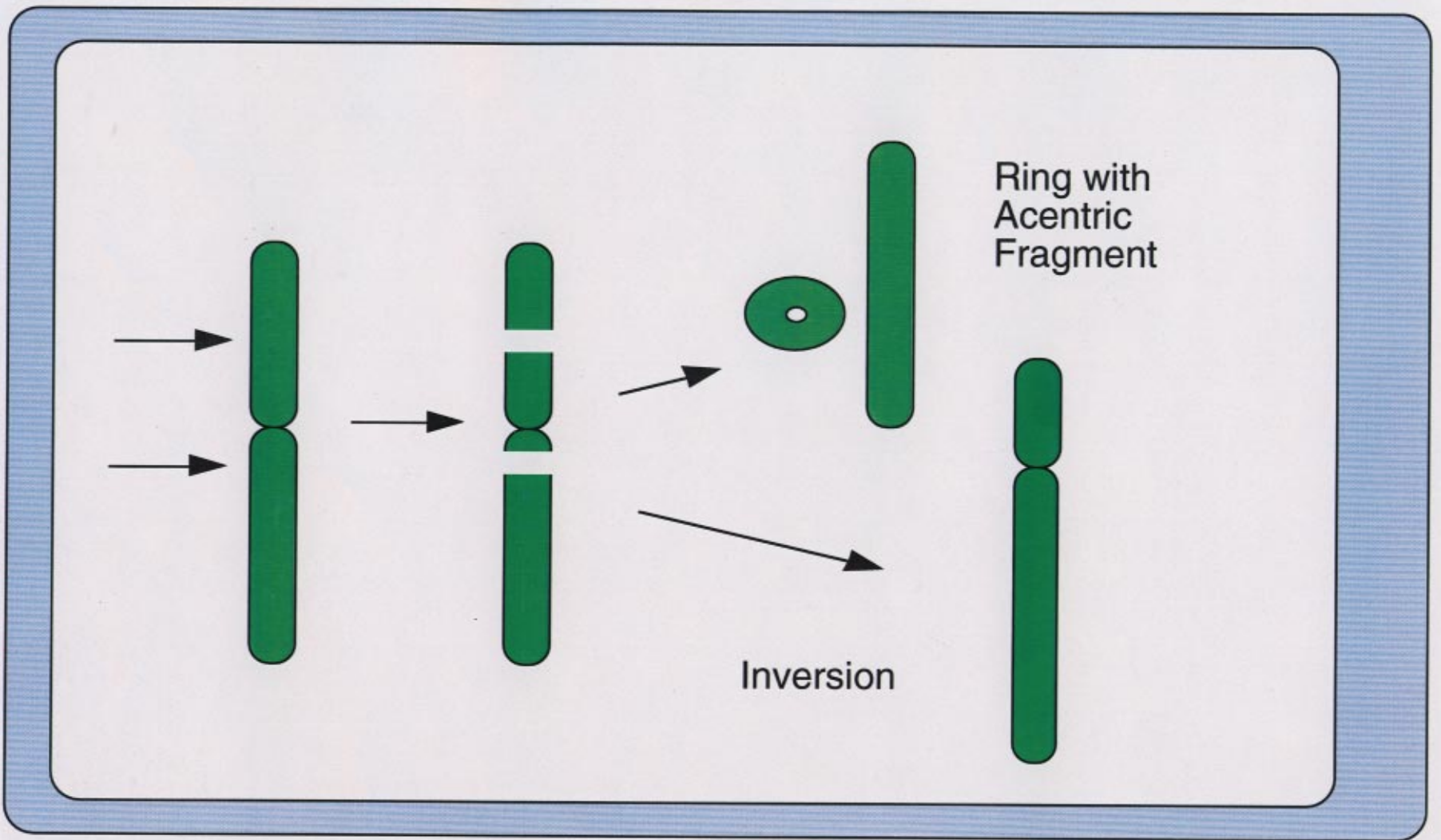


Figure 2: Example of an intrachromosomal aberration, resulting in either a pericentric inversion or a centric ring.

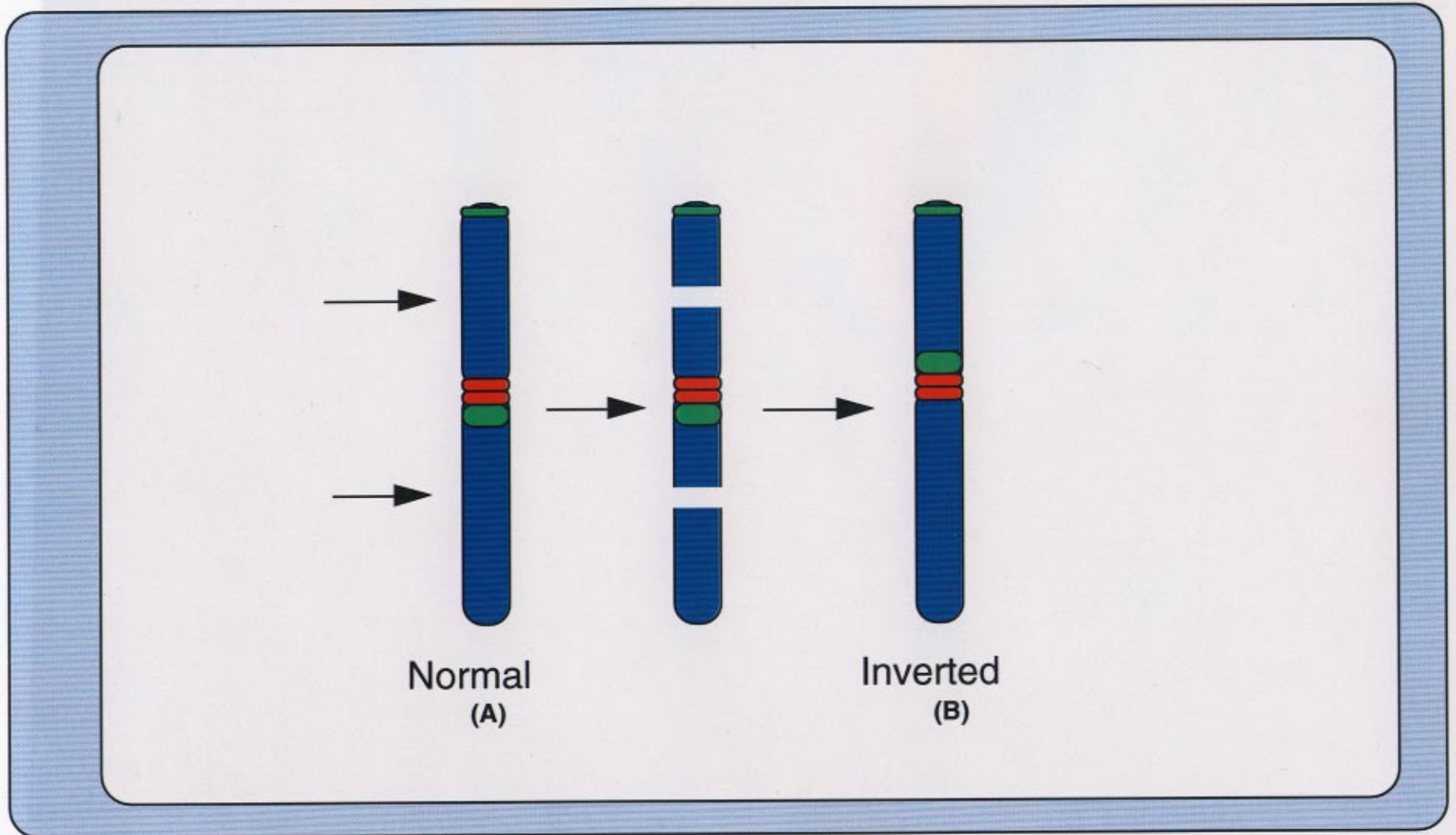


Figure 3: Schematic representation of the design of specific chromosomal probes to detect pericentric inversions. (A) Normal chromosome with a telomere probe and a heterochromatin probe on opposite arms labeled green, and a centromere labeled red. (B) Schematic of a pericentric inversion showing the green probes in (A) on the same arm.

References

- BRENNER, D. J., 1996, Direct biological evidence for a significant neutron dose to survivors of the Hiroshima atomic bomb. *Radiation Research*, **145**, 501-507.
- CHEN, A. M., LUCAS, J. N., HILL, F. S., BRENNER, D. J. and SACHS, R. K., 1996, Proximity effects for chromosome aberrations measured by FISH. *International Journal of Radiation Biology*, **69**, 411-420.
- GRIFFIN, C. S., MARSDEN, S. J., STEVENS, D. L., SIMPSON, P., SAVAGE, J. R., 1995, Frequencies of complex chromosome exchange aberrations induced by ²³⁸Pu alpha-particles and detected by fluorescence *in situ* hybridization using single chromosome-specific probes. *International Journal of Radiation Biology*, **67**, 431-439.
- GUAN, X. Y., ZHANG, H., BITTNER, M., JIANG, Y., MELTZER, P. and TRENT, J., 1996, Chromosome arm painting probes. *Nature Genetics*, **12**, 10-11.
- HLATKY, L. R., SACHS, R. K. and HAHNFELDT, P., 1992, The ratio of dicentrics to centric rings produced in human lymphocytes by acute low-LET radiation. *Radiation Research*, **129**, 304-308.
- KOVACS, M. S., EVANS, J. W., JOHNSTONE, I. M. and BROWN, J. M., 1994, Radiation-induced damage, repair and exchange formation in different chromosomes of human fibroblast determined by fluorescence *in situ* hybridization. *Radiation Research*, **137**, 34-43.
- LUCAS, J. N., AWA, A., STRAUME, T., POGGENSEE, M., KODAMA, Y., NAKANO, M., OHTAKI, K., WEIER, H.-U., PINKEL, D., GRAY, J. and LITTLEFIELD, G., 1992, Rapid translocation frequency analysis in humans decades after exposure to ionizing radiation. *International Journal of Radiation Biology*, **62**, 53-63.
- LUCAS, J. N., CHEN, A. M. and SACHS, R. K., 1996, Theoretical predictions on the equality of radiation-produced dicentrics and translocations detected by chromosome painting. *International Journal of Radiation Biology*, **69**, 145-153.

- LUCAS, J. N., TENJIN, T., STRAUME, T., PINKEL, D., MOORE II, D. M., LITT, M. and GRAY, J. W., 1989, Rapid determination of human chromosome translocation frequency using a pair of chromosome-specific DNA probes. *International Journal of Radiation Biology*, **56**, 35–44.
- MORTON, N. E., 1991, Parameters of human genome. *Proceedings of the National Academy of Sciences (USA)*, **88**, 7474–7476.
- MUHLMANN-DIAZ, M. C. and BEDFORD, J. S., 1995, Comparison of gamma-ray-induced chromosome ring and inversion frequencies. *Radiation Research*, **143**, 175–180.
- SACHS, R. K., AWA, A., KODAMA, Y., NAKANO, M., OHTAKI, K. and LUCAS, J. N., 1993, Ratios of radiation-produced chromosome aberrations as indicators of large-scale DNA geometry during interphase. *Radiation Research*, **133**, 345–350.
- SAVAGE, J. R. K. and PAPWORTH, D. G., 1982, Frequency and distribution studies of asymmetrical versus symmetrical chromosome aberrations. *Mutation Research*, **95**, 7-18.
- SIMPSON, P. J. and SAVAGE, J. R. K., 1995, Estimating the true frequency of X-ray-induced complex chromosome exchanges using fluorescence in situ hybridization. *International Journal of Radiation Biology*, **67**, 37-45.
- SIMPSON, P. J. and SAVAGE, J. R. K., 1996, Personal communications.

Optimization of Chromosome Painting Probes for Scoring of Incomplete Translocations

Samihah Ragland
Spelman College
Lawrence Livermore National Laboratory
Livermore, California 94550

December 18, 1996

Prepared in partial fulfillment of the requirements of the Science and Engineering Research Semester under the direction of Dr. Joe N. Lucas, Research Mentor, in the Lawrence Livermore National Laboratory.

*This research was supported in part by an appointment to the U.S. Department of Energy Science and Engineering Research Semester (hereinafter called SERS) program administered by LLNL under Contract W-7405-Eng-48 with Lawrence Livermore National Laboratory.

Optimization of Chromosome Painting Probes for Scoring of Incomplete Translocations

Samihah Ragland

ABSTRACT

The purpose of this project is to synthesize a two color whole chromosome probe mixture for use in scoring incomplete translocations. An incomplete translocation occurs when one chromosome derivative fails to rejoin, leaving one bicolored chromosome and one painted chromosome segment. The painted chromosome segment has a centromere. Flourogreen labeled probes for chromosomes 3, 5, and 6 were generated by DOP-PCR and Random Priming techniques. Spectrum Orange labeled probes for chromosomes 1,2 and 4 were purchased from VYSIS. After ethanol precipitation, the probe DNA was resuspended in buffer and visualized by FISH on metaphase spread.

The signals produced by this bicolored probe mix provide a rapid and sensitive means for scoring incomplete translocations. These probes will facilitate the understanding and quantification of incomplete translocations by providing a sharper image of small translocated chromosome segments on bicolored chromosomes.

INTRODUCTION

Do incomplete translocations exist? One group believes they are, " hidden reciprocals due to one translocated segment being too small to detect"(Kodama et al, 1996). They further hypothesize that the smallest detectable sizes for painted and unpainted translocated segments to be 11.1 Mb and 14.6 Mb respectively. These assumptions are based on the collection of cytogenetic data from 120 Atomic bomb survivors. In that study, chromosomes 1,2 and 4 were stained with fluorescein isothiocyanate and counterstained with propidium iodide. Non-reciprocals were scored as the visualization of one bicolored chromosome.

To provide a sharper image of chromosomes containing previously undetectable translocated segments, we propose the use of a two color whole chromosome probe mixture. This mixture will paint a defined set of chromosomes in red and the other set in green and will be used to score incompletes. The intensity of these whole chromosome signals will provide a keener detection of small translocated segments than could be found in the atomic bomb study. The success of this project would include the removal of difficulties associated with seeing small translocated segments, as well as aiding in the determination of the existence of incompletes.

MATERIALS AND METHODS

Probe Development and Hybridization:

Whole chromosome probes 3,5, and 6 were generated by performing three consecutive rounds of DOP-PCR. The probes were directly labeled with Flourogreen using Random Priming. Whole chromosome paints 1,2 and 4 were purchased from VYSIS. All probes were ethanol precipitated and combined with Master Mix 1.0 and Cot1 into a hybridization mixture. The mixture was then hybridized to slides T#4G and T#6K(see next section) overnight at 37 degrees Celsius. The following morning the slides were washed for 25 minutes and counterstained with 4,6-diamidino-2-phenylindole (DAPI).

Slides Used:

Slide	Slide Background	Treatment of Lymphocytes	Dose
T#6K	male, age 26	Tritium-chronic exposure	0.9 Gy
T#4G	male, age 62	Tritium-chronic exposure	0.9Gy

Scoring:

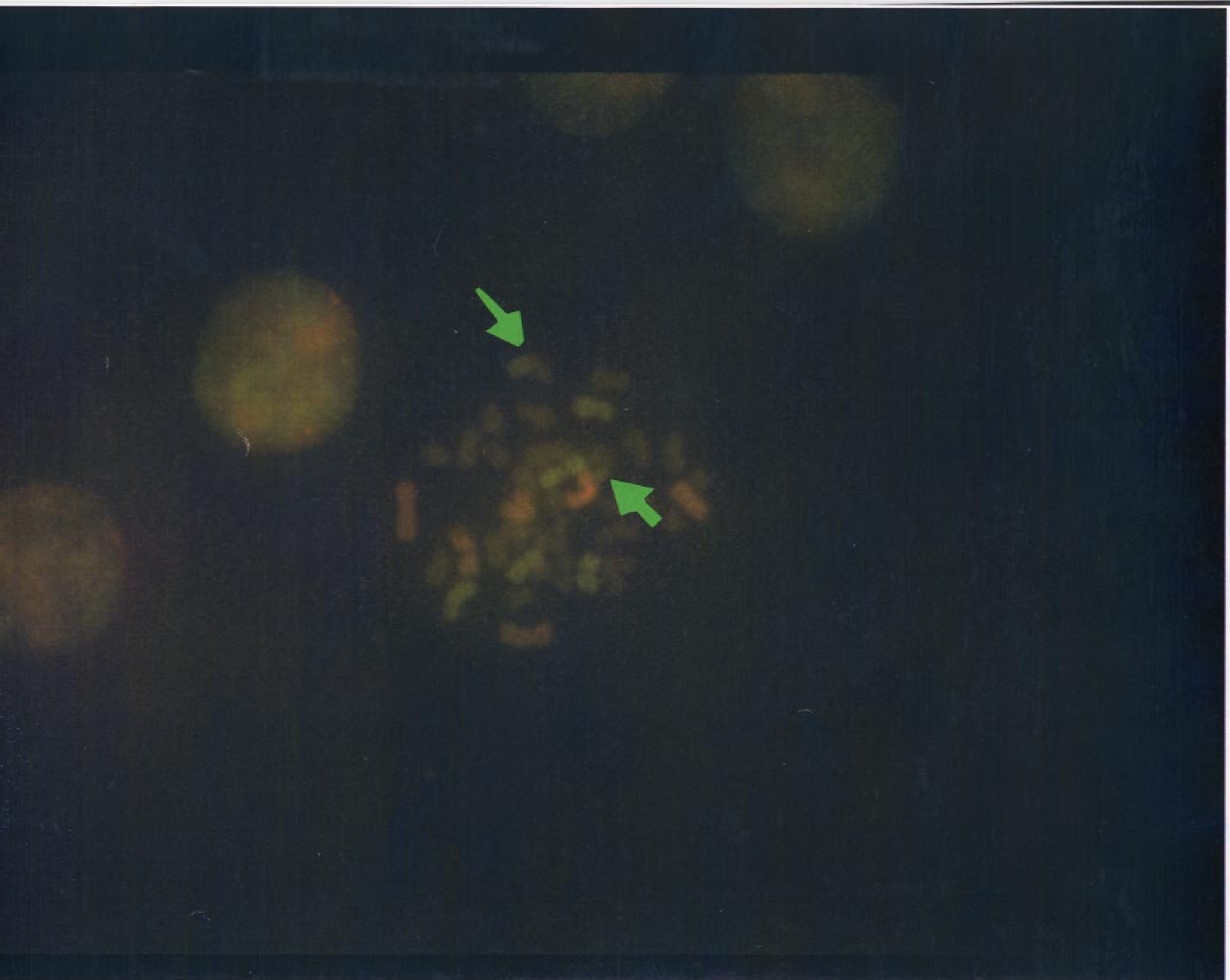
T#6K and T#4G were scored for reciprocal and incomplete translocations between painted and unpainted chromosomes. All aberrant metaphases were photographed and recorded.

RESULTS

The amount of data collected is not sufficient to provide a results section. The figures provide examples of some of the preliminary results.

DISCUSSION

At this time, substantial amounts of data have not been collected involving translocations between painted chromosomes. The intensity of the signals found on reciprocal translocations carrying translocated segments of substantial sizes(See Figure 3), suggests that small painted translocated segments can be detected. Our earliest results involving incomplete translocations between a painted and unpainted chromosome(See Figures 1& 2), reinforce the visual difficulties we associated with the study of Kodama et al (1996).



Figure

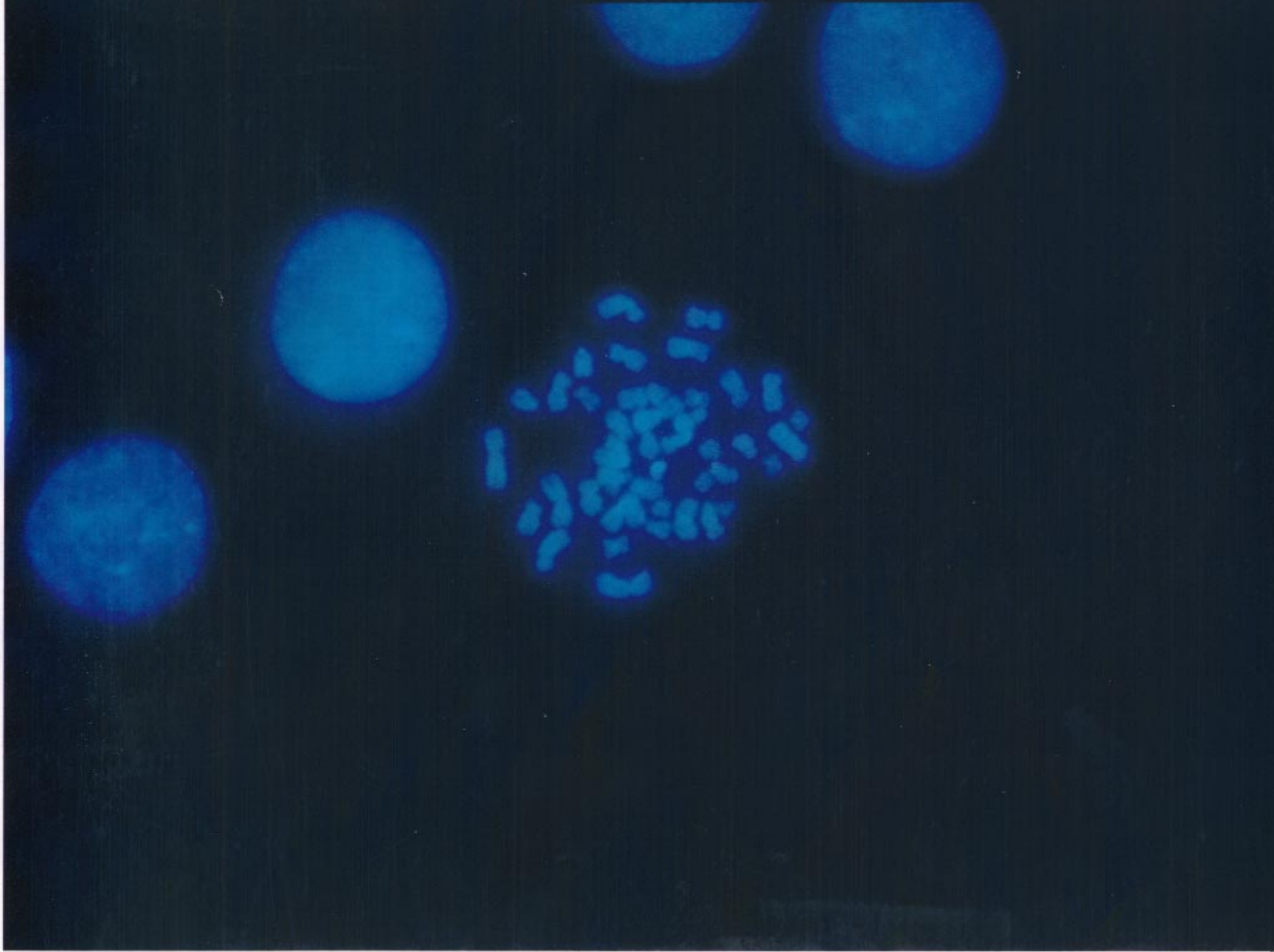


Figure 2

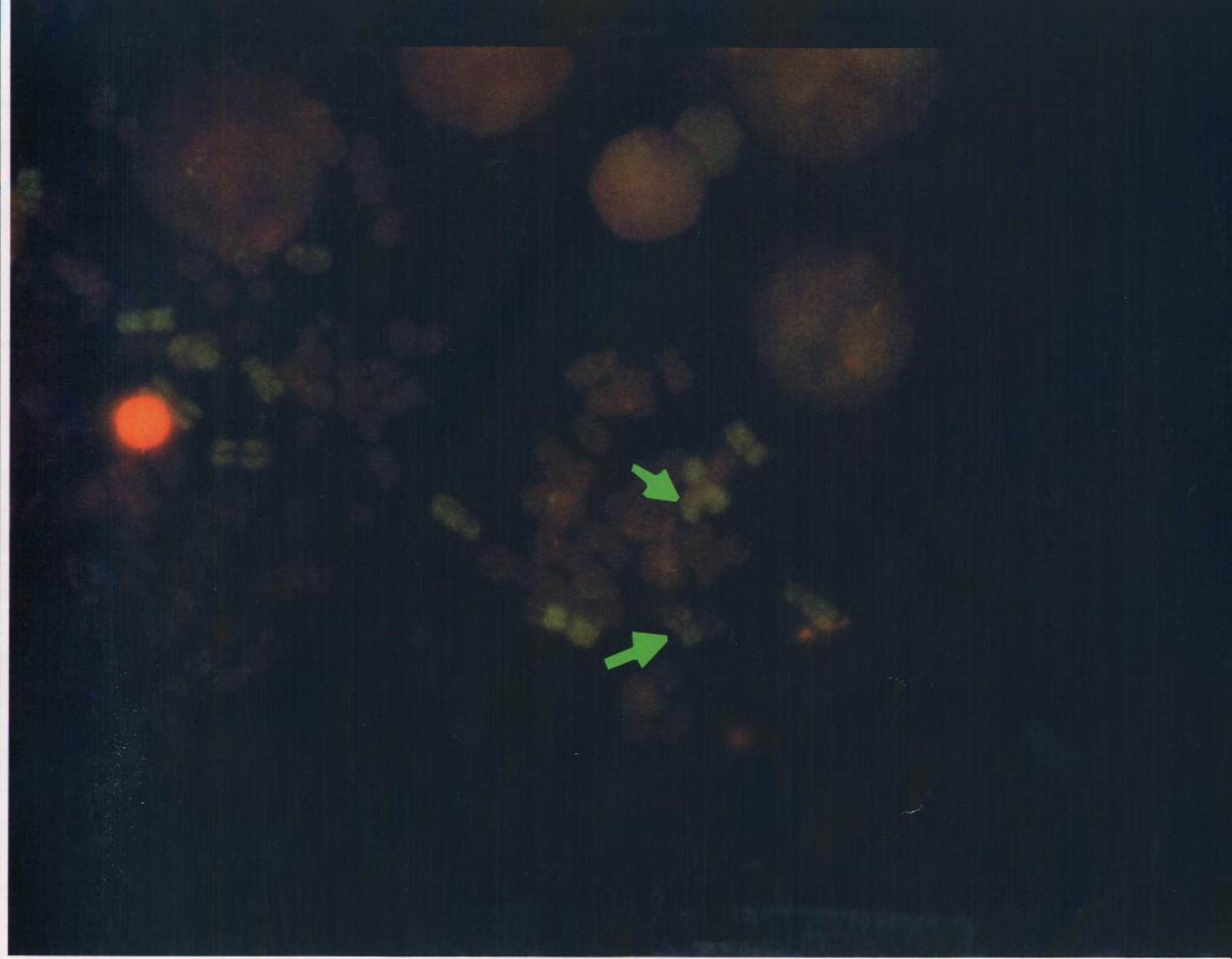


Figure 3

LEGENDS

Figure 1 shows a incomplete translocation between chromosome 5 and an unpainted chromosome as it is seen on a Texas Red/FITC filter.

Figure 2 shows Figure 1 as it is seen on a DAPI filter.

Filter 3 shows a reciprocal translocation between chromosome 1 and chromosome 6 as it is seen on a Texas Red/FITC filter.

CONCLUSION

The optimization of a two color whole chromosome probe mixture provides sharper visualization of small translocated segments on bicolored chromosomes. The signals produced by this probe mixture provide a detection of incomplete translocations that will facilitate the rapid uptake of data as well as a means of discovering the existence of incompletes.

REFERENCES

Carter, N. P. Cytogenetic analysis by chromosome painting. *Cytometry*. 18: 2-10; 1994.

Kodama, Y., Nakano, M., Ohtaki, K., Delongchamp, R., Awa, A. A. and Nakamura, N. Estimation of minimal size of translocated chromosome segments detectable by FISH. *International Journal of Radiation Biology*. 126: 1-13; 1996.

DOE
and
Lawrence Livermore
National Laboratory

192
Timm Wulff
8000 Soldiers Road
Penngrove, CA 94951
Phone 707 792-1957

Cyber Sight ,

a 3D Motion Camera,

Moves to the PC Platform

By: Timm Wulff
Student: CSU, Chico
Focus: Mechatronics Engineering
Electrical Engineering Department
Mentor: Shin-Yee Lu

Abstract

The advent of the PCI bus on the Personal Computer (PC) has suggested that the PC may have become a more effective platform from which the Cyber Sight project could be executed. The purpose of this paper is to document the steps made to convert the Cyber Sight project from a UNIX to a PC platform, including evaluation of possible hardware and software options.

Research Methods

- 1.) exploring the Targa 2000 hardware as a source of video input.
- 2.) exploring 3D Studio MAX software as a imaging output tool.
- 3.) development of software to convert 3D image data to a format that is supported by 3D Studio MAX.

Research Results

- 1.) Targa video format is compressed to keep up with real time video data rate. The video format is in 60 fields per second, and 2 fields per frame.
- 2.) images could be imported into 3D Studio MAX in a dxf format.
- 3.) a program was developed to convert output image data to a dxf format.

Based on Results

- 1.) The fields of the Targa video image make the Targa video useless to application in the Cyber Sight project.
- 2.) Importing the dxf format into 3D Studio MAX is an effective method of displaying system output.
- 3.) Software has been developed to build a series of DXF files from a series of 3D data sets.

⋮

Table of Contents

Title Page	1
Abstract	2
Table Of Contents	3
Introduction	4
Video Input Options	5
Video Format Conversion	8
Output Introduction	9
DXF File Format	10
Program Algorithm	13
Image Output Display in 3D Studio MAX	15
Video Output Using Targa 2000	18
Appendix A	20

Introduction

Cyber Sight is a innovative technique for capturing 3 dimensional motion in the real world at video rates with high resolution. The imaging is done by comparing 2 light intensity images from different positions from the same moment in time . Similarities in intensity patterns across horizontal lines through the image and the position of these patterns in each image allows a range image to be generated. This range image describes the distance to points on the surface of the objects in the camera field of view at the assigned scale. Video rate, 30 frames per second, is accepted as continuous motion by the human eye.

Analysis of an object may be done at 33ms intervals of non rigid bodies. The high resolution of this imaging system will yield detailed information of the objects surface behavior. This technology can be applied in fields such as

- Manufacturing
- Ergonomics
- Biometrics
- Security
- Body Analysis
- Robotics Guidance

Cyber Sight was developed on a UNIX station. The UNIX system was selected for its rapid data transfer rate and open architecture. This system can capture 45 frames (or 1.5 seconds) of motion, due to memory limitations. However, recent advances in PC computing may now allow video data to be captured directly to disk. The invention of the PCI bus allows for fast data transfer rates (100Mb/s) directly to the hard drive. This rate surpasses that needed for real time video data rate. This direct to disk data storage will increase the volume of video captured from 45 frames to thousands.

The purpose of this report is to present the work done in converting the Cyber Sight project from the UNIX to the PC in the areas described below.

- Video input hardware evaluation.
- Evaluation of software to display 3D output.
- Program development for formatting of 3D data into models.

Video Input Options

Method

The hardware used to grab video frames on the UNIX system is platform specific. A new source of video input needed to be selected for operation on the PC that would meet the project requirements. Target specifications include

- 30.0 frames per second (fps) video rate to capture real time motion.
- No compression of video data for details can be lost in the compression process.

Previous to my arrival, the Targa 2000 PCI Version hardware and software were installed into the workstation. This multimedia package was studied for its general abilities and then optimized to meeting the previously stated specifications.

A frame grabbing board made by Matrox is also being explored for its abilities. The parts have been ordered but has not arrived to date.

Targa Results

Targa 2000 is a product of the Truevision company. The product is claimed to transform your desktop computer into a non-linear digital editing system. The features include

- RGB or S-video input and output
- Full-screen full motion video capture and playback
- NTSC at 30 fps/60 fields per sec. and PAL at 25fps/50 fields per sec.
- Real-time JPEG video compression, with adjustable compression ratio
- Simultaneous real time display to graphics and video monitors
- Genlock via separate sync input or to a video source

The package met the video capture rate requirement of 30 fps. The length of time recorded by 'Targa \Digital VCR' software limited to 2 GigaBytes. The user sets the size of the file to be recorded and the program automatically sets a default time length and degree of compression. Typically, default settings for data throughput are around 4Megs/second of video.

The Targa board fails to capture video with no compression of data. The maximum video through-put rate is 8.2 Mb/sec. The ability to capture uncompressed video of this sort (640x480, 24 bit RGB NTSC at 30 fps) requires a rate of 27.6 Mb/sec is required.

The video data capture by the Targa product is captured in two fields (odd and even). These two fields divide the time segment for the frame (33ms) into 2 separate images. One field shows the image at $t=0\text{ms}$ and the other show the image at $t=16.5\text{ms}$. This gives the video a fluid motion when viewed by the human eye.

There is a option to field double the video on capture. The attempts to use this option proved vain. The video data contained one active field (it would change frame to frame). The field that did not change through time contained an initial image that is ever present. So, the n th frame contained one field from the n th frame and one field from first frame.

Targa Discussion

These 2 fielded images are not good for using as input data. The nature of the interlacing of the 2 fields would blur motion of the target object.

The field doubling option would provide a data set the shows 30fps motion. The field that remained constant would need to be filtered out of the image. Also the single field would only provide half the data that would be contained in a full frame.

The Targa board may be able to be applied to stationary or slow moving objects. However, other unknowns arise.

The Targa 2000 hardware can not capture video at real time rate without being compressed. The concerns of this compression damaging the actual image data set is valid. However, the data set may not be significantly be altered by some compression for 2 reasons;

- Each frame would experience an minimum of 11% compression. Currently the system uses 2 frame grabbing boards. Each board grabs one black and white image. If the Targa 2000 were used in a similar fashion the required data rate of 9.2 Mb/s is not far from the Targa's through-put of 8.2 Mb/s.
- The compression will primarily occur in areas of no interest. The target of the camera only fills 50-70% of the data field. The background image area is black. The compression should prefer working in this black, low intensity, highly continuous, background area to a high intensity, textured, modeled and moving target.

The data from compressed images should be analyzed and for surface data loss. This would determine if compression is acceptable and if acceptable, at what rate is data altered.

Specifications suggests that the Targa board can work in parallel with another frame grabbing device by using a Genlock sync. Thus, 2 Targa boards could be used on the PC in the same manner the 2 frame grabbers are of the UNIX type. More studies are required to make a formal recommendation.

The single Targa board, being color, could eliminate the need for a second frame grabber. The image received by the computer from the camera is divided into its three primary color, intensity images. Using a sync signal, the intensity images of the left and right cameras could be attached to the color board's component input. For example, the left camera would be the seen as the blue intensity image, and the

right camera could be the red intensity image of a color frame. These 2 components of a single color image could be accessed for their intensities of the left and right camera images. The data books giving camera specifications have been ordered. Once received, the verification of this process can be made.

The Next Step

The abilities of the Targa board are very promising for stationary or slow moving objects, but certain questions still must be answered if this is to be perused.

- How much detail is lost when an image is compressed by the Targa hardware?
- How much compression may occur before the accuracy of the Cyber Sight surface model is effected?
- Can the work of two black and white boards (as per the UNIX design) be done with one color board? Would doubling the data volume through the hardware damage the detail of the data set?
- If two Targa boards are used in parallel, can bus contention be resolved? The nature of the hardware bypasses the CPU while passing video data to memory. This direct to disk access is what make the 8.1Mb/s throughput possible. Coordinating a Master and slave setup is speculated to be difficult without loss to data rata.

Conclusions

The Targa board should not be perused as the source for video input for the Cyber Sight project. The data from this tool would be incomplete and/or blurred.

Recommendation

Investigate the Matrox frame grabbing products. The company, Matrox, builds leading edge machine vision systems. Matrox products are a combination of easy-to-use, device-independent, software tools, and powerful hardware. Machine vision commonly requires that there be no compression to the data set. This being true, the Matrox product would meet the 'no compression of data' specification. However, the data through-put rate is unknown. From communication with people who have used Matrox products, video data can be captured to video tape and loaded into memory at a latter time and at a rate that will not overload throughput rates. A Matrox frame grabber has been ordered.

Video Format Conversion

Method

The data file is generated in the video capture process using the Targa hardware is stored in a single, partially compressed digital video movie (.DVM) format. The DVM file must be decompressed to become a useful format for analysis. The individual frames of the video image must also be able to be discerned.

Results

A efficient way of decompressing the data was found in the Targa software. This single video file can be processed post capture in the 'Targa \Video Tool Box'. This software can convert between DVM and a TGA Series. TGA is the Targa companies own image format. The TGA Series are a actual series of files that are numerically ordered as they appeared in the DVM video data. These sequential files have no compression.

This TGA file format lends itself to the dissimulation of data. Each of these TGA files is 1.2 Mb in size. This size sets 4 bytes describing each pixel. One byte describing each primary color (blue, green, and red) and one byte designated for attribute data.

The first few bytes of a TGA file describe what data format will follow. Once beyond this point, a byte of data describing the intensity of one pixel of an image can be found in every fourth byte in the file. This data can be extracted, and placed into a 2-dimensional array that is 640 x 480 in size to completely describe the image a camera sees in black and white. Once the data for both left and right camera images has been collected, the transformation from 2, two dimensional images to one, 3 dimensional image can begin.

Conclusion

The TGA format lends itself to easy access to its component colors making it a excellent option for use with the project.

Output

Introduction

3D Studio MAX was selected as a possible tool to display the output of Cyber Sight. The successfulness of this software to display the output was firstly founded on if the 3D data could imported into 3D Studio MAX (MAX).

The vehicle of a file type known as DXF was implemented to transfer the 3D range images into the MAX software. A C language base program was written to generate the DXF files for each set of 3D range images.

MAX provided an environment in which the 3D data sets could be examined for surface quality . The data could easily be viewed from any angle and at any scale desired.

MAX also provided tools that allowed the surface data to be given attributes for display and presentation purposes. Shading, colors, and textures can be applied to objects as needed. The image can also be rendered into component images (of various file type) or into animated formats (with timed controllers for angle, position, background).

The rendered images can be compiled into video with the aid the Targa 2000 software discussed in the previous chapter. Targa can output video or animated feature, generated by the MAX software, to the monitor (computer or TV) or directly to any video recording device.

In the sections that follow the topics discussed above are described in detail. The procedures used in software are outlined to provide future users with enough information to repeat the tasks necessary for generating output.

1. DXF file format outline.
2. Programming Algorithm for building DXF files.
3. Using MAX to display and render data.
4. Producing Video Output.

DXF file format

Introduction

3D Studio MAX was selected as a possible tool to display the output of Cyber Sight. The successfulness of this software to display the output was firstly founded on if the 3D data could imported into 3D Studio MAX. MAX currently allows 3 types of data format to be imported and exported. These are file type extensions are

- .SHP Little information could be found
- .DXF ASCII file, describes an object using vertexes and there associations.
- .DWG. a denser, binary AutoCAD format

The DXF format was chosen to be studied due to its simplicity, popularity, and ASCII nature.

Method

Simple objects (i.e. a cube) were constructed in MAX and exported from that environment for examination of file format.

A wide variety of geometric figures or 'ENTITIES' could be used to construct a model of the 3d data. These possible construction algorithms were examined for ease of implementation toward building a surface to be

- ease of construction
- reliability for use with any data set

Results

All DXF file contain the following sections

1. Initial conditions describing world control parameters.
2. Layers, line types, text, and entities to be constructed.
3. Description of specific of each entity in turn.
4. Declaration of vertexes
5. Declaration of meshes
6. End of File statement.

Below these 6 sections are described in more detail. The information is curved toward its impact on the project. For a more general and extensive report please Email: pdbourke@ccu1auckland.ac.nz

- 1 The file begins with code governing the basic world conditions and environment. These sections tell AutoCAD the X and Y direction vectors, minimum and maximum extents.
- 2 This section states line type and defined layers.
- 3 Declare entities and the number of vertexes and meshes included in each.
- 4 The geometry of a type '3DMESH' was selected to display the image. The '3DMESH', unlike others, allowed for all the vertexes of the entire object to be built in a single group. Each vertexes is described by its (x,y,z) Cartesian location. The order in which these points are constructed is critical, for the each point will be referenced by the order they appear in the file.
- 5 Meshes are a summation of many smaller planes. Each plane is comprised of 3 to 4 points. Each points' location in space is referenced by referenced an integer. This integer points to the vertex location in the earlier section. The vertices number by the order in which they were constructed. (The first vertex is pointed to by a 1, the 123rd vertex is pointed by 123, etc....)
- 6 EOF

The following page display the outline of the DXF file format.
See Appendix A for further details on the DXF file format

Format Outline

```

1 SECTION
  HEADER
  $ACADVER
  AC1008
  $UCSORG
    (0.0,0.0,0.0)
  $UCSXDIR
    (1.0,0.0,0.0)
  $TILEMODE
  $UCSYDIR
    (0.0,1.0,0.0)
  $EXTMIN
    (0.0,0.0,0.0)
  $EXTMAX
    (110.0,110.0,110.0)
  ENDSEC

2 SECTION
  TABLES
    TABLE
      LTYPE
      LTYPE
      CONTINUOUS
      Solid line
    ENDTAB
    TABLE
      LAYER
      LAYER
      3DMESH01
      CONTINUOUS
    ENDTAB
    TABLE
      STYLE
      STYLE
      STANDARD
      txt
    ENDTAB
    TABLE
      UCS
    ENDTAB
  ENDSEC

3 SECTION
  ENTITIES
    POLYLINE
    3DMESH01
      # Verts in SEQ
      # Meshes in SEQ
4      List all Verts in 3DMESH01
5      List all Meshes in 3DMESH01
    SEQEND
  3DMESH01
  ENDSEC

6 EOF

```

Program Algorithm

Introduction

The program developed writes DXF files for the importing of 3D data into MAX.

Program's Method

The flow for the program is as follows:

- 1 Start a loop to increment through the data file to be converted
- 2 Open the files
- 3 Write to DXF generic code for the world parameters
- 4 WHILE the flag is not set loop through data file array
 - N is read from Data, the integer states the number of data points in the first column of data
 - IF N is not EOF
 - Read the float values for X, Y, &Z point coordinates
 - Write these coordinates to the DXF in the proper format.
 - Else set the flag to end loop
- 5 Close data file.
- 6 FOR loop through once for every column of good data -1
 - DO build meshes from the vertexes. Continue to increment through the points up the column WHILE the number of points being meshed does not exceed the number of points in that column.
 - IF Y value of the point in the left column is less than or equal to Y value of the point in the right column build the mesh.
 - Write the mesh so that the points appear in the DXF file in the proper format.
 - IF Y value of the point in the right column is less than or equal to Y value of the point in the left column build the mesh.
 - Write the mesh so that the points appear in the DXF file in the proper format
- 7 Write the sequence and EOF to the DXF in the proper format.
- 8 Close the DXF file.
- 9 FOR Loop back to 1 and build the next DXF file from the next data file.

From this extensive outline, and the DXF file format describe in the previous section, it should be possible to recreate a program that would build meshes in a DXF file format.

Results

There are two procedures written to handle different sorts of file types. The preceding described the one named MeshBuilder.c The procedure MeshBuilder.c was written in the C programming language. It is intended to be integrated into the main body of the Cyber Sight project. Running the MeshBuilder procedure constructs numerically sequential DXF files from similarly sequenced data files.

Currently, the procedure requires values to be entered into the program directly.

- 1 The data file name.
- 2 The DXF file name to be built.
- 3 The number of 3Ddata sets must be entered in the code of the procedure.
- 4 The data set given to the procedure must have a certain format
 - The data set must begin with an integer.
 - This number is the number of data points that follow in the file
 - The data points that follow are floating point.
 - Each point is defined by X, Y and Z coordinates in respective order.
 - The last floating pt. Z coordinate is followed by an integer describing the number of points in the next sequential column of data
 - No carriage returns.
 - Terminated with EOF character

Example:

```

3,  fx,fy,fz, fx,fy,fz, fx,fy,fz,
5,  fx,fy,fz, fx,fy,fz, fx,fy,fz, fx,fy,fz, fx,fy,fz,
9,  fx,fy,fz, fx,fy,fz, fx,fy,fz, fx,fy,fz, fx,fy,fz, fx,fy,fz, fx,fy,fz,

```

Discussion

The program was written to import files into MAX. Do not expect the DXF file to load into AutoCAD or other like design package. That is to say this DXF file builder is not completely true to form. The generic code written that states conditions (the X and Y direction vectors, minimum and maximum extents, line type, defined layers and the number of vertexes and meshes included) is the only variation from the true DXF format. However, these values are ignored by MAX. So, accordingly, the program was written as needed to import files into MAX as needed. This is the same reason that DXF files generated by MAX can not be to loaded into AutoCAD or other like design package. MAX doesn't care about the world the way CAD does.

Output Display in 3D Studio MAX

Introduction

The 3-dimensional data generated requires a tool to display the 3D image in an environment that allows

- the data to be visually inspected for completeness and accuracy and
- the meshed surface to be rendered for presentation

The software evaluated for its wide variety of applications for use in the Cyber Sight project is 3D Studio MAX (or MAX).

Method

The DXF file generated from the range images can be imported into MAX. The meshed data can also be rendered for presentation. The processes involved as they apply to the Windows NT 3.51 operating system are described below to display data was done in the.

To Import the DXF file

Open the 3D Studio MAX program

1. In the **Kinetix** window locate the **3D Studio MAX** icon.
2. Double Click on it, wait a minute and the program will eventually open.

From the **File** pull down menu (top left), select **Import**

Select File to Import window will open.

1. Change the **List File of Type** (lower left) from the options provided, select type **AutoCAD (*.DXF)**
2. Set the **Drive** path (bottom center) to the location of the DXF file you wish to import.
3. Set the **Directory** path (right center) to the location of the DXF file you wish to import.
4. The DXF should now be listed in the **File** listing (left).
5. Select the DXF file to import from the list (left center) by clicking on it.
6. Click on the **OK** button (right top).

Import DXF File parameter window will open.

Accept the defaults by clicking **OK**.

The default values, in the past, have been accepted and provided excellent results. Layer is selected and all options are set to default values. These parameters allow the objects to be smoothed on import. These parameters effect the esthetic of the surface of the object only.

To Render a View

From the **Rendering** pull down menu (top center), select **Render...**

Render Scene window will open.

1. **Time Output** set to single
2. **Output Size** Set to 640x480, this size is compatible with the video image captured by Targa hardware.
3. **Options** These will vary. None need to be selected. If the Surface of the mesh is constructed up side down, such that surface normal can not be seen from what should be the above vantage point, the force two side option selection will remedy this.
4. **Output** Will allow you to save the render in a variety of formats, to any file you wish. Here is how to make a TGA series image to be used with Targa at a later time
5. Click on **Files**

Render Output File window will appear

1. Change the **List File of Type** (lower left) from the options provided, select type **Targa Image File (*.tga, *.vda,*,*....,*)**
 2. Set the **Drive** path (bottom center) to the location you wish to create the file.
 3. Set the **Directory** path (right center) to the location you wish to create the file.
 4. Type the name you wish to save the file as in the **File** listing (top left). This name can not be greater than 8 character in length. It must also contain space for a three digit number before the .tga extension. For example, TestF000.tga.
 5. Select the select the **Setup..** (right center) by clicking on it. Set the **Bits-Per-Pixel** to **24**. This is required by Targa software. Select the **Compression** option. Adding comments in the information area is not necessary.
 6. Click on the **OK** button (right top).
- Render Output File** window will close.
6. Click the **Render** button (center bottom). Image renders to file.

Results

Importing DXF files

The import will take anywhere from 3 minutes (for 10-15K points) to 30 minutes (for 40K points). The time varies with the length of the file and on the quality of the mesh.

Often the progress prompt (center bottom) will stop at 50% and will not up data until the Import is complete. If the import progress prompt reaches the 50% point, the DXF file has successfully been loaded. The building of the MESH is now only a matter of time.

If the import fails before 50% is prompted, the error is in the DXF file. It has been my experience that the DXF file has tried to mesh points that were not constructed in the vertex defining section of the file. When this occurs, it is the fault of the programming. This commonly occurs when there are thin (1 to 10 points wide) extremities or noise around the object. Building a new file is

recommended. Editing the current file is very difficult and time consuming due to the size of the file.

Should this occur here are 3 possible solutions.

- Filter out the noise by limiting the meshing of data only when it occurs in columns of points greater than a limit (i.e. 13)
- Eliminating the first and last several columns of data.
- I recommend altering the program to count the number of vertexes constructed. Use This value as a limit that will terminate the construction of the meshes.

Rendering

The file type varies on the use of the rendered image.

- The TGA format can be used by Targa Digital VCR hardware if it is in the 640x480 pixels, 24 bit and a TGA series format.
- The FLC format can be used to generate animated files. These too can be processed by the Targa Digital VCR hardware if the size is 648x480 pixels.
- The AVI format can be used with another Targa software called AVI player. The AVI is a high resolution image, but is not compatible with the file types previously discussed.

Discussion

The MAX software is an excellent tool for examining individual frames of data for accuracy and completeness. Once in the MAX environment, the mesh and rendered surface, can be viewed from any angle, and at any scale.

Video Output Using Targa 2000

Method

The generation of 3D video output from the PC would demonstrate the PC to be an effective platform from which the Cyber Sight project operate. The current generation of the 3D video motion requires support from several different software tools. In brief, the follow steps were made to build a Cyber Sight 3D motion video.

- I. Sequential DXF format files are constructed from like numbered 3D data sets from the transform matrix.
- II. The numbered DXF files built by the meshing program are sequentially imported into 3D Studio MAX. Here each frame is rendered into a like numbered TGA Series file type.
- III. The Targa\DVM Tool Box software is used to convert the TGA Series into a DVM video movie.
- IV. Targa\Digital VCR can play this DVM file to a terminal or video monitor or video recorder for future viewing and demonstrations.

Details of process

- I. Converting Range Images into a DXF Series
See Chapter: Programming Algorithm
- II. Converting DXF Series into a TGA Series
 - A. Import the first (or next) DXF file (*****000.dxf)
See Chapter: Image Output Display in 3D Studio MAX,
Method: To Import the DXF file
 - B. Render the Object
See Chapter: Image Output Display in 3D Studio MAX,
Method: To Render a View
 - C. Save the Meshed surface into a MAX file for future use.
 Repeat steps A and B until all files have been converted from DXF to TGA series.
- III. Converting the TGA Series into a Digital video movie
Open the **DVM Tool Box** from the **Targa 2000** window
 - A. Select **Add** from the **Clip** pull down menu.
File window will open
 1. Change file type to Targa Series (*.TGA)
 2. Set Path to the Series generated in MAX
 3. Select the 0th file in the TGA Series.
 4. Select OK
 An **Option Window** will Appear

- B. If you wish to load all files in the Series, click OK.
1. Else, Deselect the include all option and correct the frames to be recorded.
 2. Select OK.

Option Window will disappear.

- C. Select Save from the File pull down menu, and save it as a *.clp.
- D. Select Write Options from the File pull down menu.
1. Confirm the 640x480 resolution setting.
 2. If correct, select OK.
 3. If incorrect, correct it.
- E. Select Write Sequence from the File pull down menu.
1. Change the file type to the *.DVM if already set as default.
 2. Set the path to write the file name with extension .DVM in the file name box
 3. Select OK

The TGA series will then be written to a DVM format.

- F. When writing is complete. Exit and Close the DVM Tool Box.

IV Play the DVM Movie

Open the Digital VCR program from the Targa 2000 (Common) window

1. Select Open File...
2. confirm the DVM file type is in the file type box.
3. Find the DVM file you just created
4. select it and click OK.
5. **DESELECT the Audio Enable option (top right)**
6. Click on the Play button.
7. Video will play to monitor and also to two remote locations via the cable interface. Remotely video data can be output as a composite signal (CS), or as a S-video. These outputs can be hooked up to a TV monitor to display or a VCR to record

Helpful hints;

- Until the error is resolved, always **DESELECT** the Audio Enable option. It may need to be done every time you open, play or build a file. Doing so will crash the system in a bad way.
- When building a Settings window is open, do not use any other button or device until you close that window. Doing so will lock up the system.

Results

This process successfully shows that the PC can generate a real time video output from 3D data sets.

Discussion

Video frame construction is an iterative process using 3D Studio MAX. The MAX upgrade, Release 1.1, is being promoted as containing the source code for the MAX commands. This being true, a program will be written to automate this repetitive and time consuming task. Currently, one cycle of steps 1-6 takes approximately 5 minutes. Automating and removing the human element would remove at least 2 minutes per frame.

Appendix A Extended Format Outline

1

```
SECTION
HEADER
$ACADVER
AC1008
$UCSORG
(0.0,0.0,0.0)
$UCSXDIR
(1.0,0.0,0.0)
$TILEMODE
$UCSYDIR
(0.0,1.0,0.0)
$EXTMIN
(0.0,0.0,0.0)
$EXTMAX
(110,110,110)
```

ENDSEC

2

```
SECTION
TABLES
TABLE
LTYPE
LTYPE
CONTINUOUS
Solid line
ENDTAB
TABLE
LAYER
LAYER
3DMESH01
CONTINUOUS
ENDTAB
TABLE
STYLE
STYLE
STANDARD
txt
```

```
ENDTAB
TABLE
UCS
ENDTAB
ENDSEC
```

3

```
SECTION
ENTITIES
POLYLINE
3DMESH01
80000 v
80000 M
```

4

```
VERTEX
3DMESH01
(14.000000
36.000000
63.124760)
```

```
VERTEX
3DMESH01
(14.000000,
37.000000,
62.366665)
```

```
VERTEX
3DMESH01
(15.000000,
38.000000,
61.199299)
```

```
.
.
.
.
.
```

5

```
VERTEX
3DMESH01
(vert1,
vert2,
vert3)
```

```
.
.
.
.
.
```

6

```
SEQEND
3DMESH01
ENDSEC
EOF
```

These are actual exerts from a DXF file

First 2 Columns Set Control Conditions 3rd declares entity 4th declares vertexes 5th declares meshes 6th close with EOF

0	0	0	0	0	0
SECTION	SECTION	SECTION	VERTEX	VERTEX	SEQEND
2	2	2	8	8	8
HEADER	TABLES	ENTITIES	3DMESH01	3DMESH01	3DMESH01
9	0	0	10	10	0
\$ACADVER	TABLE	POLYLINE	14.000000	0	0
1	2	8	20	20	ENDSEC
AC1008	LTYPE	3DMESH01	36.000000	0	0
9	70	66	30	30	EOF
\$UCSORG	1	1	63.124760	0	
10	0	70	70	70	
0.0	2	1	192	128	
20	CONTINUOUS	64	0	71	
0.0	70	71	0	12381	
30	64	80000	VERTEX	72	
0.0	3	72	8	12400	
9	Solid line	80000	3DMESH01	73	
\$UCSXDIR	72	0	10	12382	
10	65		14.000000	74	
1.0	73		20	12381	
20	0		37.000000	0	
0.0	40		30	VERTEX	
30	0.0		62.366665	8	
0.0	0		70	3DMESH01	
9	ENDTAB		192	10	
\$TILEMODE	0		0	0	
70	TABLE		0	20	
1	2		0	0	
9	LAYER		VERTEX	30	
\$UCSYDIR	70		8	0	
10	1		3DMESH01	70	
0.0	0		10	128	
20	LAYER		14.000000	71	
1.0	2		20	12401	
30	3DMESH01		38.000000	72	
0.0	70		30	12382	
9	0		61.199299	73	
\$EXTMIN	62		70	12400	
10	1		192	74	
0.000000	6		.	12401	
20	CONTINUOUS		.	0	
0.000000	0		.	VERTEX	
30	ENDTAB		.	8	
-200.000000	0		.	3DMESH01	
9	0		.	10	
\$EXTMAX	TABLE		.	0	
10	2		.	20	
300.000000	STYLE		.	0	
20	70		.	30	
300.000000	1		.	0	
30	0		.	70	
200.000000	STYLE		.	128	
0	2		.	71	
ENDSEC	STANDARD		.	12382	
	70		.	72	
	0		.	12401	
	40		.	73	
	0.0		.	12383	
	41		.	74	
	1.0		.	12382	
	50		.	0	
	0.0		.	VERTEX	
	71		.	8	
	0		.	3DMESH01	
	42		.	10	
	0.2		.	0	
	3		.	20	
	txt		.	0	
	4		.	30	
	0		.	0	
	ENDTAB		.	70	
	0		.	128	
	TABLE		.	71	
	2		.	12402	
	UCS		.	72	
	70		.	12383	
	0		.	73	
	0		.	12401	
	ENDTAB		.	74	
	0		.	12402	
	ENDSEC		.		

Technical Information Department • Lawrence Livermore National Laboratory
University of California • Livermore, California 94551

